DEPARTMENT OF COMMERCE
LUTHER H. HODGES, Secretary

WEATHER BUREAU
F. W. REICHELDERFER, Chief

# MONTHLY WEATHER REVIEW

JAMES E. CASKEY, JR., Editor

Volume 89, Number 7 | Washington, D.C. | July 1961

## MEAN CIRCULATION PATTERNS BASED ON 12 YEARS OF RECENT NORTHERN HEMISPHERIC DATA

JAMES F. O'CONNOR

Extended Forecast Section, U.S. Weather Bureau, Washington, D.C.

[Manuscript received March 23, 1961]

### ABSTRACT

A new set of long-period means for sea level pressure and 700-mb. height, based on 12 recent years of reliable upper-level and surface observations in the Northern Hemisphere, is constructed. Comparison with the normals currently in use, which are based on data prior to 1950, reveals additional information and some significant differences, principally at high and low latitudes. The three cells of the polar vortex at 700 mb. are not as deep as shown in the normals, the cells over Baffin Island and the Siberian Arctic are farther north, and the Kamchatka cell is found primarily over the Bering Sea rather than over land. The Pacific High at 700 mb. is tricellular on an annual basis, with the additional Philippine cell becoming the dominant cell in late winter. Other new features in the 700-mb. means include troughs near Spitzbergen, Alaska, the Philippine Sea, and the Bay of Bengal; and Highs in northeastern Siberia and the Caspian Sea area. Patterns of height differences between the new means and the normals suggest that a long-period trend toward increased blocking has been in progress during the last decade, particularly in the Baffin Bay area.

### 1. INTRODUCTION

In the preparation of a study of the frequencies of 5-day mean 700-mb. Highs and Lows for the years 1947–1958 (to be published), it was noted that there was poorer correspondence than might be expected between some areas of maximum frequency and the long-period mean circulation pattern in the Northern Hemisphere currently in use as a normal; i.e., the normals published in 1952 [1] and based on data prior to 1950. In January, for example, the frequencies showed a secondary maximum of mean Lows near the Denmark Strait and a clustering of Highs over Greenland, features not adequately reflected (by vorticity maxima) in the 1952 normals. Similar discrepancies could be noted by comparison of the 1952 normals with the frequencies of 5-day mean 700-mb. troughs and ridges during the period 1947–1955 published by Klein and Winston [2].

It might be argued that any disparity between the frequencies and normals may be due to a different circulation regime in the 12 years embraced by the frequency studies (1947 and later years) than in the earlier period prior to 1950 embraced by the normals. To the extent that this is true, then, the earlier normals no longer adequately reflect current modes of synoptic behavior, so that it might be desirable to adopt a more up-to-date set of normals which more accurately represent current trends. (In this connection, it might be noted that the Weather Bureau following the World Meteorological Organization *Technical Regulations* [3] adopted the policy of revising 30-year surface temperature normals once every 10 years by adding data of the most recent decade and dropping the earliest decade.)

As a result of the above considerations, a new set of long-period means for the years 1947–1958 was prepared. This was the longest continuous period of relatively accurate hemispheric analyses for 700 mb. available on punched cards in the files of Extended Forecast Section, and it embraced the same period as used in the frequency study of mean Highs and Lows. Subject to the reserva-

tions discussed later, the 12-year means presented here probably reflect as accurate a portrayal of the long-period circulation as could be obtained.

The principal charts to be presented consist of four sets, as follows: (a) 12 monthly 700-mb. means; (b) 12 charts showing the differences between the 700-mb. 12-year means, by months, and their 1952 normal counterparts; (c) 12 monthly sea level means; and (d) 12 charts showing the differences between the 12-year mean 1000–700-mb. thicknesses by months (not shown) and their 1952 normal counterparts. Obviously these charts may be used, if desired, without any reference to the text, which points out in some detail the deficiencies of earlier data (section 2), composition of the 12-year means (section 3), differences in circulation features at 700 mb. (section 4), annual oscillation of the 12-year mean circulation features at 700 mb. (section 5), comparison of height differences at 700 mb. in relation to long-period changes (section 6), differences in the 700-mb. zonal indices (section 7), stability of the 700-mb. height differences (section 8), comparison of sea level patterns (section 9), comparison of thickness patterns (section 10), and conclusions (section 11).

## 2. DEFICIENCIES OF EARLIER DATA

The 1952 normals presented in [1] were a heterogeneous combination of different periods of data from different areas, and, especially for the upper levels, relied to a great extent on daily analyses arrived at indirectly. This is not surprising when one realizes that the history of direct upper-air measurements is short compared with that of surface observations. It was not until the end of the decade of the 1930's that radiosondes came into extensive use even in the United States, although some measurements were made from airplanes early in this period. Upper-air meteorology based on actual measured data, and of a scope even resembling a hemispheric basis, is thus barely 25 years old at this writing. Furthermore, because of the disruptions in data coverage at various times by wars, etc., only since the end of World War II has there been a relatively uninterrupted flow of data on a hemispheric basis on which a reliable long-period upper-air mean could be based. Over the oceans, for example, prior to near the end of World War II, synoptic upper-air observations from shipboard weather stations and regularly scheduled aerial weather reconnaissance observations were non-existent. Thus the oceanic circulations at upper levels were largely derived from surface observations prior to 1946.

It is well known, as pointed out by Namias [4], that prior to World War II, analyses over the Polar Basin were largely unreliable owing to lack of adequate observations, both surface and aloft. In fact, the analyses during the 1946–1950 period, on which the 1952 normals relied heavily in some areas [1], were still far from adequate in the polar regions, although there was an unprecedented increase in observations during that period. The same deficiencies existed in other parts of the world, particularly in parts of Asia (e.g., China, where upper-air data did not become available until 1956), and at lower latitudes over both land and sea. For these reasons, short-period means based on recent observed data have been used in place of the normals by numerous authors, including Namias [5], Reed and Kunkel [6], Bryson, Lahey, Somervell, and Wahl [7], and Jacobs [8]. In no case however, has any previous mean been based on a continuous period of record even as long as 12 years.

In view of the heterogeneous combination of different periods of record and different methods of obtaining data used in the 1952 normals, it would be indeed surprising if differences could not be found between them and more recent long-period averages, especially considering the tremendously increased data coverage in the last decade or so. It will be observed that both the 1952 normals and the 12-year means presented in this paper contain four of the same years; i.e., 1947–1950. Therefore the comparisons presented here are essentially between features of the eight years 1951–1958, which probably contain the best observational basis in the history of upper-air meteorology, and features of a period of sparse data prior to 1946.

## 3. COMPOSITION OF THE 12-YEAR MEANS

Figures 1–12 portray the new monthly 12-year means at sea level and 700 mb., together with thickness and height departures from the 1952 normals.

These means were obtained by averaging, for each calendar month, the 12 monthly means for the years 1947–1958. Each monthly mean in turn represented an average of 60 synoptic analyses; i.e., 30 days of twice-daily data. Through the years each 12-hourly analysis has been placed on punched cards in the form of heights and pressures interpolated at standard intersections of latitude and longitude in the shape of a diamond grid. The intersections employed are those formed by latitudes and longitudes both of which are evenly divisible by 10, and also by those intersections both of which end in digit 5. For example, 40° N., 60° W. and 35° N., 55° W. are used, but not 35° N., 60° W., etc. The same grid was used in the preparation of the 1952 normals (see fig. 1 of [1]).

The punched card data fell short of providing a full 12-year average in some areas. Over much of Asia north of 40° N., only the months November and December are true 12-year averages, the other 10 months representing 11-year averages in this area. Over Africa east of 10° E. and Asia between 30° N., and 40° N., the patterns represent 10-year averages, and at 20° N. and 25° N. they represent only 8-year averages in this region. These averages, however, are the most recent years in all cases.

Although the punched-card data over China and Southeast Asia represent 10- to 12-year averages, actual daily observations during much of this period were

mostly absent, especially from China. Of course, this is almost always the case over some parts of the world, especially the oceans, even to the present day. Over these ocean areas vertical extrapolations from generally available surface data usually permit delineation of relatively reliable upper-air patterns, especially where the lapse rates are normally not excessively stable at low levels. These extrapolated values are then integrated with actual upper-air reports from ocean weather vessels and islands. However, over China the absence of surface as well as upper-air observations required dependence on horizontal space and time continuity only. It is therefore believed that the patterns presented here may be considered least reliable in the interior of Southeast Asia, but, interestingly enough they are not as different from earlier normals as they are in some other areas. This might be explained by the necessity of using the same techniques of extrapolation in both periods since data were largely absent for both.

The 1000–700-mb. thickness charts (not presented) from which the departures in figures 1D to 12D were computed, were prepared by converting the new mean sea level pressures at each grid-point into heights of the 1000-mb. surface by using a constant height equivalent of 26 feet for each millibar of departure from 1000 mb. This height equivalent is valid near 32° F. This results in varying degrees of error depending on both the extent to which average temperatures depart from 32° F., and the extent to which the mean pressures depart from 1000 mb. (see table 58 of [9]). Thus over the eastern portions of continents in winter north of about 50° N., where mean pressures are relatively high and temperatures may average as low as −50° F., the thicknesses computed by this method are less than actual thicknesses, and positive corrections might be needed locally (such as in the vicinity of Verkhoyansk, USSR, near 67° N., 133° E.) of perhaps as much as 100 feet in the months of January and February.

Similarly in the vicinity of the subtropical oceanic Highs in summer, negative corrections of perhaps as much as 50 feet have to be applied. Elsewhere the thickness difference patterns should be reasonably accurate since the magnitude of the error introduced by the above method diminishes as the mean pressure approaches 1000 mb.

## 4. DIFFERENCES IN CIRCULATION FEATURES AT 700 MB.

The principal features of the 12-year mean 700-mb. charts (figs. 1A–12A) will now be described and compared to corresponding features of the 1952 normals.

(1) Baffin Island Low

At 700 mb. this center is generally not as deep and is farther north on the 12-year means by as much as 7° of latitude in the winter months, as compared with the normal.

(2) Cyclonic Vorticity in the Denmark Strait

In the 12-year means this feature is present at 700 mb. from November to February, with a low center from June to October, but these features are not as pronounced in the normals.

(3) Atlantic Subtropical High

This High is slightly weaker on the 12-year means during most of the year, with the western cell centered east, instead of west, of Cuba in November and December. The trough between the two cells in the cold months is generally 7° or 8° east of the normal position. The westward extension of the Atlantic ridge becomes a separate High center in the southern United States in August, September, and October, a feature absent in the 1952 normals.

(4) Spitzbergen Trough

A short trough shows up in nearly all months at 700 mb. near Spitzbergen in the 12-year means, whereas the normal shows a ridge in this area in most months, notably February.

(5) North American East Coast Trough

This trough at 700 mb. appears farther east on the 12-year means in some months, notably October, while in other months, such as December, it is farther west.

(6) Alaskan Trough

A distinct trough or shearline appears in the new 12-year 700-mb. means during winter months over Alaska, in contrast to ridge conditions in the normals, notably in January and February.

(7) Pacific High

The 12-year means at 700 mb. reveal that the Pacific High is tricellular in the fall and winter months, bicellular in the spring, and single-celled and strongest in July. In August a weak central Pacific cell and a weaker Philippine cell become evident, with the central cell becoming predominant in the fall months. The central Pacific cell and the Philippine cell become equally dominant in December, while in the winter months the Philippine cell becomes the strongest cell in the Pacific High. In April and May the eastern cell disappears, reappearing strongly in June. Little of this detail is apparent from the 1952 normals.

(8) Hawaiian Trough

A distinct trough at 700 mb. occurs near the Hawaiian Islands from November to about March, separating the eastern and the central Pacific High cells. In March this trough appears to be associated with a Low south of the Islands. The proximity of this trough is closely related to the winter rainfall maximum in Hawaii, while the absence of a trough in summer is associated with relative dryness there.

(9) Philippine Sea Trough

From July to November a trough appears in the 12-year 700-mb. means just east of the Philippine Islands, separating the Philippine or South China Sea High from the

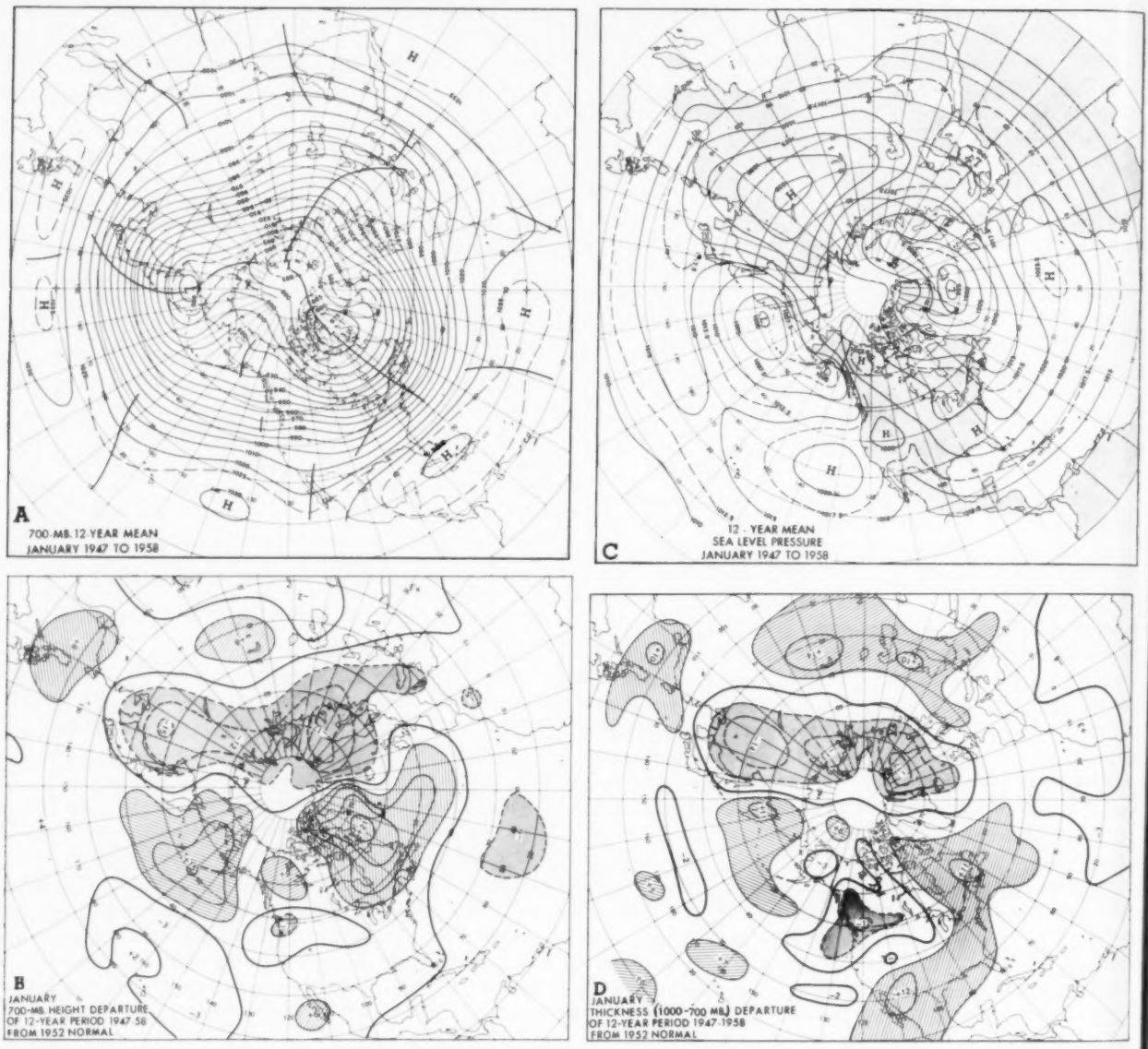


FIGURE 1:

A. 12-year average contours of the 700-mb. surface (tens of feet), drawn at intervals of 100 ft. with selected intermediate contours dashed. Trough lines (heavy solid) delineate the loci of height minima along adjacent latitude circles.

B. Height differences (tens of feet) between 12-year average 700-mb. heights (A charts) and corresponding 1952 normals [1]. Heavy solid lines indicate zero differences. Hatched areas have poitive sdifferences and stippled areas have negative differences of more than 50 ft. The lines are drawn at intervals of 50 ft. with positive differences solid and negative differences dashed.

C. 12-year average isobars of sea level pressure (millibars) drawn at intervals of 5 millibars with selected intermediate isobars dashed.

D. Differences between12-year average thicknesses (1000–700 mb.) (tens of feet) and corresponding 1952 normal values [1]. Heavy solid line indicates zero differences. Hatched areas have positive differences and stippled areas have negative differences of more than 50 ft. The lines are drawn at intervals of 50 ft. with positive differences solid and negative differences dashed.

central Pacific cell. This trough probably reflects the locus of typhoon activity which reaches a maximum at this time of year.

(10) Kamchatka Low

In the winter months this Low at 700 mb. is farther west and not so deep as shown in the 1952 normals. In July and October the vorticity maximum or Low is found over the Bering Sea rather than over adjacent Siberia as in the normal. In November this Low is found near the Kamchatka side of the Bering Sea, in contrast to the position in the normal nearer Alaska.

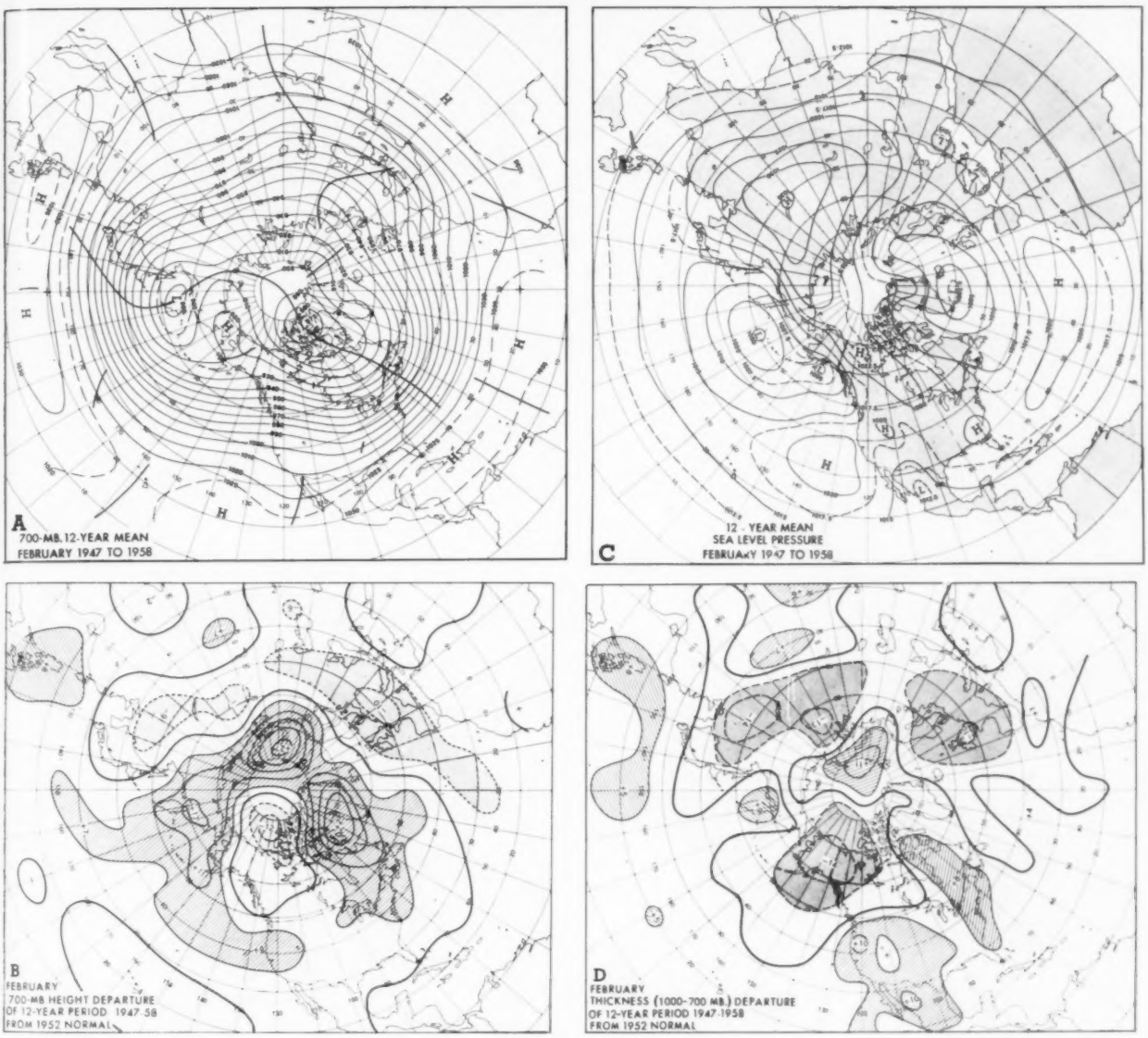


FIGURE 2.—(See legend to fig. 1.)

(11) Northeastern Siberian High Cell

A small High cell appears in extreme northeastern Siberia in the new 12-year means at 700 mb. in some of the colder months such as November, December, and February. This feature does not appear on the earlier normals. Its existence is associated not only with greater heights in this area than in the earlier normals, but also with the Alaskan trough which is also a new feature found in the 12-year means. This High cell is essentially a cut-off portion of the Yukon Ridge.

(12) Siberian Arctic Low

The 12-year means at 700 mb. show marked differences in the position and intensity of the second deepest cell of the polar vortex, the Siberian Arctic Low. In January this Low is deeper than the Kamchatka Low, a reversal from the situation in the earlier normals, while in February this Low disappears as a circulation center, although it is still shown as such on the normal. In April it becomes the largest cell of the polar vortex, whereas the normal map shows only one deep center over Baffin Island. In June the Siberian cell becomes the deepest system in the Northern Hemisphere, and from July to September it apparently becomes *the* polar vortex, close to the North Pole on the Siberian side. In October and November this center is connected by a trough to the Baffin cell, whereas the normal shows a ridge separating the two. In December this center is found considerably farther

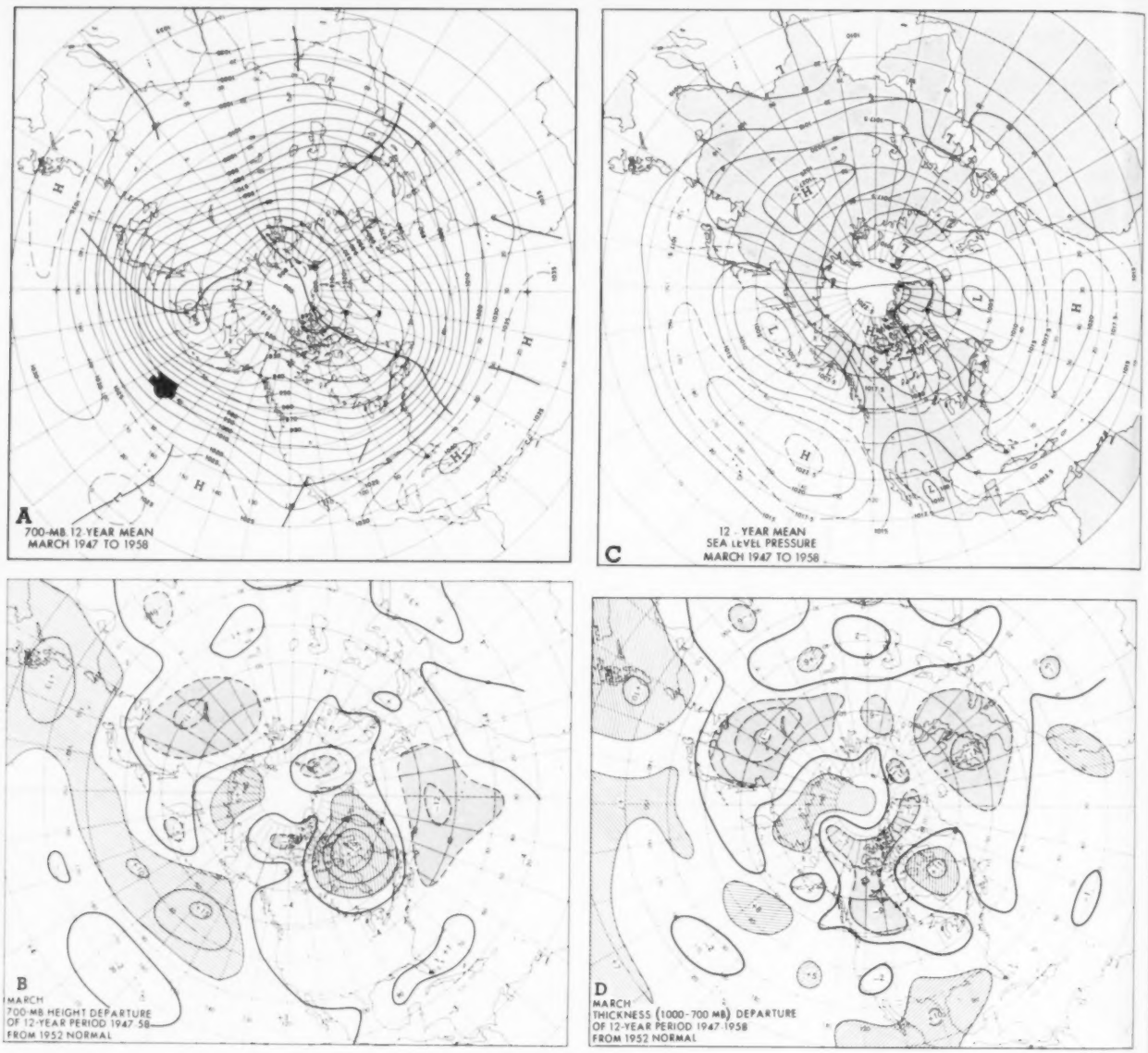


FIGURE 3.—(See legend to fig. 1.)

west near Spitzbergen, where a ridge is shown on the 1952 normals.

(13) Bay of Bengal Trough

In the new 700-mb. means a trough is found near the Bay of Bengal in all months, primarily over Burma in the first half-year, and near India in the summer. In contrast, the normals show this trough near the Philippines during some months, where the 12-year means show a High cell predominating from the fall to the end of spring.

(14) Caspian Sea High

In the summer months an anticyclone builds up at 700 mb. near the southern shore of the Caspian Sea, reaching a maximum height in August. This feature is not evident from the normals.

(15) Russian Trough

A trough oscillates throughout the year about a mean position in western Russia, generally extending across the Black Sea into the eastern Mediterranean. This trough does not usually connect directly with the Siberian Arctic Low, since another persistent trough connects the latter across northeastern Siberia with the Kamchatka Low. In April and May there are marked differences from the normals in orientation and location of the Russian trough. In July this trough appears to be well developed southward along 40° E. longitude, where in

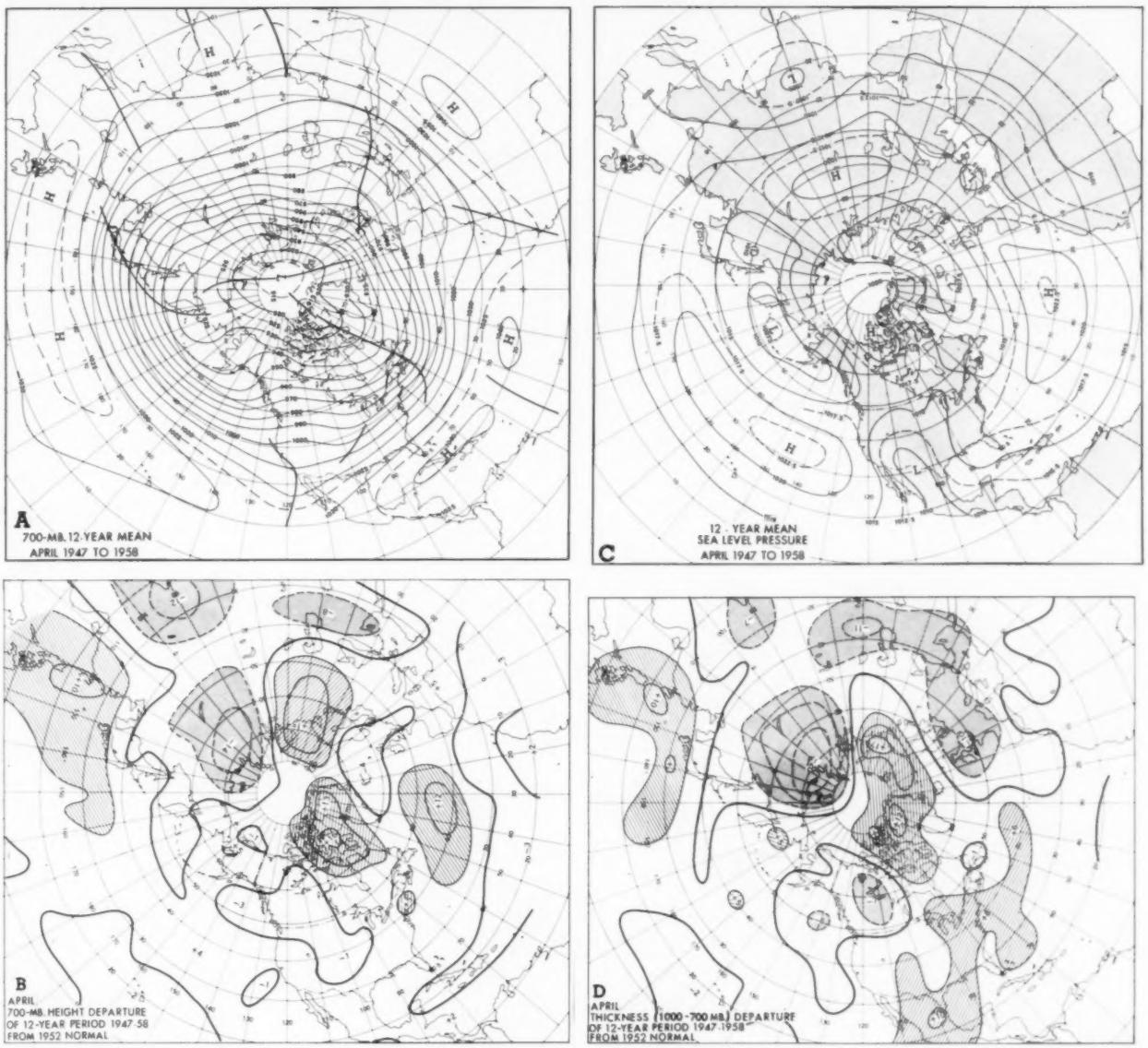


FIGURE 4.—(See legend to fig. 1.)

the 1952 normals, a ridge is located at higher latitudes. In July and August this trough is fairly strongly developed from the eastern Black Sea southward, while the normal indicates little or no trough there. In the winter months the southern position of the Russian trough snaps back westward to the Italian peninsula.

## 5. ANNUAL OSCILLATION OF THE 12-YEAR MEAN CIRCULATION FEATURES AT 700 MB.

Many of the mean circulation features at 700 mb. oscillate with considerable regularity according to the season. Some of the prominent oscillations are as follows:

(1) Alaskan Trough

This trough migrates eastward from the Bering Sea in the fall to its easternmost position in central Alaska in February, after which it disappears.

(2) Pacific Coastal Trough

This feature at 700 mb. oscillates within about 15° of longitude west of Lower California throughout the year. It elongates northward along the west coast of the United States during spring, reaching its northwesternmost position in late summer about 5° off the coast of the Pacific Northwest. Subsequently it retreats southeastward, reaching southern Arizona in December. The North African coastal trough behaves in almost precisely the same fashion.

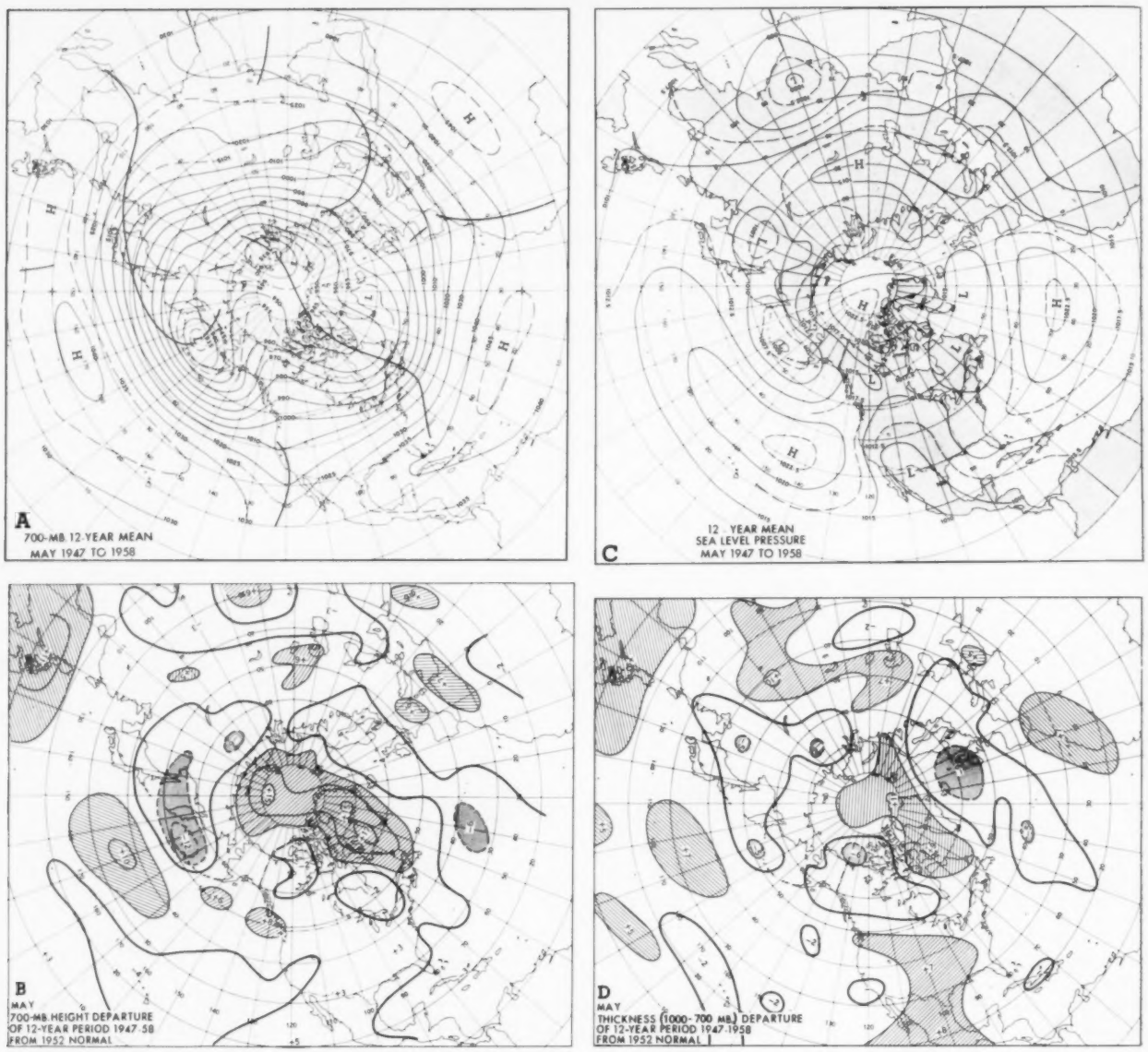


FIGURE 5.—(See legend to fig. 1.)

(3) Eastern Cell of Pacific High

This cell at 700 mb. migrates discontinuously northwestward about 25° of latitude from its southeasternmost position between Hawaii and Lower California in January and February to its northwesternmost position north of Hawaii at 35° N. in July and August, after which it returns to its southernmost position near year's end. This oscillation is similar to that of the west coast trough, but over a greater span of longitude.

(4) Central Pacific High Cell

This cell migrates northeastward at 700 mb. about 15° of latitude from its southwesternmost position in winter to its most northeastern position in late summer and early fall. It retreats rapidly to its southernmost position after October.

(5) Philippine High Cell

This cell is very stable in position from January to May east of Luzon. It disappears in June, reforming as a weak cell in August and September over the southern Philippines. During the remainder of the year it is located north or west of the Philippines.

(6) Bengal Trough

In the first five months of the year this trough migrates eastward across Burma at 700 mb. It appears on the west side of the Bay of Bengal from June through October, in association with the Nepal or Indian Low. By year's

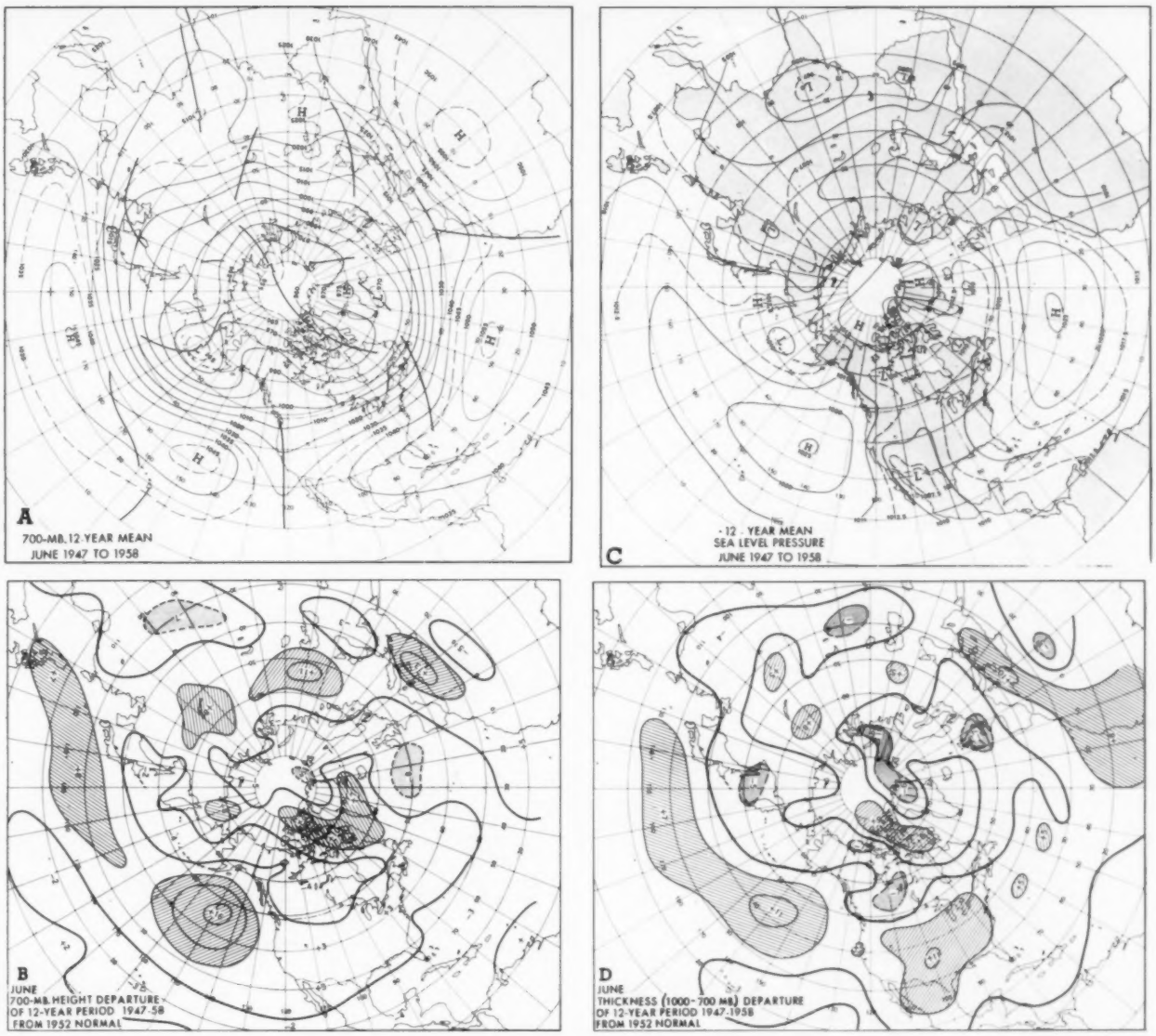


FIGURE 6.—(See legend to fig. 1.)

end it is located in the central Bay of Bengal, heading eastward toward Burma.

## 6. COMPARISON OF HEIGHT DIFFERENCES AT 700 MB. IN RELATION TO LONG-PERIOD CHANGES

Figures 1B to 12B show that there is a good correspondence, as reflected in smaller height differences at 700 mb., between the new 12-year averages and the earlier normals in some areas, such as the contiguous United States, where earlier data were fairly plentiful and relatively accurate. This might lead to the inference that the more substantial differences in other areas reflect earlier errors rather than long-period changes. However, this is not necessarily true in all areas, since the difference patterns frequently show up as couplets of adjacent height difference patterns of opposite sign.

The existence of these couplets in certain areas and seasons suggests that departures of a certain sign in one area are dynamically linked with departures of opposite sign upstream or vice versa. For example, the negative differences in January at 700 mb. over Manchuria (fig. 1B) are associated with the positive departures of similar magnitude in the north-central Pacific probably through barotropic propagation of vorticity. In other words, if the negative differences over Manchuria merely represent a compensation for erroneous heights on the earlier normals, then the positive departures in the Aleutians are quite a coincidence. Or reasoning conversely, since reliable data of the recent 12-year period in the Aleutian area indicate

595485—61——2

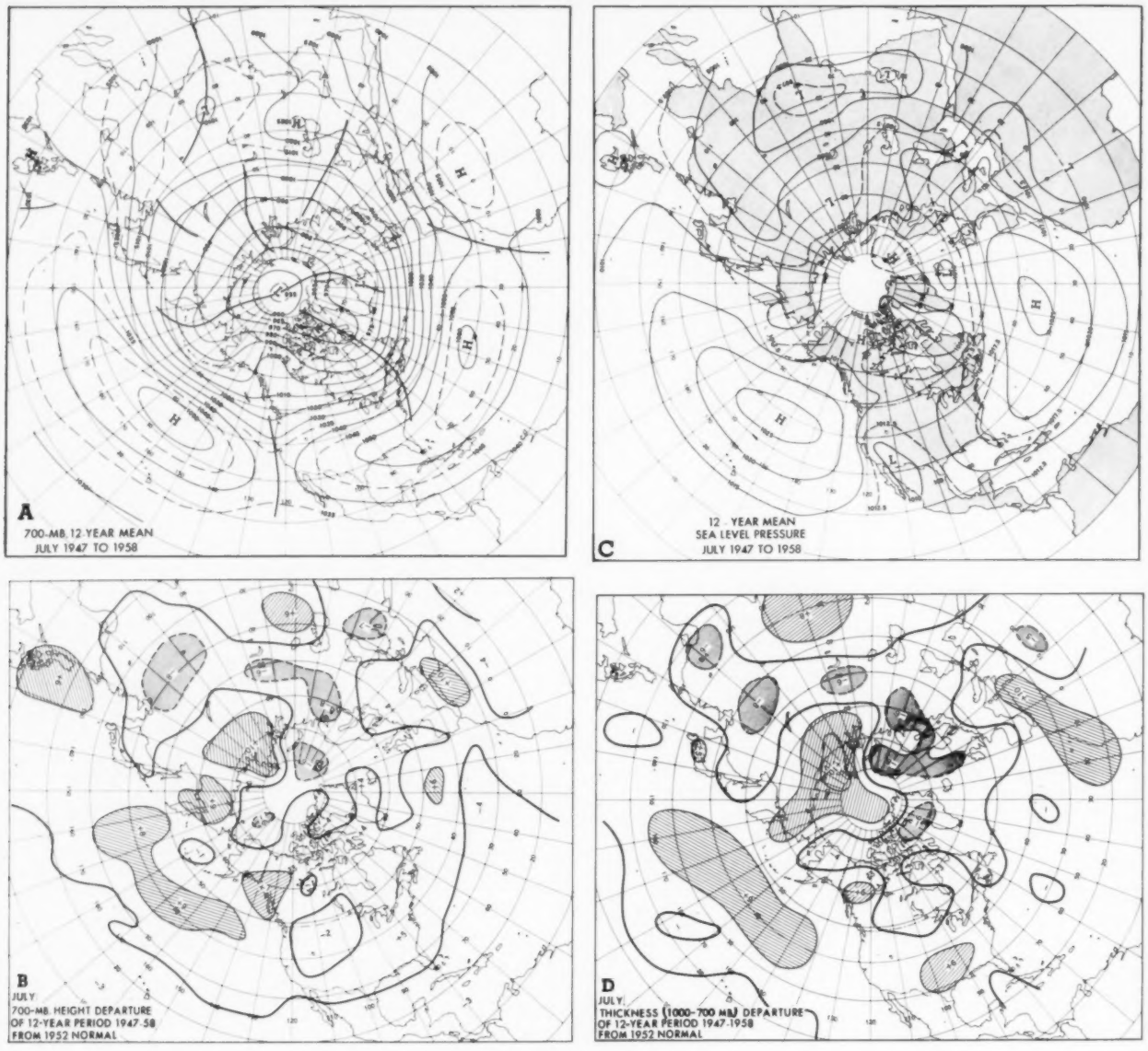


FIGURE 7.—(See legend to fig. 1.)

a trend toward greater heights than in earlier normals, this trend can be confidently attributed to an error in the 1952 normals *only* in the absence of a negative trend of the height differences upstream.

Another area of relatively large height differences at 700 mb. is in eastern Canada and Baffin Bay, from November to June, with a maximum of 250 ft. in February. That these differences are at least partially a manifestation of increased blocking in recent years is suggested by the fact that in some months e.g., December and January, strong negative differences are found immediately to the east, over Europe. Similar patterns were found by Martin [10] in seasonal averages, for the 5-year period 1947–1951, of interrelated 5-day mean height anomalies at 700 mb.

Negative departures from the 1952 normals are greatest in the colder months from the eastern Atlantic across Europe and eastward to Asia at middle and high latitudes. Strong negative differences still exist over Siberia and to a lesser extent over the eastern Atlantic in spring. In the summer and fall months, the negative differences are greatest over the North Atlantic and northern Europe.

A striking alternation from a large negative to a positive difference occurs between January and February near northern Scandinavia and Novaya Zemlya, and to a lesser extent continues through March and April. The 270-ft. positive difference in February over Novaya Zemlya is the greatest difference from the earlier normals observed

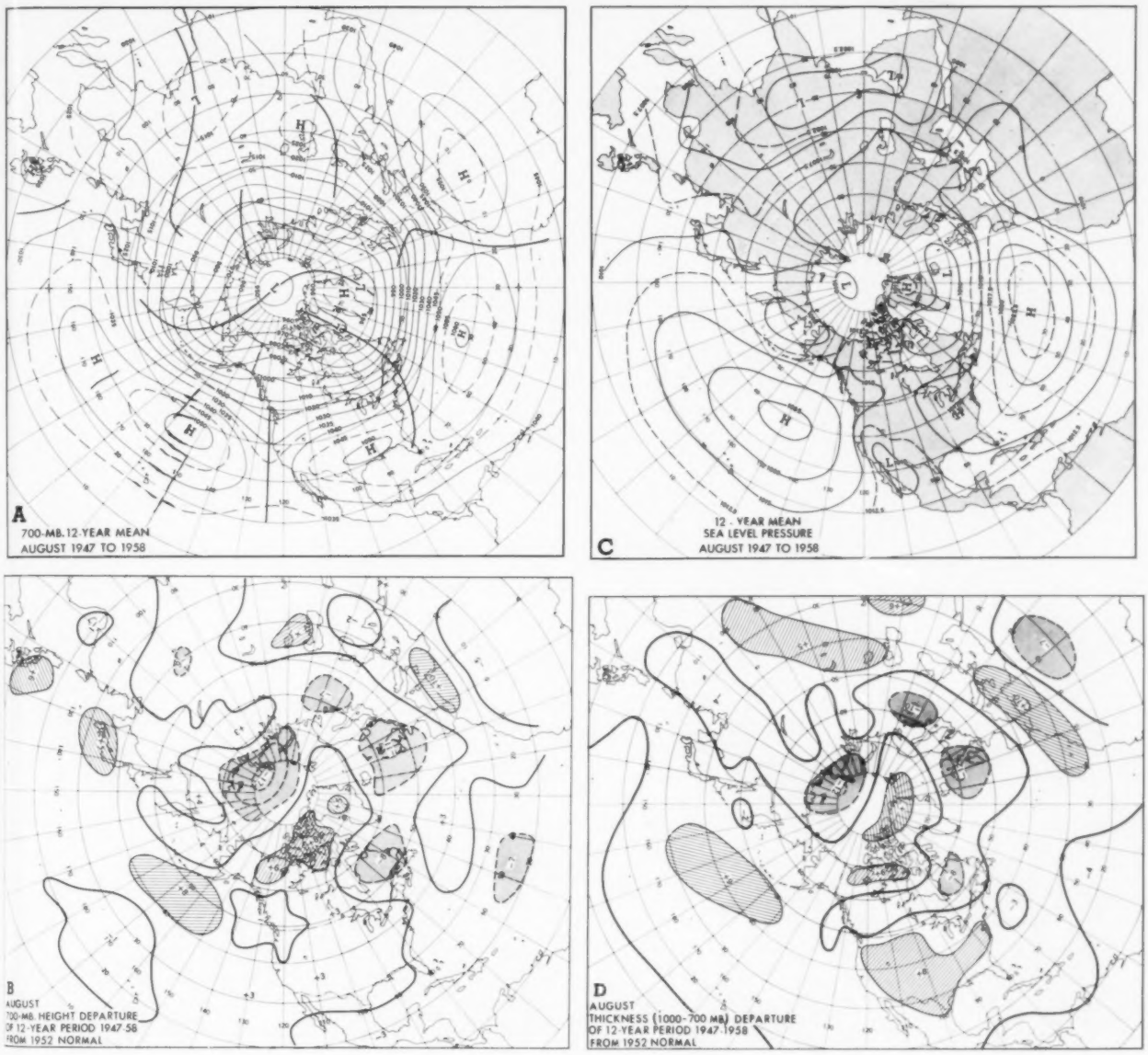


FIGURE 8.—(See legend to fig. 1.)

at 700 mb. This may reflect either an increased blocking trend or a correction of errors of analyses in earlier years.

October (fig. 10B) is also an unusual month in the sense that negative differences appear in the 12-year means throughout the higher latitudes. This implies stronger westerlies in the polar latitudes during October than in the earlier normals.

On a hemispheric basis the positive height departures exhibit a northward migratory trend, primarily in the western sector of the hemisphere, from about December to May, after which they recede southward to middle latitudes in the last half of the year. The negative departures, on the other hand, dominate the high latitudes from late summer to October, after which they recede southward, primarily into the eastern sector. The net effect of these height differences on the westerlies in the western sector of the hemisphere is shown in figure 13.

## 7. DIFFERENCES IN THE 700-MB. ZONAL INDICES

Figure 13 gives a comparison of the annual variation of zonal indices at 700 mb. for the western sector of the Northern Hemisphere, between the new 12-year means and the 1952 normals. Overall, the 1947–1958 average westerlies are slower than those in the normals, with the polar westerlies averaging 0.26 m.p.s. less, and the subtropical westerlies 0.75 m.p.s. less.

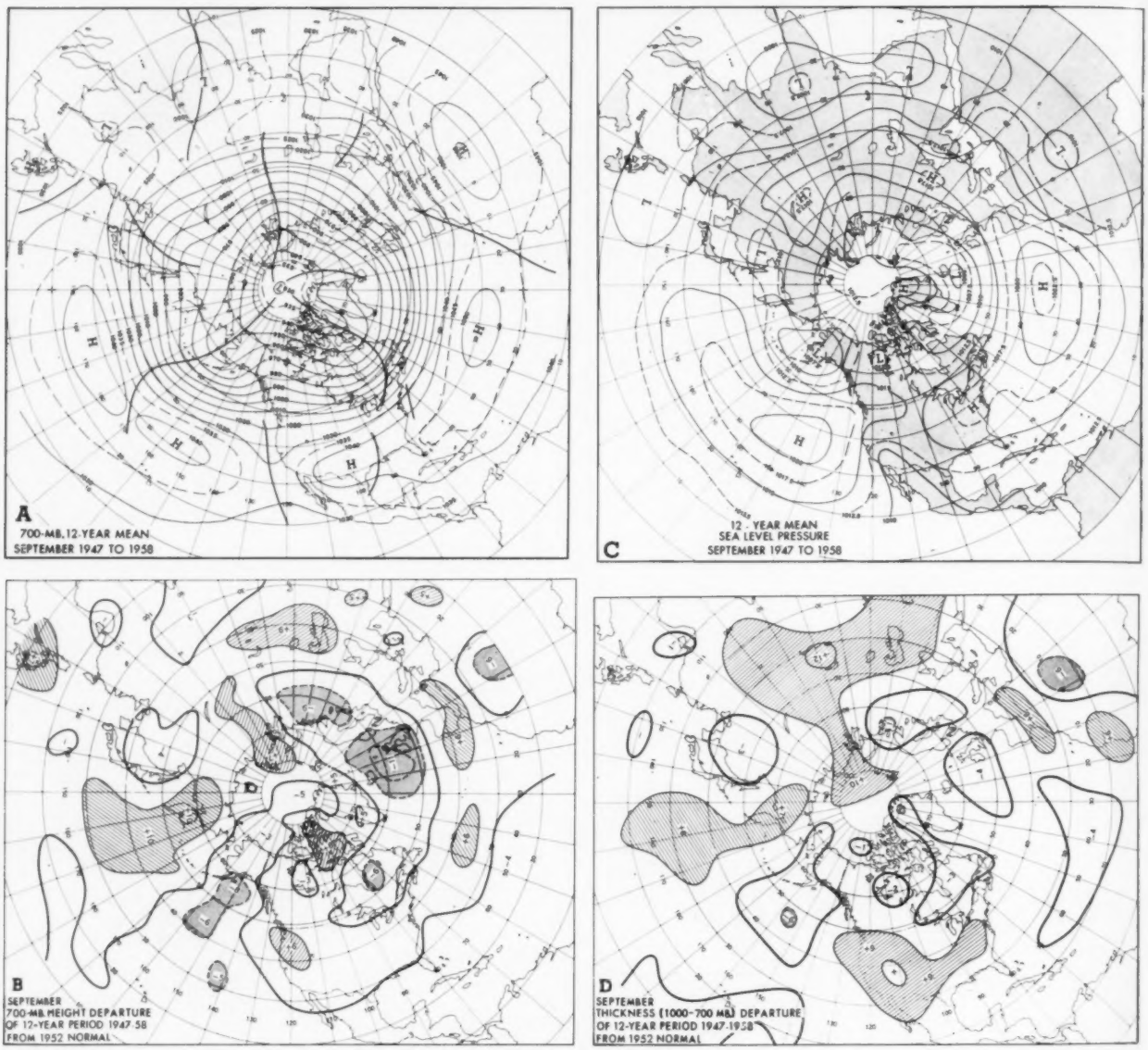


FIGURE 9.—(See legend to fig. 1.)

The subtropical westerlies at 700 mb. are slower in all months in the 12-year means, with the minimum speeds occurring in July instead of in August. At mid-latitudes, the westerlies are stronger in the 1947–1958 means than in the normals in summer and fall and weaker in winter, with the annual maximum in December instead of in January, and a single minimum in July instead of a double minimum in June and August. In the polar latitudes, the westerlies reach a sharp maximum in October on the 12-year means.

## 8. STABILITY OF THE 700-MB. HEIGHT DIFFERENCES

One criterion of the reliability of a new set of long-period averages is the relative stability of the differences between the new means and the earlier ones. Ideally this would require two new sets of consecutive averages and a sufficiently long sample of new data to justify this procedure. Since such a new sample was not available, it was decided to compare the departures of the new 12-year means (1947–1958) with the departures of a set of 8-year means (for the years 1946–1953) which had previously been prepared in the Extended Forecast Section. Maps at high latitudes for the period 1948–1955 were published by Namias [4] for the months of January, April, July, and November. A mean of 8 Mays from 1946 to 1953 was published by Klein [11] in 1954 (see his fig. 9). Figure 14 shows the departures from the 1952 normals of 8-year means at 700 mb. for the period 1946–1953 for

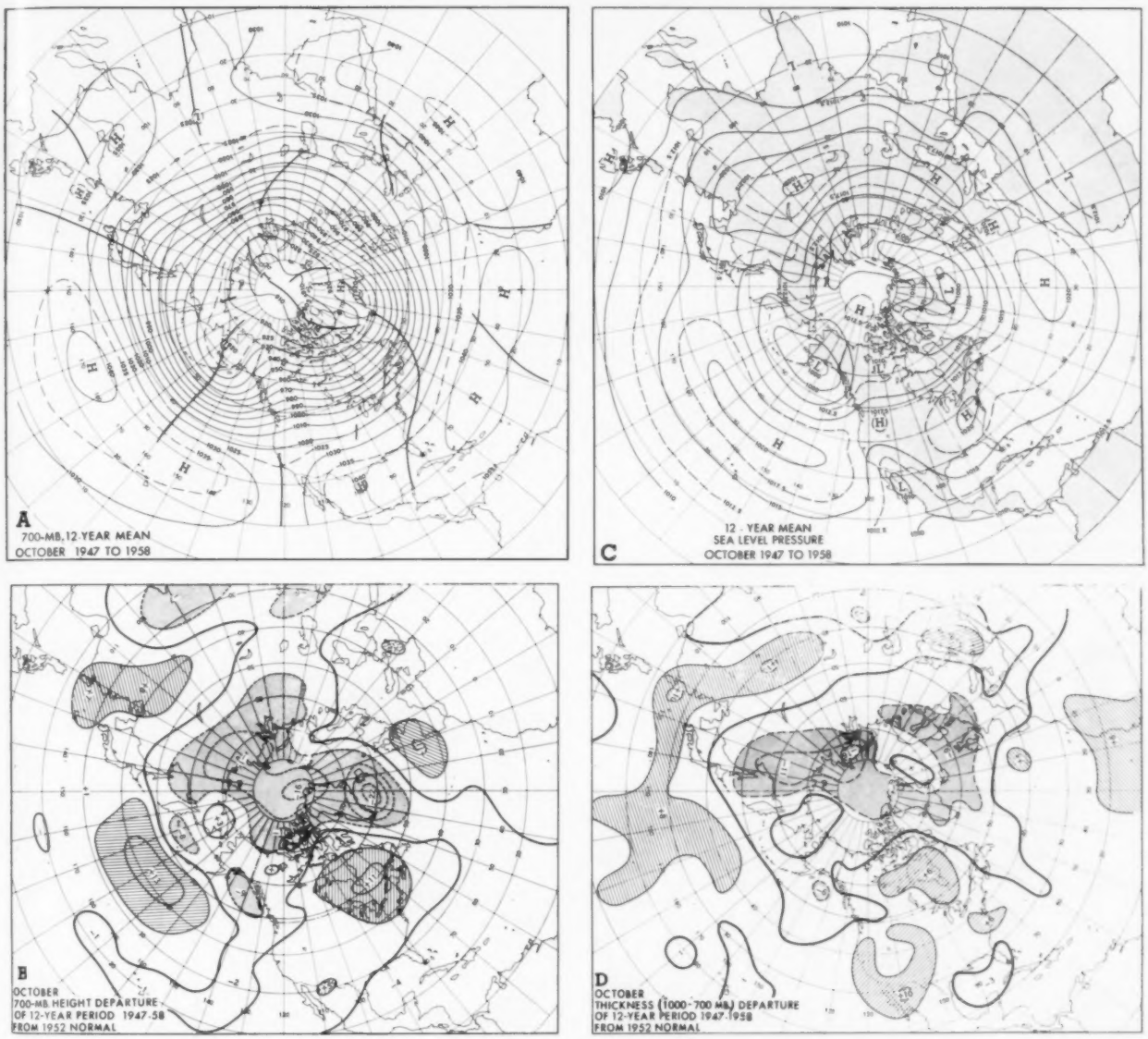


FIGURE 10.—(See legend to fig. 1.)

three additional selected months, February, June, and October. These may be compared with the differences from the 1952 normals of the 12-year means in figures 2B, 6B, and 10B, respectively.

The similarity of the departures of the 8-year and 12-year means for these months is equally strong for the other months (not shown). In general the patterns show considerable stability and, with few exceptions, the differences between the departures of the 8-year and 12-year means, where they exist, are generally in a direction away from the earlier normals.

In February, for instance, the departures almost without exception, are greater in the 12-year average than in the 8-year average. In June the majority of the departure centers have intensified with time, except for some in the western sector of the hemisphere. In October, the departure patterns show greater stability, but the trend if any, is still that of increased differences from the earlier normals with the larger sample of new data. A very stable departure pattern is observed in the region of northeastern United States and southeastern Canada, where the +110-ft. departure remains unchanged.

There appears to be little doubt that the large differences between the departures of progressively longer-period averages, which are observed in some areas such as Baffin Island, Scandinavia, and the Bering Sea, reflect, in addition to compensation for earlier errors, important secular trends in the average circulation from that represented by the earlier normals. The more stable differences in other areas are more likely to reflect the locations of

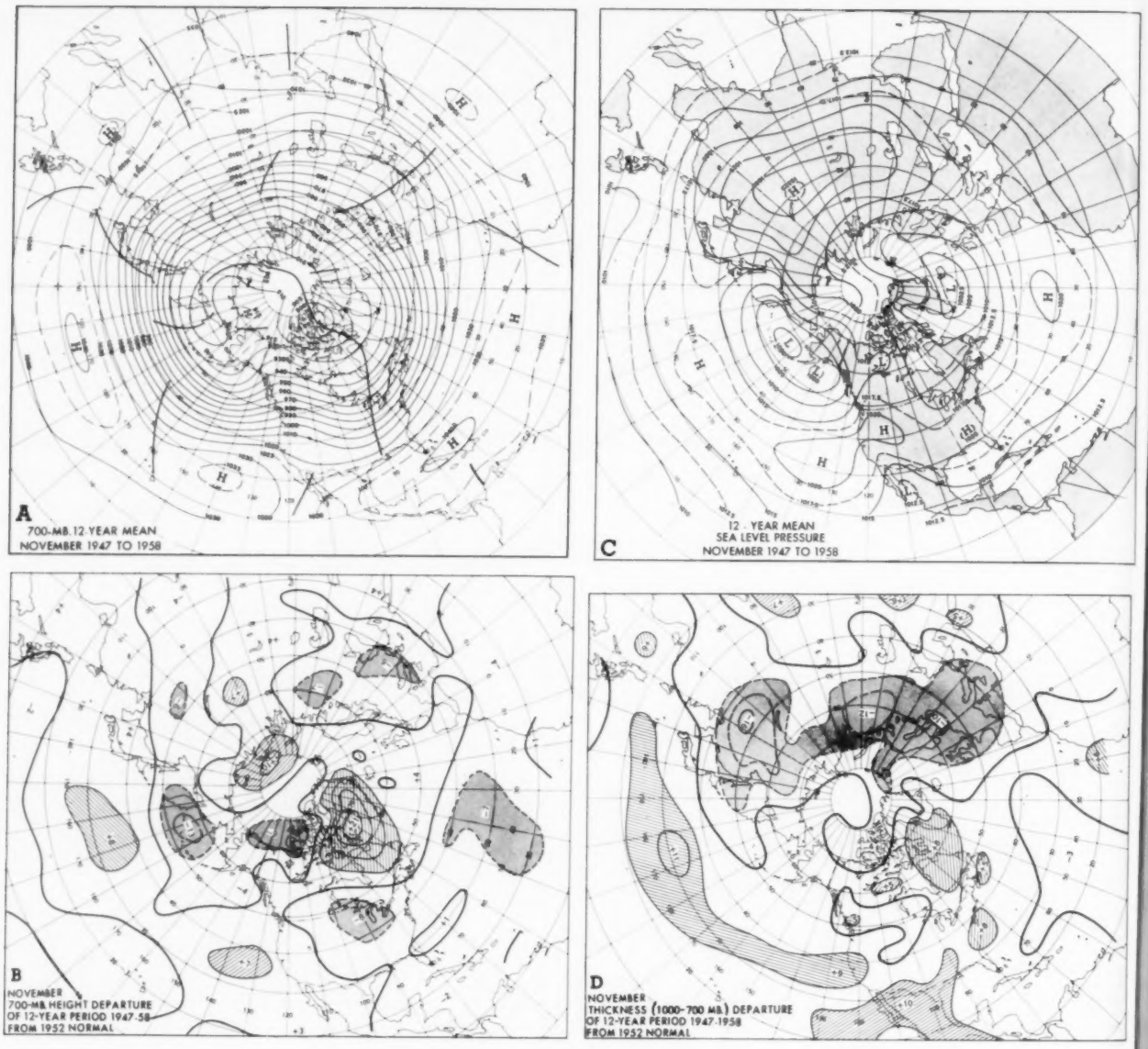


FIGURE 11.—(See legend to fig. 1.)

errors in the earlier normals. In the few areas where the trend of the departures is back toward the 1952 normals, the departures of the 8-year means probably represent an overcorrection of earlier errors, and also in part a cyclical trend of a more temporal nature.

## 9. COMPARISON OF SEA LEVEL PATTERNS

Figures 1C to 12C portray the 12-year averages for the years 1947–1958 at sea level. Some of the noticeable differences from the 1952 normals are pointed out below. There are many additional differences, of course, and these generally correspond to those previously observed at 700 mb.

Systems which appear on the 12-year means but not on the normals are:

(a) Secondary Lows appear in the Gulf of Alaska in January and February.
(b) A Low is found in the Adriatic and the ridge connects across Europe in April.
(c) There is a Low over Quebec in May.
(d) In June a closed Low appears southwest of Iceland.
(e) A weak High is found over the Philippines in July.
(f) In September an inverted trough makes its appearance over Hatteras.
(g) A separate Low forms in the Bering Sea in November

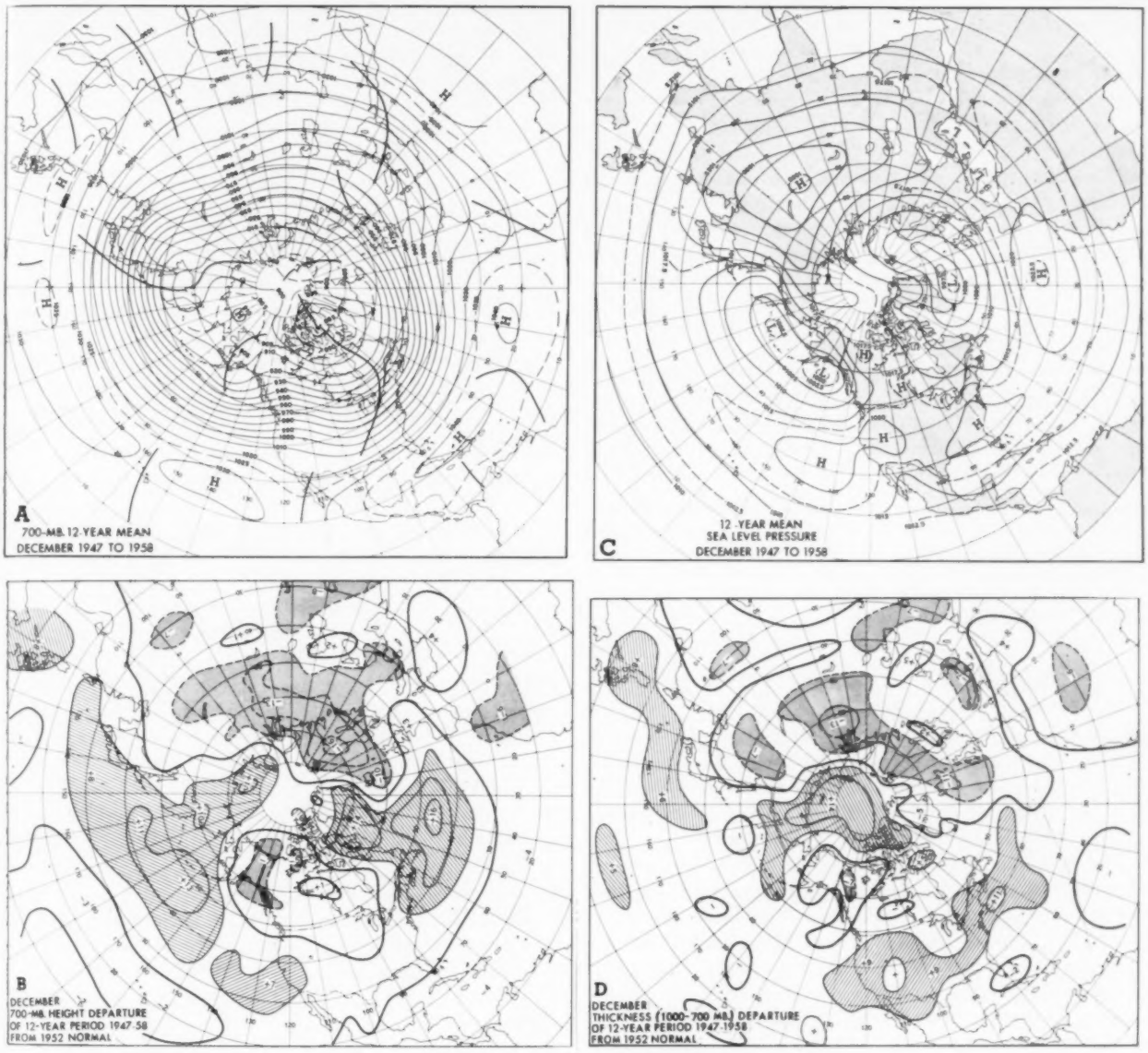


FIGURE 12.—(See legend to fig. 1.)

Systems which appear in the normals but are not found in the 12-year means are:

(a) Highs show up in the Arctic in January, July, and August.
(b) In July there is a Low over southern China.
(c) A Low appears in Davis Strait in November.
(d) The Colorado Low appears in December and January.

Some other features of the 12-year means which differ from the 1952 normals are:

(a) The Yukon High has an unbroken connection with the southeastern United States High, and in February the latter is disconnected from the Atlantic High.
(b) In April the main Low center is in the Bering Sea instead of near Kodiak.
(c) In May the Indian Low is deeper and farther southeast, while the Bering Sea Low is farther west.
(d) In June the Indian Low is much farther southeast and deeper on the 12-year mean.
(e) In July a stronger ridge extends from the Mediterranean over North Africa, forcing the Sahara Low west to near 0° longitude.
(f) In August a Low appears near the North Pole in the area of high pressure shown in the earlier normals.
(g) In September, the deepest Low is centered near Iceland instead of over Davis Strait, and in the

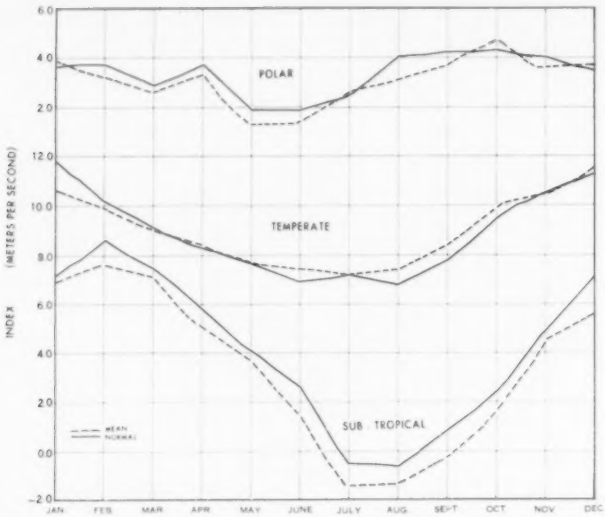


FIGURE 13.—Annual variation of 12-year average monthly 700-mb. indices (dashed) in meters per second for the western sector of the Northern Hemisphere (0–180° W.). Subtropical index applies between latitudes 20° N. and 35° N., temperate between 35° N. and 55° N., and polar between 55° N. and 70° N. "Normal" indices (solid) are averaged from maps in [1].

Pacific a low center exists east of the Philippines instead of over the South China Sea.

(h) In October a single deep center occurs near Iceland instead of weaker double centers in the normal.

(i) In December the Azores High is about 5° farther north, while in the Pacific, the deepest Low is near Kodiak instead of the Bering Sea.

The patterns of monthly pressure differences between the 1947–1958 sea level means and the normals (not shown) correspond fairly closely to the height differences at 700 mb. shown in figures 1B to 12B, especially for the major centers. One of the areas in which persistent differences from the earlier normals show up is in the vicinity of the North Pole where pressures on the 12-year means are lower than in the normals in all months, except May, to varying degrees from 1 to 4 millibars. The largest departures occur in July and August and again in December. The differences are not as great in July as suggested by Reed and Kunkel [6]; the patterns conform more nearly to the 8-year average published by Namias [4].

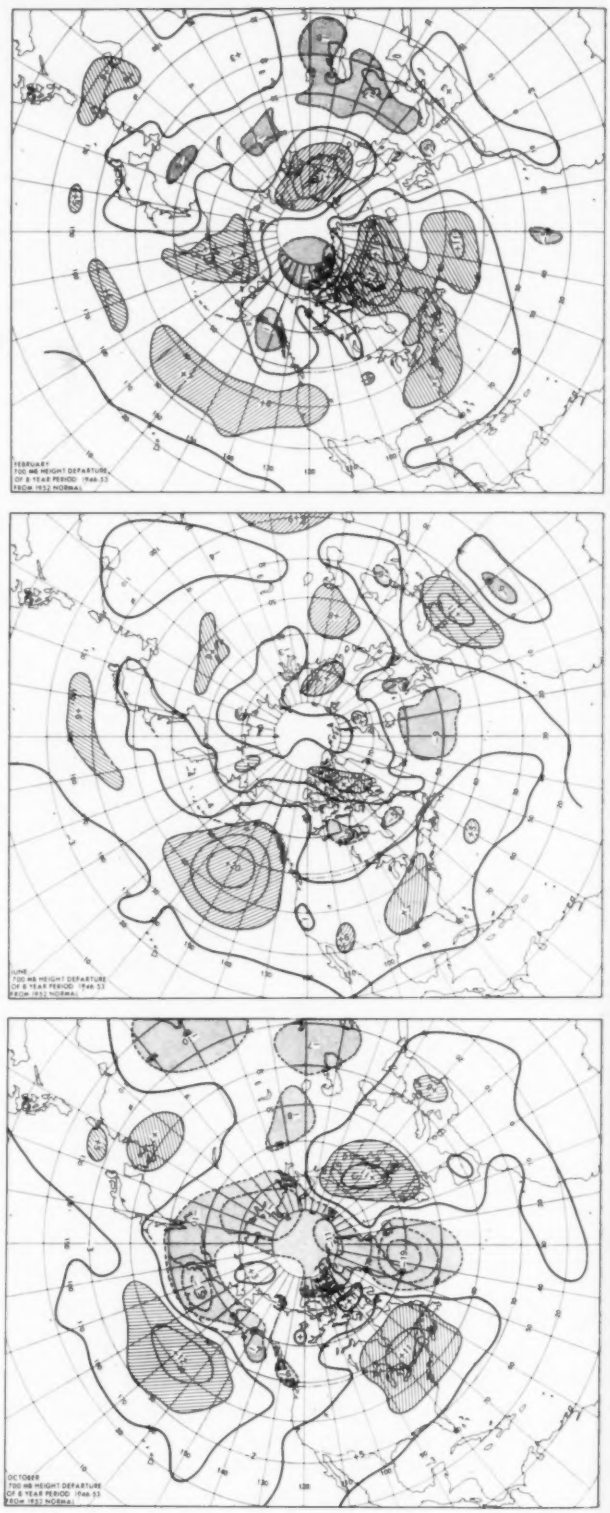

FIGURE 14.—Height differences (tens of feet) between 8-year average 700-mb. heights and corresponding 1952 normals [1]. Heavy solid lines indicate zero differences. Hatched areas have positive differences and stippled areas have negative differences of more than 50 ft. The lines are drawn at intervals of 50 ft. with positive differences solid and negative differences dashed.

In other areas there are displacements of the sea level departure centers from the corresponding 700-mb. centers. For example, a negative sea level departure center in January in the Sea of Okhotsk (not shown) is probably related to the negative 700-mb. center (fig. 1B) over Manchuria. This implies that thicknesses were greater in the 1947–1958 period over Kamchatka and less over Siberia than in the earlier normal.

An overall integration of the local differences between the sea level pressure departures and the 700-mb. height departures of the 1947–1958 means from the 1952 normals is probably best portrayed by the monthly 1000–700-mb. thickness departures (figs. 1D–12D). In addition, the patterns of monthly thickness departures show how the mean virtual temperature regime of the years 1947–1958 compares with the earlier period embraced by the 1952 normals.

## 10. COMPARISON OF THICKNESS PATTERNS

Figures 1D to 12D show the monthly departures of the 1947–1958 average thicknesses between 1000 and 700 mb. from the 1952 normals. Some of the departures may be due to the fact that the method used to reduce sea level pressure to height of the 1000-mb. surface differs in the two cases. (See section 3 above and page 4 of [1].)

From October to April the European and Asiatic sectors of the hemisphere, especially at higher latitudes, show decreased thicknesses from the 1952 normals, the largest departure (200 ft.) appearing in April near the Laptev Sea. This is equivalent to about a 10° F. decrease in virtual temperature. During the remainder of the year, thickness differences over Asia and Europe are smaller and more variable.

Over the North American area, thicknesses appear generally greater in practically all months except in western Canada from November to June. The largest decrease and associated cooling occur in February with a 140-ft. center over Alaska and the Yukon. Increasing thicknesses of about 100 feet occur in a number of months over the southeastern United States, the Northeast, and the Maritime Provinces.

In the North Atlantic, thickness differences are generally small, except in the extreme northeastern part, where thicknesses near the United Kingdom decrease in practically all months, sometimes 100 feet or more.

In the Pacific, thickness differences are generally positive especially from June to November.

## 11. CONCLUSIONS

The 1947–1958 means at 700 mb. are based upon actual data that are superior to the data used in the 1952 normals. Significant differences from the earlier period as well as additional information come to light. Some of the differences appear to reflect compensation for errors in the earlier normals, while others seem to be more clearly linked to secular changes. The latter are manifested in couplets of contiguous positive and negative differences, which are dynamically compatible.

The new 12-year means more accurately reflect current modes of synoptic behavior, as shown in a separate study of the frequencies of 5-day mean Highs and Lows. When three more years of data, 1959–1961 have been added, it is planned to supplant the 1952 normals with a new set of long-period (15-year) means. This new set will be based on essentially hemisphere-wide post World War II upper-air data coverage and should more accurately reflect the long-period circulation.

595485—61——3

## ACKNOWLEDGMENT

The author is indebted to Messrs. Jerome Namias and William Klein for encouragement and helpful criticisms, and to Messrs. Raymond Green, Paul Stark, William Lockhart, Joseph Mangum, Frank Smallwood, and Mrs. Evelyn Boston for assistance in various phases of preparation of the charts.

## REFERENCES

1. U.S. Weather Bureau, "Normal Weather Charts for the Northern Hemisphere," *Technical Paper* No. 21, Washington, D.C. 1952.
2. W. H. Klein and J. S. Winston, "Geographical Frequency of Troughs and Ridges on Mean 700-mb. Charts," *Monthly Weather Review*, No. 86, No. 9, Sept. 1958, pp. 344–358.
3. World Meteorological Organization, *Technical Regulations*, Vol. 1, Chap. 8, Par. 8.4.2.5, 2d Edition, Geneva, 1959.
4. J. Namias, "The General Circulation of the Lower Troposphere over Arctic Regions and its Relation to the Circulation Elsewhere," pp. 45–61 of *Proceedings of the Polar Atmosphere Symposium, Oslo, July 2–8, 1957, Part I Meteorology Section*, Pergamon Press, London, 1958.
5. J. Namias, "Synoptic and Climatological Problems Associated with the General Circulation of the Arctic," *Transactions, American Geophysical Union*, vol. 39, No. 1, Feb. 1958, pp. 40–51.
6. R. J. Reed and B. A. Kunkel, "The Arctic Circulation in Summer," *Journal of Meteorology*, vol. 17, No. 5, Oct. 1960, pp. 489–506.
7. R. A. Bryson, J. F. Lahey, W. L. Somervell, Jr., and E. W. Wahl, "Normal 500 mb. Charts for the Northern Hemisphere," *Scientific Report*, No. 8, on Contract AF19(604)–992, Dept. of Meteorology, University of Wisconsin, Nov. 1957.
8. I. Jacobs, *5- and 40-Year Monthly Means of the Absolute Topographies of the 1000-mb., 850-mb., 500-mb., and 300-mb. Levels and of the Relative Topographies 500/1000 mb. and 300/500 mb. over the Northern Hemisphere and Their Month-to-Month Changes*, Institut für Meteorologie und Geophysik der Freien Universität Berlin, vols. I and II, Berlin, 1957 and 1958.
9. R. J. List (Editor), *Smithsonian Meteorological Tables*, 6th revised edition, The Smithsonian Institution, Washington D.C., 1951, 527 pp.
10. [D. E. Martin] "Anomalies in the Northern Hemisphere 700-mb. 5-Day Mean Circulation Patterns," *Air Weather Service Technical Report*, 105–100, Air Weather Service, 1953.
11. W. H. Klein, "The Weather and Circulation of May 1954—A Circulation Reversal Effected by a Retrogressive Anticyclone During an Index Cycle," *Monthly Weather Review*, vol. 82, No. 5, May 1954, pp. 123–130.

# Publications By Weather Bureau Authors

D. I. Blumenstock (with F. R. Fosberg and C. G. Johnson) "The Re-Survey of Typhoon Effects on Jaluit Atoll in the Marshall Islands," *Nature*, vol. 189, No. 4765, Feb. 25, 1961, pp. 618–620.

D. C. House and J. T. Lee, "A Case Study of Extreme Turbulence Possibilities Based on Considerations of Buoyancy and Horizontal Divergence," *Bulletin of the American Meteorological Society*, vol. 42, No. 3, Mar. 1961, pp. 175–184.

C. G. Knudson, "The New Weather Bureau Office in Rockefeller Center," *Weatherwise*, vol. 14, No. 2, Apr. 1961, pp. 43–46.

H. E. Landsberg, "Some Patterns of Rainfall in the North Central U.S.A.," *Archiv für Meteorologie, Geophysik und Bioklimatologie*, Serie B, Band 10, Heft 2, 1960, pp. 165–174.

H. E. Landsberg, "Review of 'Bioclimatologie Humaine de Saint-Luis de Senegal', by Jean-Paul Nicolas, *Memoires de l'Institut Francais d'Afrique Noire*, No. 57, Ifan-Dakar, 1959, 340 pp.," *Bulletin of the American Meteorological Society*, vol. 42, No. 3, Mar. 1961, pp. 222–223.

H. E. Landsberg, "Review of *Pflanze und Strahlung*, by F. Sauberer and O. Härtel, Leipzig, 1959, 268 pp.," *Bulletin of the American Meteorological Society*, vol. 42, No. 3, Mar. 1961, pp. 221–222.

D. K. Lilly, "Review of *Dynamics of Climate, The Proceedings of a Conference on the Application of Numerical Integration Techniques to the Problem of the General Circulation, held October 26–28, 1955*, Ed., R. L. Pfeffer, Pergamon Press, 1960, 137 pp.," *Bulletin of the American Meteorological Society*, vol. 42, No. 3, Mar. 1961, pp. 220–221.

J. K. McGuire, "History of the Weather Bureau Office in New York City," *Weatherwise*, vol. 14, No. 2, Apr. 1961, pp. 50–52, 71.

L. Machta, "Inverted Concentration Profiles from a Ground Source," *Journal of Meteorology*, vol. 18, No. 1, Feb. 1961, pp. 112–113.

L. Machta and R. J. List (with L.T. Alexander, R. H. Jordan, R. F. Dever, E. P. Hardy, Jr., and G. H. Hamada), *Strontium-90 on the Earth's Surface*, U.S. Atomic Energy Commission, Office of Technical Information, TID-6567, Feb. 1961.

H. Wexler, "Additional Comments on the Warming Trend at Little America, Antarctica," *Weather*, vol. XVI, No. 2, Feb. 1961, pp. 56–58.

H. Wexler, "Ice Budgets for Antarctica and Changes in Sea Level," *Journal of Glaciology*, vol. 3, No. 29, Mar. 1961, pp. 867–872.

J. S. Winston and L. Tourville, "Cloud Structure of an Occluded Cyclone over the Gulf of Alaska as Viewed by TIROS I," *Bulletin of the American Meteorological Society*, vol. 42, No. 3, Mar. 1961, pp. 151–165.

O. R. Wulf (with S. B. Nicholson), "The Diurnal Variation of K Indices of Geomagnetic Activity on Quiet Days in 1940–1948," *Journal of Geophysical Research*, vol. 66, No. 4, Apr. 1961, pp. 1139–1144.

# A SOUTHERN HEMISPHERE CASE STUDY WITH TIROS I DATA

LESTER F. HUBERT

Meteorological Satellite Laboratory, U.S. Weather Bureau, Washington, D.C.

[Manuscript received March 24, 1961; revised April 24, 1961]

## ABSTRACT

On April 28, 1960, TIROS I obtained pictures of an exceedingly sharp-edged cloud deck over the Pacific Ocean west of Chile, of cirrus associated with the jet stream on the west coast of South America, and of a mature cyclone in the central South Atlantic. Surface, upper-air, and cross section analyses are presented and compared with pictured cloud features.

Because of the wide spacing of the data, the locations of double jet streams had to be deduced by examining the horizontal temperature gradients associated with Northern Hemisphere jets and assuming that the same general relation holds in the Southern Hemisphere.

An operational surface analysis is shown to be inconsistent with the pictured data in the oceanic region where the analysis was based on a single ship report. A modification of the analysis is suggested to illustrate the potential of meteorological satellite data in data-sparse regions.

## 1. INTRODUCTION

TIROS I, the meteorological satellite launched on April 1, 1960, photographed interesting cloud patterns over many parts of the earth. From about mid-April until early May 1960 its camera orientation changed in such a manner that pictures of the Southern Hemisphere were obtained. Near the end of April some unusually interesting pictures showed what appeared to be cirrus clouds streaming off the eastern coast of Argentina. Cirrus patterns have been studied in relation to the jet stream in the Northern Hemisphere so these pictures provided an attractive case for comparison. In addition to the cirrus clouds were a sharp-edged cloud deck off the Pacific coast of South America and the classical spiral cloud pattern of a cyclone in the Atlantic east of South America. In order to examine the several interesting features of this sequence, upper-air and surface observations were obtained for a comparison between the standard meteorological data and the picture data.

The Director of the Argentina Servicio Meteorologico kindly furnished plotted and analyzed maps from their files along with some tabulated upper-air data. All observations so collected have been plotted and reanalyzed. There is little difference between the common features of the upper-air analysis furnished by the Argentina Meteorological Service and that shown here—the changes are mainly details added by incorporating the results of the cross-section analysis.

Two versions of the surface analysis are shown—the first is a copy of the operational analysis made by the Argentinian meteorologists (the oceanic portion of which is done on the basis of a single ship report), the second is modified on the basis of picture data. The purpose of the latter is to illustrate how satellite data provide invaluable information where no standard observations are available.

## 2. PICTURE DATA

Figures 1 through 6 are individual frames on which have been superimposed grids of latitude and longitude, while figure 7 is a schematic nephanalysis showing the major features. In the latter figure the picture outlines are shown with shading inside those boundaries to represent cloudiness. Inspection of the pictures will show that little can be seen near the horizon; consequently the useful part of each picture does not actually extend all the way to the horizon boundaries shown on figure 7. The various cloud patterns are described here briefly for comparison with the nephanalysis, but will be referred to again in more detail in connection with the meteorological analysis, and the analysis superimposed on the pictures will also be deferred to a later section.

Figure 1, viewing toward the western horizon, shows a sharp cloud edge in the Pacific 52° to 48° S. between a stratus deck and cumuliform clouds to the south. The sharp edge of the stratus in the left foreground is along the Andes Mountains, showing the western slopes cloudy and the eastern slopes clear. The breaks in the stratus deck near 40° S. in the Pacific correspond to the limb of the Pacific anticyclone.

Figure 2 shows a bright band across the middle of the picture which is probably cirrus and middle clouds. The stratus clouds on the west coast and the clear downslope area are again visible.

Figures 3 and 4 show the region with few scattered clouds from 40° to 50° W. longitude that is probably associated with a pressure ridge in the low troposphere.

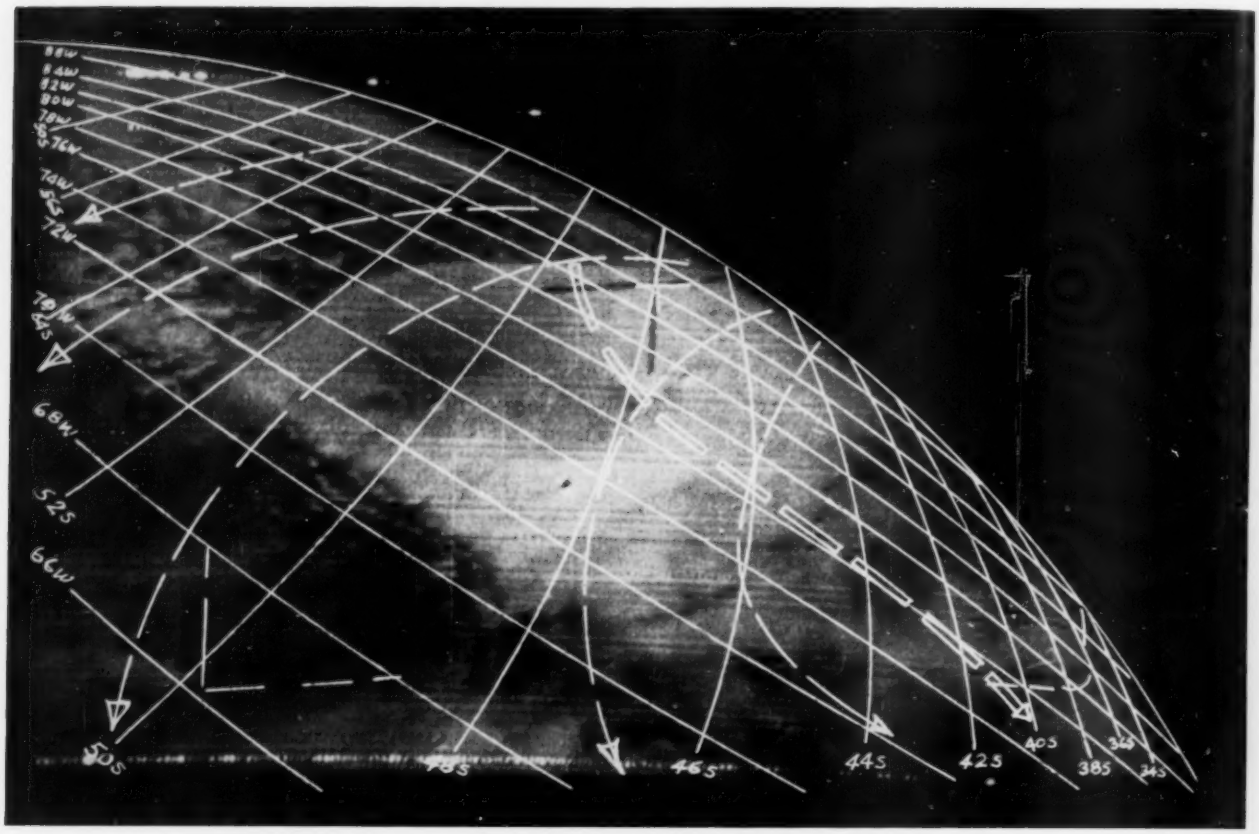


FIGURE 1.—TIROS picture toward the west from above Argentina. Superimposed broken lines are mean streamlines for 700–500-mb. layer; doubled broken line is jet stream axis. 1600 GMT, April 28, 1960.

Figure 5 is a view of the edge of the cyclone where a dry cool air mass has circulated toward the north around the center which is at 17° W.

Figure 6 is nicely centered on the cyclone and shows the dry air completely around the northern (equatorial) side of the cyclone. Of particular interest in this picture are the clouds standing above the lower cloud undercast, near the storm center. The shadows that appear along the eastern edge of each cloud make it clear that these are well above the lower cloud deck and have the appearance of cumulonimbus towers. However, since these elevated features are 30 to 60 miles long, they must represent a combination of cumulus towers and sheared-off cirrus nothus and perhaps some middle clouds.

## 3. METEOROLOGICAL ANALYSIS

One purpose of this investigation was to determine the location of the jet stream in the pictured area in order to associate it with the cloud features. Data for 1200 GMT April 28 and 29, 1960 were analyzed, but only analyses for April 28, corresponding to the picture time, are shown.

A space cross section approximately normal to the jet in the pictured area proved to be the critical analytical tool for this purpose. The section extended some 1500 n. mi. from northwest to southeast, but incorporated data from only three stations.

In order to estimate the proximity of the jet stream axis to a given station, the horizontal gradient of potential temperature in the various atmospheric layers was computed from 14 winter cases studied by Palmén and Newton [1] and for four autumn cases assembled for this study, all in the Northern Hemisphere. The latter limited sample was computed only for the purpose of estimating any differences that might exist between winter and autumn gradients near and beneath the jet—no claim for statistical significance is made.

The potential temperature gradients shown in figure 8 were derived as follows: temperature gradients (°C. per 60 n. mi.) for various pressure surfaces were measured

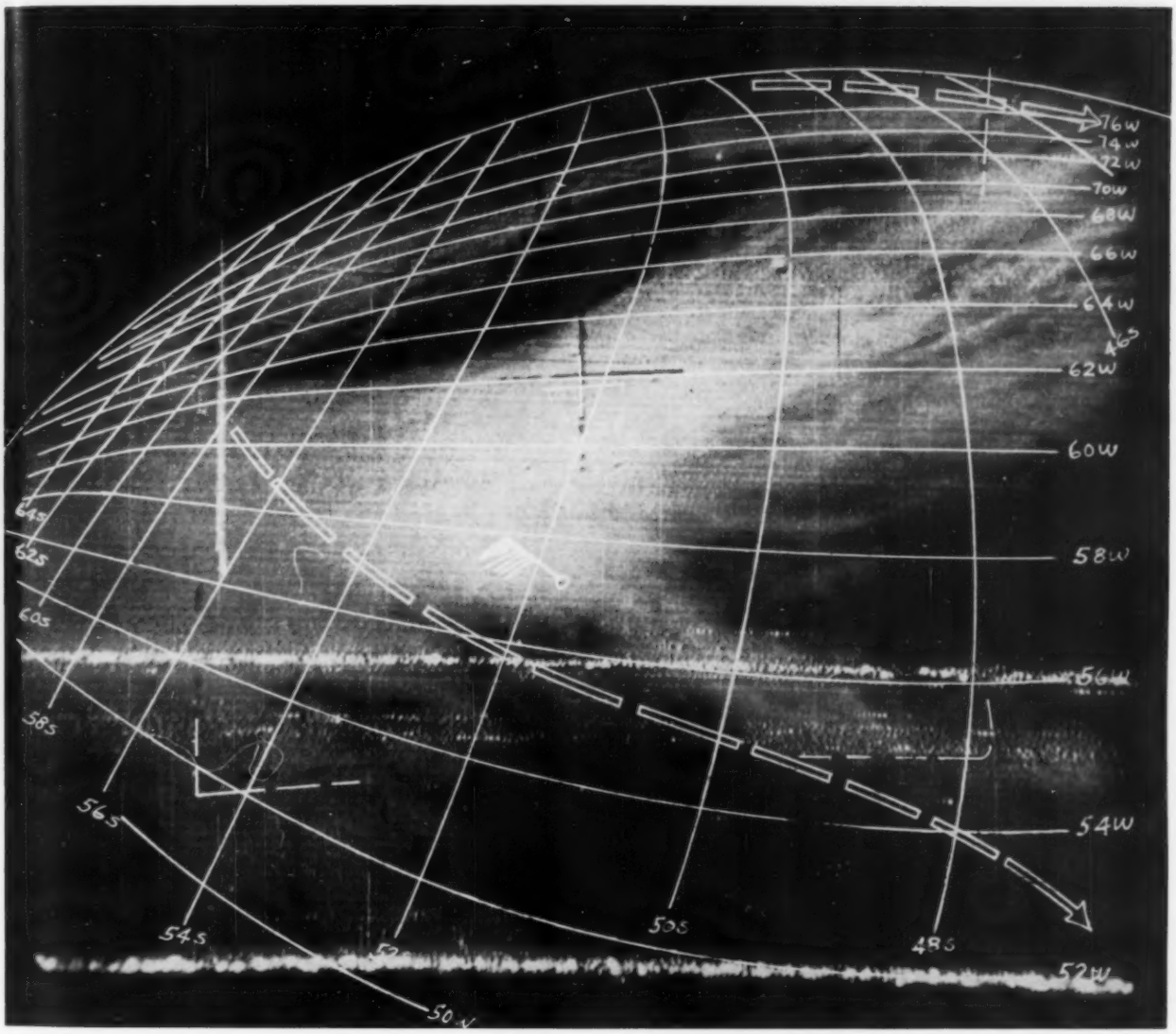


FIGURE 2.—TIROS picture over South Atlantic with South America on horizon. Doubled broken line represents jet stream axis; 200-mb. wind shown from Stanley, Falkland Islands. 1600 GMT, April 28, 1960.

from the mean cross sections of the Northern Hemisphere jets mentioned above. The potential temperature gradients were then approximated by application of equation (1):

$$\left(\frac{\partial\theta}{\partial n}\right)_p = \frac{\partial}{\partial n}\left[T\left(\frac{1000}{p}\right)^{\kappa}\right] = \frac{\theta}{T}\frac{\partial T}{\partial n} \qquad (1)$$

where the subscript $p$ means differentiation at constant pressure, $T$ is temperature, $\theta$ is potential temperature, $n$ is horizontal space coordinate parallel to the pressure gradient, $p$ is pressure in millibars, $\kappa$ is $R/c_p$, the universal gas constant $R$ divided by specific heat of air $c_p$.

Reference to figure 8 shows that the potential temperature gradient maximum is nearly 4° C. per 60 n. mi. The maximum gradient near 700 mb. for the winter cases and near 400 mb. for the autumn cases reflects the intense thermal gradient of frontal regions in the low troposphere during winter contrasted to the maximum gradient occurring high in the troposphere during the warmer season. The feature used here is the value of gradient 100

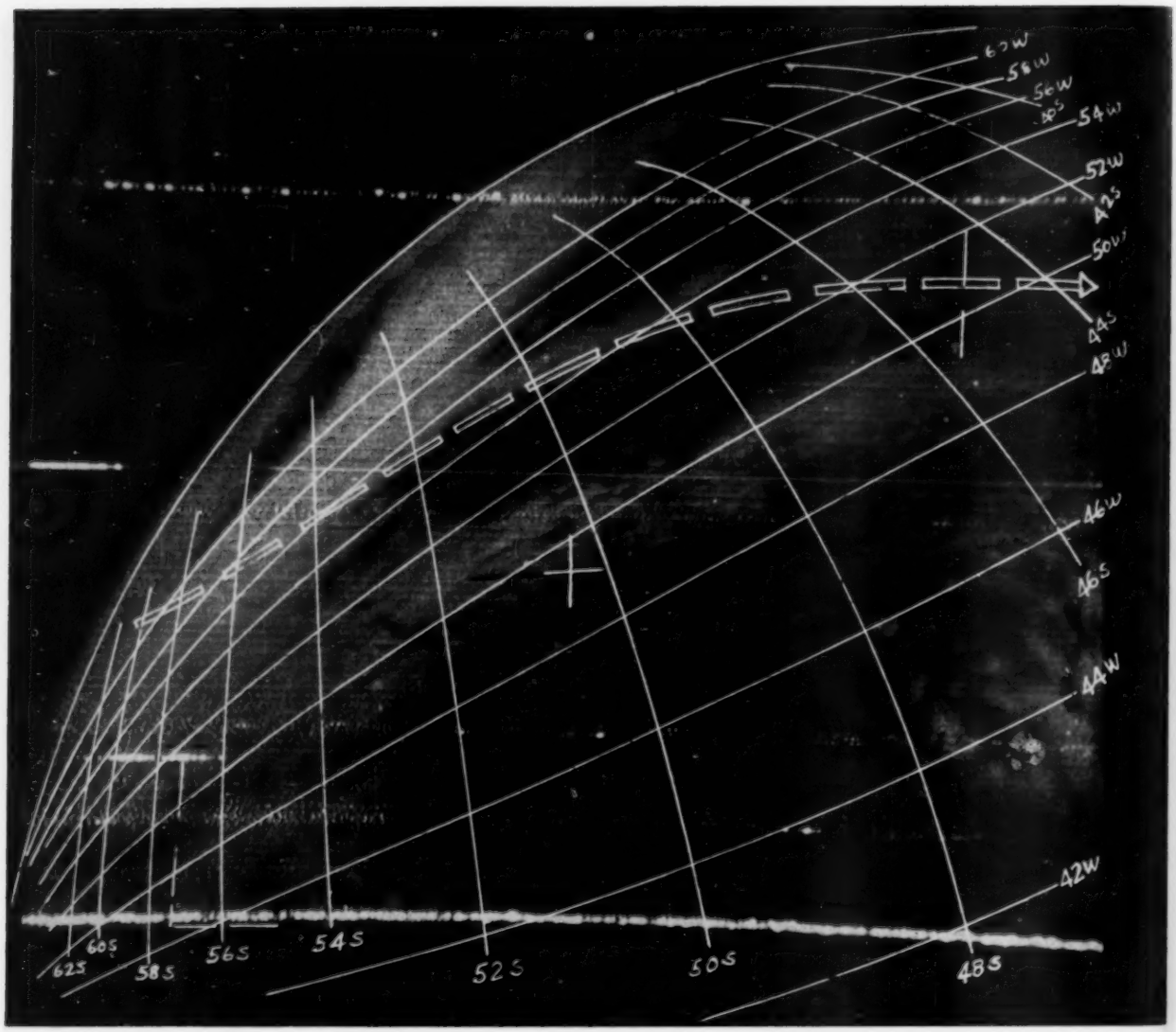


FIGURE 3.—TIROS picture of high pressure area in South Atlantic. Doubled broken line represents jet axis. 1600 GMT, April 28, 1960.

to 200 miles from the jet axis. In both autumn and winter the gradient of 2.0° C. per 60 n. mi. exists no more than 150 to 200 n. mi. from the jet axis and it is this fact that will be applied to the situation under investigation here.

Figure 9 is the space cross section for 1200 GMT April 28, 1960. The line of this section is shown on the 300-mb. map, figure 10, running from Puerto Montt, Chile (41.5° S., 72.8° W.), through Stanley, Falkland Islands (51.7° S., 57.9° W.), to the Naval Observatory at Orcadas, South Orkney Islands (60.7° S., 44.7° W.). The section is plotted with standard radiosonde and wind data. In addition the potential temperatures and potential temperature gradients are shown. The latter were computed by combining the thermal wind equation with equation (1) to give,

$$\frac{\Delta\theta}{\Delta n} \approx \frac{\theta f}{g} \frac{\Delta c}{\Delta z} \tag{2}$$

where $f$ is the Coriolis parameter, $g$ is the acceleration of gravity, and $\Delta c/\Delta z$ is the vertical wind shear.

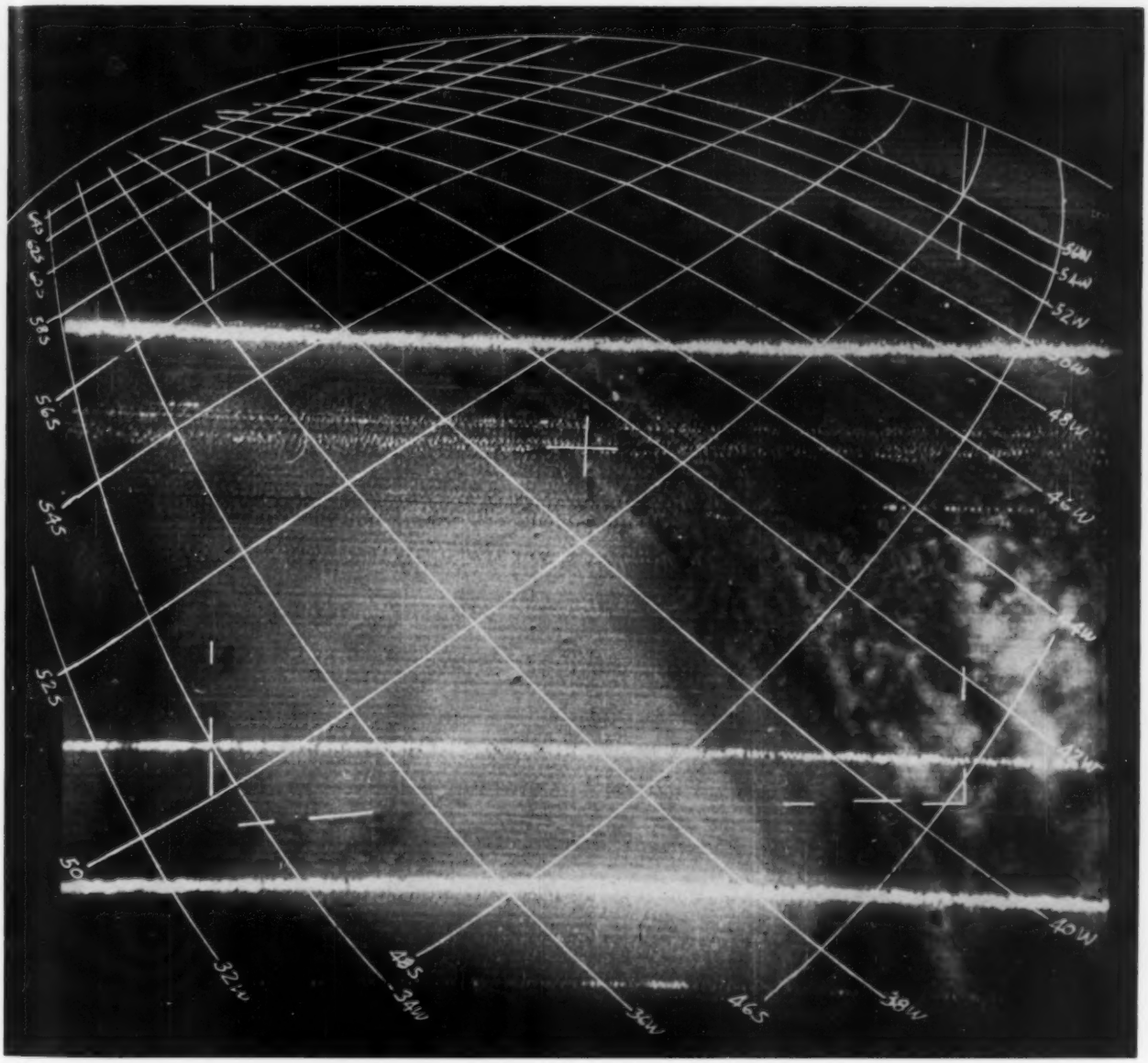


FIGURE 4.—TIROS picture showing transition area between high and low pressure areas in South Atlantic. 1600 GMT, April 28, 1960.

The vertical wind shear was computed for each atmospheric layer reported and the $\theta$-gradient was computed from equation (2) and plotted on the cross section in the same units as those used in figure 8.

Since the cross section is not strictly along the gradients or normal to the mean motion, and because of the probable existence of ageostrophic wind components, absolute consistency cannot be expected between the slope of the isentropes and the plotted gradients. Especially at the northern end of the section the shear vector and wind are not normal to the plane of the section. The analyzed slopes of the isentropes were made consistent with smaller values of $\Delta\theta/\Delta n$ (approximately 60 percent of the plotted values) in figure 9a.

In particular, shear in the layer 300 to 250 mb. over Puerto Montt implies a very large temperature gradient,*

*The gradient of 3.4° C. per 60 n. mi. immediately above a gradient of 0.5° C. per 60 n. mi. hints at an error in the wind report at 300 mb., but even if the two values are averaged, the mean value of 2.0 for the layer 400 to 250 mb. is good evidence for the implication made here.

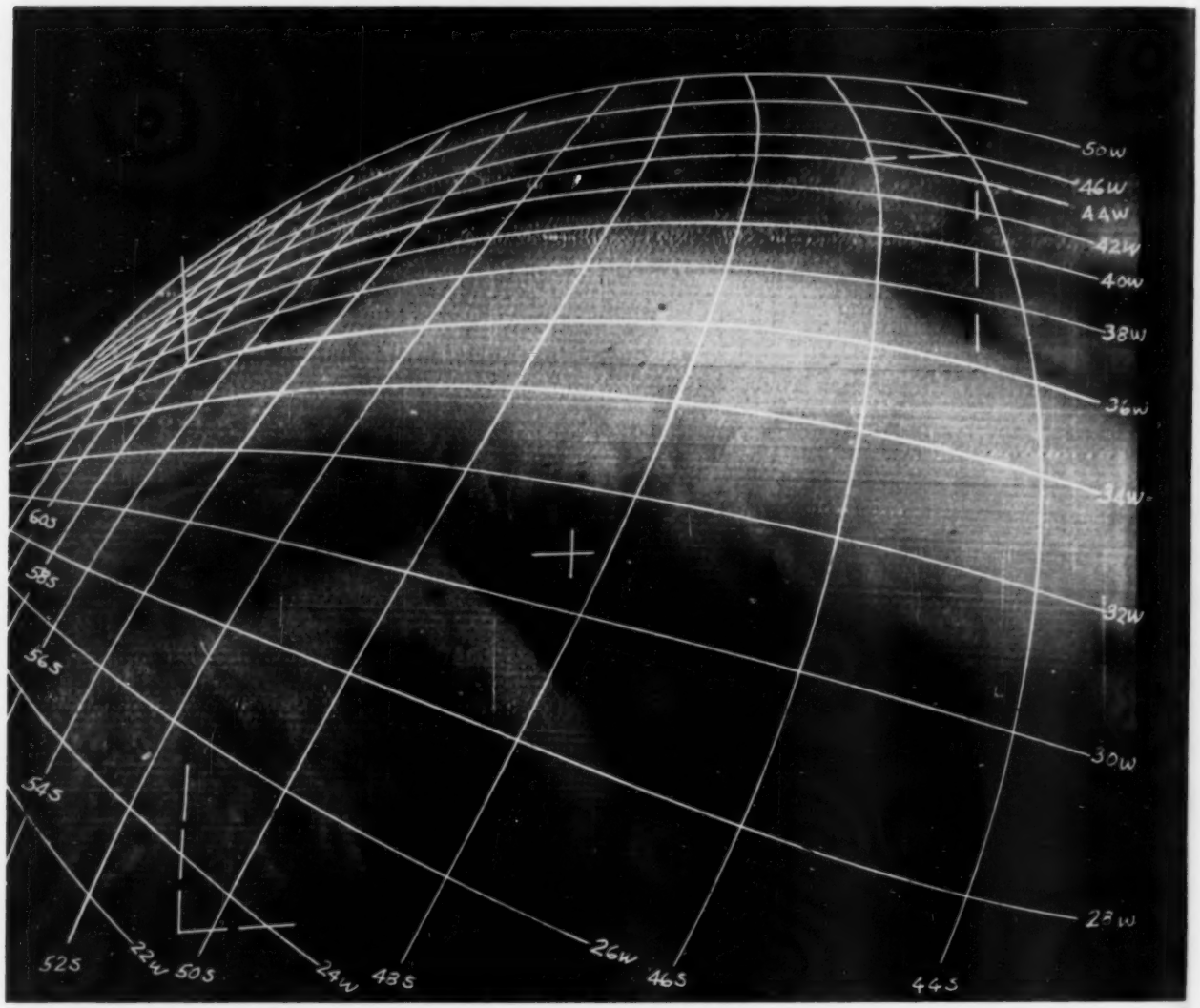


FIGURE 5.—TIROS picture showing curved cloud pattern at edge of cyclone in South Atlantic. 1600 GMT, April 28, 1960.

while the region between that station and Stanley must have a very small gradient in order to retain a reasonable pattern of isentropes. It therefore appears reasonable to postulate the existence of a jet axis northwest of Puerto Montt, and the large gradient indicates the jet axis is probably within 100 to 150 miles of the station. The data from Stanley also indicate a jet axis nearby probably within 150 miles to the southeast since the larger temperature gradients exist southeast of the station.

Figure 9b represents the same cross section but shows the isotach analysis along with lines representing the loci of maximum and minimum temperature gradients. In the low troposphere the maximum gradient is probably associated with a frontal surface and as such is shown sloping poleward. The maximum gradient near Puerto Montt, being high in the troposphere and quite similar to the jet stream gradient found at 400 mb. in figure 8b, may not be directly associated with a frontal surface.

Although it has not been included in the analysis of figure 9b, it appears that the isotach pattern between Stanley and Orcadas might have been more complex than shown here, with a primary speed maximum at the subtropical tropopause and a secondary maximum at about 350 mb., the level of the polar tropopause.

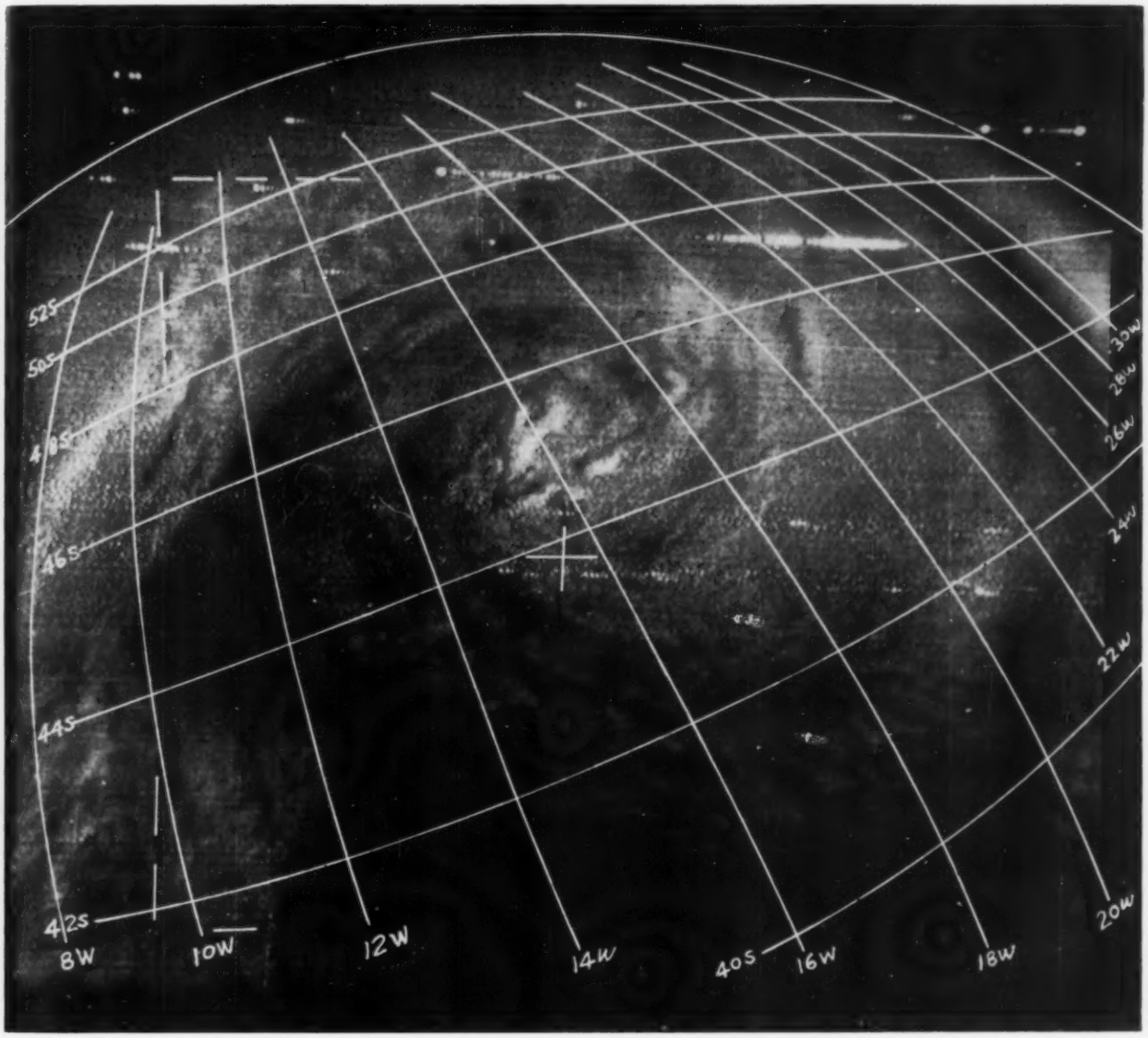


FIGURE 6.—TIROS picture showing cyclone centered at 17° W. in South Atlantic. 1600 GMT, April 28, 1960.

Figure 10 is the 300-mb. analysis for 1200 GMT April 28, 1960 on which the location of both jet axes is shown. Reference to the cross section will show that 300 mb. is not the level of maximum winds, but the general flow pattern for both jet axes is accurately represented by this level.

The closed Low was placed here because such a Low is a frequent feature of the upper flow when a double jet stream appears on Northern Hemisphere maps. The 70-kt. wind at Buenos Aires, 35° S., 59° W., lent credence to the existence of this northern jet axis, and the presence of the closed Low at this time was validated when it moved over that station 24 hours later, producing a wind of 10 kt. from the southwest.

Figure 11 shows three soundings plotted with radiosonde data also used on the cross sections. Both of the soundings over the Atlantic (Stanley and Orcadas) show relatively high moisture content to mid-troposphere, while the upper air over Puerto Montt is extremely dry and shows evidence of subsidence down to the 800-mb. level.

595485—61——4

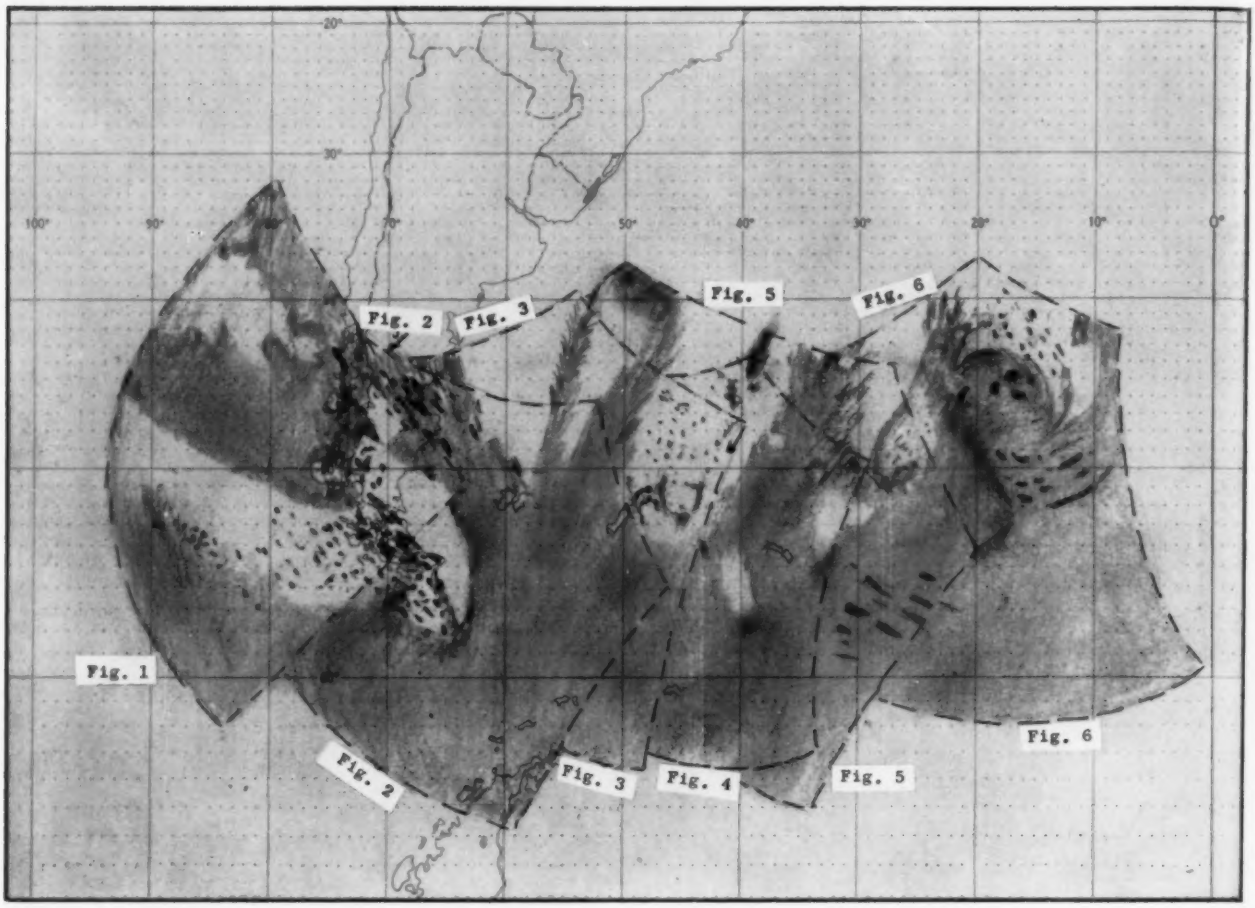


FIGURE 7.—Nephanalysis of clouds visible in TIROS pictures shown in figures 1–6. Broken outlines represent picture boundaries labeled with figures to which they refer.

Figure 12 shows a few of the surface data and analysis furnished by the Argentina Meteorological Service. Data from many continental stations have not been replotted for this illustration, but the isobaric analysis is an accurate copy of that made on April 28 in Argentina.

## 4. COMPARISON OF ANALYSES WITH PICTURE DATA

It is now possible to associate the analyzed details with the pictures. The overcast cloud deck off the west coast of Chile, shown in figure 1, is clearly below the 800-mb. level because the extreme dryness above that level at Puerto Montt could not support any cloudiness. The overcast deck that ends along the sharp line of figure 1 is a combination of fog and low stratus as shown by the data on figure 12, with the fog probably confined to the coast and the cool coastal waters. South of the 52d parallel in the Pacific the cloudiness is probably stratocumulus giving way to cumulus. The sharp division no doubt represents the boundary between two streams of air that had quite different trajectories—the warmer air from the Pacific anticyclone to the north had been stabilized as it moved over cool water, while the polar air from the south was being made unstable as it moved to lower latitudes. The stratus deck ends along the Andes Mountains in the foreground (along the 71st meridian).

Superimposed on figure 1 is the jet stream axis, representing the jet location at about 250 mb. and streamlines showing motion of the 700- to 500-mb. layer. If there were any high or middle clouds associated with the jet

axis, they are invisible against the lower stratus and fog. The lower troposphere streamlines are shown here because the clouds near the Andes at 48° to 50° S. were embedded in this layer. The "bridge" of tenuous clouds at 48.5° S., 69° W. appears to be cirrus streaming across the lower cloudless area. Conditions over the pictured area of South America were unfavorable for mountain waves to occur. The sounding at Puerto Montt shows no stability in the middle and upper troposphere [2]. Probably therefore, the small cloud rows at 50° S., 70° W., lying east of the Andes, *are not* wave-produced lenticular clouds.

Figure 2 shows both jet axes transferred from figure 10 and the 200-mb. wind report from Stanley. In the upper right, the cloud area (probably middle and high clouds) 48° to 46° S. appears to have a western edge near 72° W., that is, to the cyclonic shear side of the northern jet. The cloud bands in the pattern (e.g., at 64° W.) are transverse to the wind directions at jet levels. The transverse pattern seems continuous with the bright band across the picture center which in turn lies on the equatorward side of the high-latitude (southern) jet axis. A cloud band extending from 50° S., 56° W. to 46° S., 54° W. was along the jet axis. Because of the possible error in fitting these grids to the pictures, the position of the jet axis shown here relative to this cloud band may be somewhat in error. However, this feature has the same location on an adjacent picture (not shown) and is estimated to be correctly placed within 60 to 100 miles. In any event, the main band and the finer-scale streamers are very near the jet axis, parallel to it, and probably on the equatorial side, as shown. The dark area just to the east is almost cloudless. This is associated, in the low troposphere, with a high pressure ridge containing few clouds, while at high levels there may be descent associated with the jet.

The clear area centered at 53° S., 66° W. is in the lee of the South American continent and may reflect downward motion on the lee side of the continent.

Figures 3, showing the jet axis nearer the horizon, displays more of the cloud pattern on the cyclonic shear side of the high-latitude jet. The difficulties in obtaining exact consistency between locations of the same cloud features on two different pictures are evident here when small features are compared with figure 2. Nevertheless the band of clouds and the clear areas associated with the jet axis are probably located with an accuracy of 60–100 miles and more of the general pattern near the jet can be seen. The cumuliform clouds near 47° S., 43° W. mark the transition from the high pressure ridge to the cyclone, in the low troposphere—features that are discussed below in connection with the surface analysis.

Figures 4, 5, and 6 show clouds, associated with the cyclone, which no doubt are both low and middle clouds as well as cirrus. These pictures will be used to modify the surface analysis of figure 12.

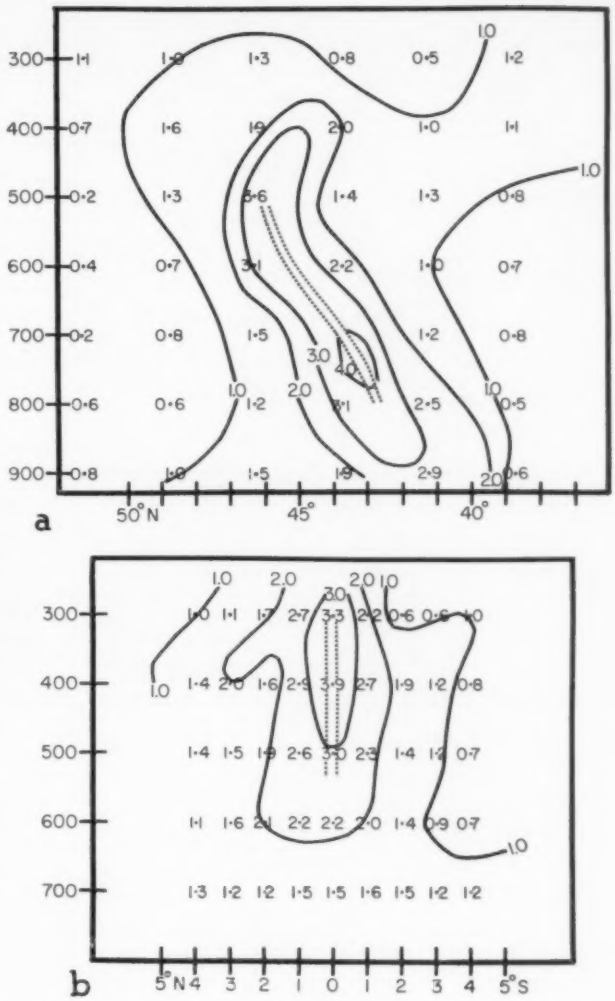


FIGURE 8.—Potential temperature gradients (°C. per 60 n. mi.) for Northern Hemisphere. Doubled broken line shows position of maximum gradient. (a) For 12 winter cases, (b) for 4 autumn cases; abscissa labeled in degrees of latitude north and south of jet axis.

## 5. MODIFICATION OF SURFACE ANALYSIS WITH PICTURE DATA

Comparison of the nephanalysis, figure 7, with the surface analysis, figure 12, shows that the low pressure area at 41° W. corresponds to the area covered with scattered to a few cumuliform clouds. While the Argentine analysis does not extend to 17° W., it does not seem reasonable that cyclones existed at both 41° W. and 17° W., with one showing the classical cyclonic spiral pattern and the other largely cloud-free. The surface cyclone was undoubtedly placed as shown in figure 12 on the basis of

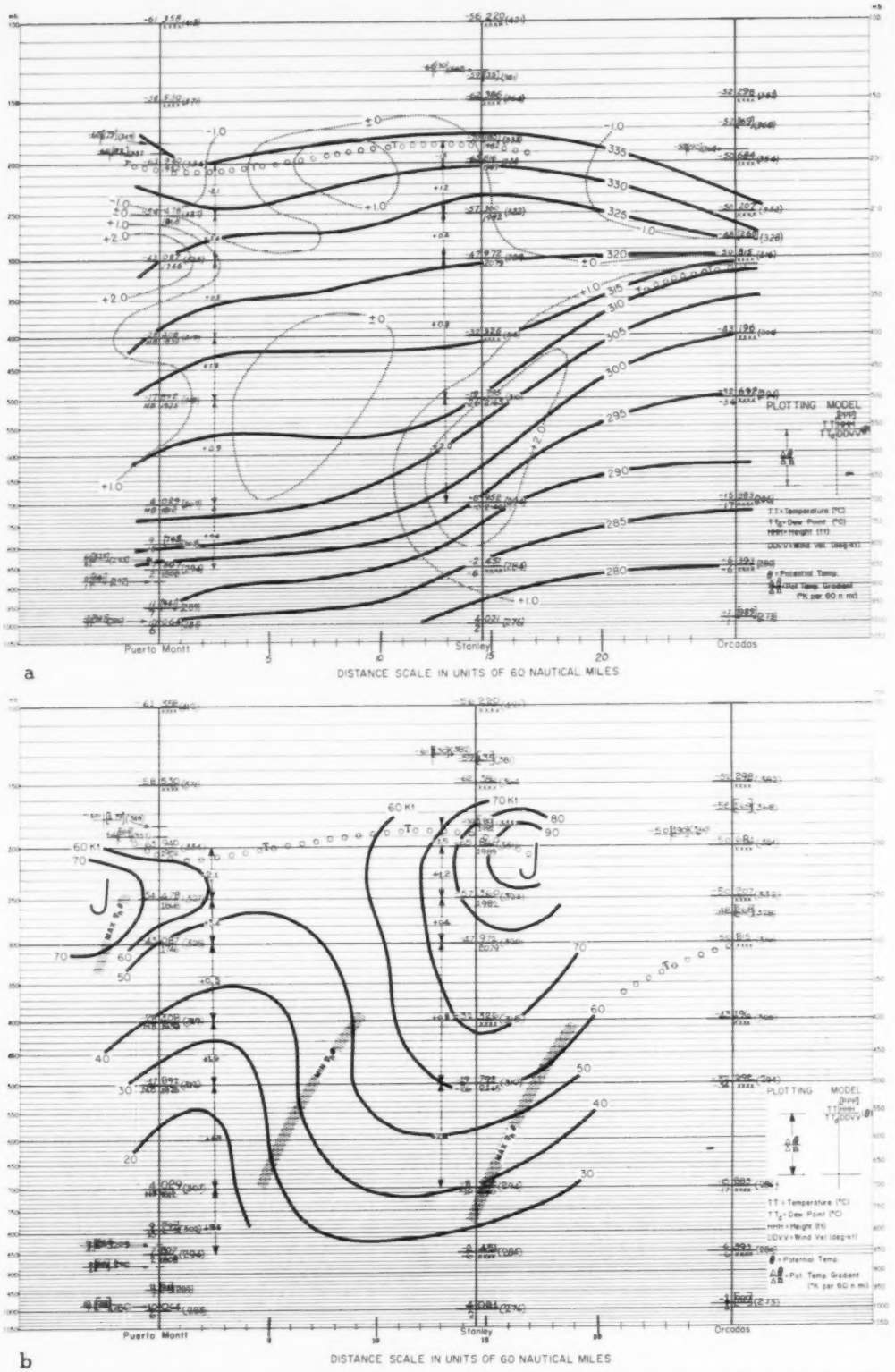


FIGURE 9.—Space cross sections for 1200 GMT, April 28, 1960; (a) showing isentropes (solid lines) and isopleths of $\Delta\theta/\Delta n$ (°C. per 60 n. mi., broken lines), and (b) showing axes of minimum and maximum temperature gradient (stippled lines) and isotachs (solid lines). Large "J" indicates best estimate of jet core location.

FIGURE 10.—300-mb. chart for 1200 GMT, April 28, 1960.

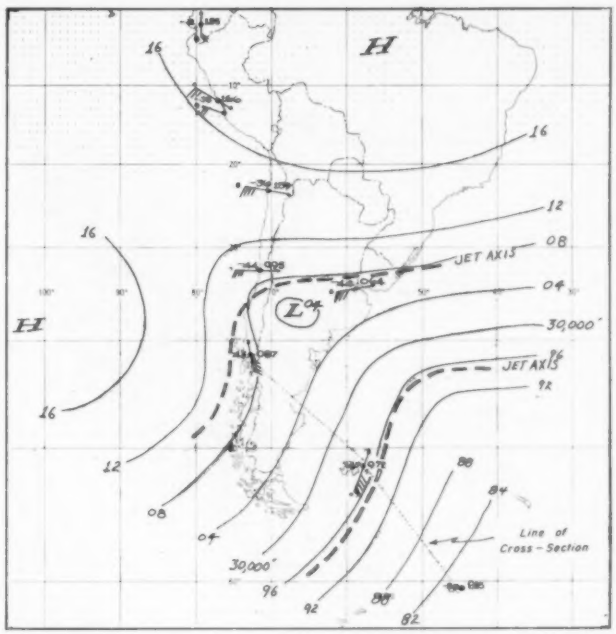


FIGURE 11.—Soundings for the three stations used in cross section (fig. 9). 1200 GMT, April 28, 1960.

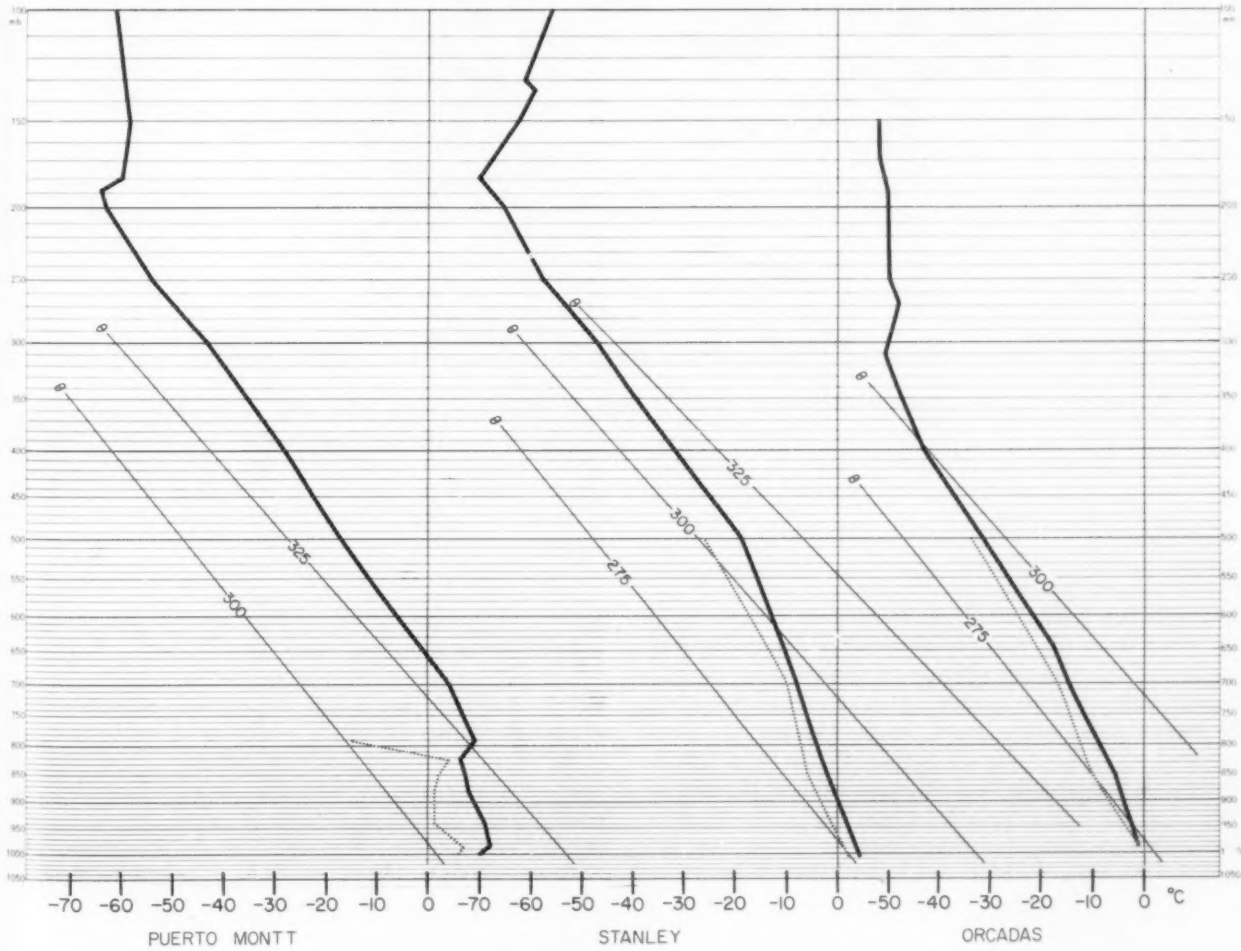

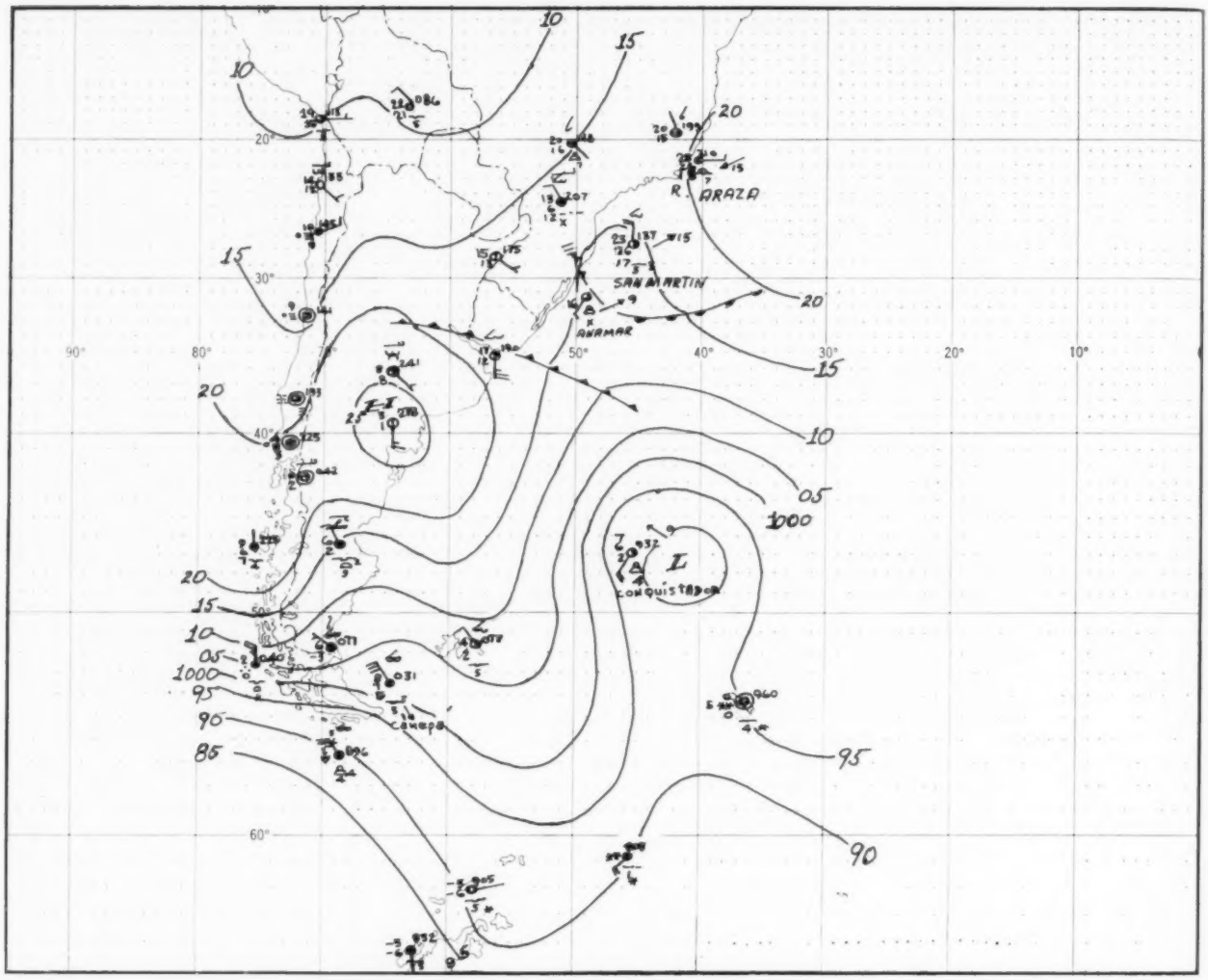


FIGURE 12.—Copy of surface data and analysis made by Argentina Meteorological Service. 1200 GMT, April 28, 1960.

the single ship report at 47° S., 45° W. In the absence of any other data the position of the Low seems entirely reasonable, but with the addition of picture data, the ship pressure appears questionable. Once doubt is thrown on the report, the analyst must decide whether the cloud type and wind speed are consistent with a deep Low so nearby. It appeared to this writer, in light of the picture data, that the ship pressure, and perhaps even the wind observation, or else the ship position, were in error. The picture data were therefore used as a basis to reanalyze the oceanic portion of the surface chart. The modified analysis is shown in figure 13.

First, the ridge line that lies on the east coast at 60° W. was extended into the zone of scattered cumuliform clouds at 50° S., 45° W. Second, an occluded cyclone (fig. 6) was located at 45° S., 17° W. That this cyclone was in the mature stage is inferred from the fact that the dry (cold) air had apparently circulated completely around the north (equatorial) side of the center and was producing a

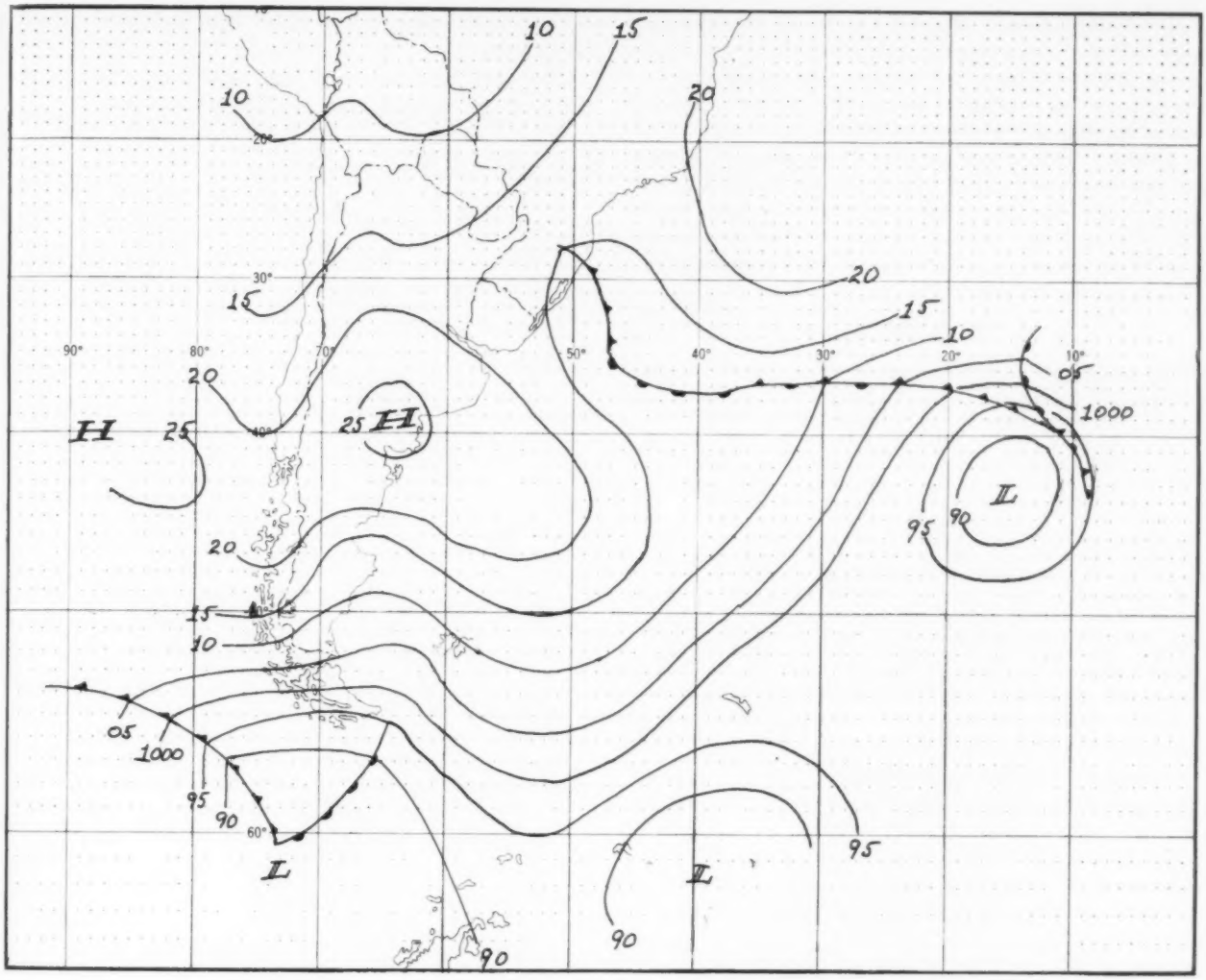


FIGURE 13.—Modification of figure 12 by use of TIROS pictures.

scattered to cloudless projection toward the center from the northeast.

Third, fog and stratus down to 52° S. along the west coast of South America indicate no front or cyclone in that immediate vicinity, but the sharp line marking the edge of the stable air implies it is a line between air masses of significantly different trajectory, and for that reason the pressure pattern southwest of South America is suggested. This portion of the analysis is of course completely outside any meteorological or picture data available at this writing and is thus little more than speculation. The cyclone in the Atlantic is, however, located with a high degree of confidence as is the ridge line extending southeastward from the continent.

## 6. CONCLUSIONS

This case study illustrates:

(1) The cloud patterns associated with cyclones and fronts are of a sufficient scale and simplicity to enable meteorologists to extract much valuable diagnostic data from satellite pictures.

(2) Cloud patterns associated with jet streams (and perhaps many other synoptic models of the upper atmosphere) are so varied and complex, that much more research must be completed before the meteorologist can exploit satellite pictures by themselves for location of the jet stream. This is true partly because the fine detail of patterns near the jet that have been documented by surface and airplane photographs are largely invisible on the currently available satellite pictures. The investigation of jet cloud patterns for satellite use must concentrate on the larger-scale distribution.

## ACKNOWLEDGMENT

The computation of the locator grids for the TIROS pictures illustrates one of the essential support functions of the Computation Section of the Meteorological Satellite Laboratory.

The work on this study has been supported by the National Aeronautics and Space Administration.

## REFERENCES

1. E. Palmén, and C. W. Newton, "A Study of the Mean Wind and Temperature Distribution in the Vicinity of the Polar Front in Winter," *Journal of Meteorology*, vol. 5, No. 5, Oct. 1948, pp. 220–226.
2. M. A. Alaka, "Aviation Aspects of Mountain Waves," World Meteorological Organization, *Technical Note No. 18*, WMO-No. 68, TP. 26, 1958, 48 pp.

# FORECASTING PRECIPITATION WITH THE AID OF A HIGH-SPEED ELECTRONIC COMPUTER

JOSEPH VEDERMAN

U.S. Weather Bureau, Honolulu, Hawaii*

[Manuscript received November 18, 1960; revised March 31, 1961]

## ABSTRACT

A high-speed electronic computer has been programmed to prepare cloud and precipitation forecasts for the Northern Hemisphere. The basic input data are derived from the Joint Numerical Weather Prediction Unit's two-level operational model of the atmosphere. The computer predicts cloudiness, rain, snow, and amounts of precipitation. Examples of computer forecasts are given and compared with observations.

## 1. INTRODUCTION

For the past five years the Joint Numerical Weather Prediction (JNWP) Unit at Suitland, Md., has been issuing upper-air forecasts based on the solution of the dynamic equations governing the large-scale flow of the atmosphere. Recently Carlstead [2] initiated experiments to see if useful forecasts of clouds and precipitation could be made based on the solution of the vorticity equation, the thermodynamic energy equation, and the continuity equations for air and moisture.

Since about 250 cloud and precipitation forecasts have now (June 1960) been made, it may be interesting to examine some of the results and to discuss some of the problems encountered. All the forecasts were made with the IBM 704 high-speed electronic computer.

## 2. THE BASIC EQUATIONS

The clouds and precipitation forecasting scheme makes use of the 500-mb. flow, the 1000–500-mb. thickness, and the vertical velocity derived from JNWP's operational 2-level forecasts. The equations governing the 2-level model of the atmosphere have been discussed by several authors, for example, 'Arnason and Carstensen [1]. For the sake of completeness, the equations are repeated here (though not in the explicit form used in calculations):

$$\frac{\partial \bar{\eta}}{\partial t}+\bar{\mathbf{V}}\cdot\nabla\bar{\eta}-K\frac{\partial \psi_5}{\partial t}=0 \tag{1}$$

$$\frac{\partial \eta'}{\partial t}+\mathbf{V}'\cdot\nabla\bar{\eta}+\bar{\mathbf{V}}\cdot\nabla\eta'=\frac{\bar{\eta}\omega}{P} \tag{2}$$

$$\sigma\nabla^2\omega-\frac{2f_0\omega}{P^2}=\frac{2f_0}{P}[\nabla^2(\bar{\mathbf{V}}\cdot\nabla\psi')-\bar{\mathbf{V}}\cdot\nabla\zeta'-\mathbf{V}'\cdot\nabla\bar{\eta}] \tag{3}$$

where $\mathbf{V}$ is the vector wind velocity, $\psi_5$ is the stream function at 500 mb., $P=500$ mb., $\sigma$ is a measure of the static stability, $\omega$ is the large-scale individual change of pressure with time, $\eta$ is the absolute vorticity, $\zeta$ is the relative vorticity, and the bar and prime superscripts refer to the mean and half the difference, respectively, between 500-mb. and 1000-mb. values of the various quantities.

However, these equations do not take into account the moisture charge of the atmosphere and so a fourth equation (see Carlstead's [2] equation (2)) is added in the form

$$\frac{\partial T_s}{\partial t}=-\mathbf{V}\cdot\nabla T_s+\gamma W \tag{4}$$

where $T_s$ is the "spread", the difference between the temperature and the dewpoint; $\gamma=-8°$ C./km., the dry adiabatic rate of change of dewpoint depression; and $W$ is the total vertical velocity taken to be $W=w+w_m$, where $w$ is the large-scale vertical velocity in cm. sec.$^{-1}$ derived from the routine 2-level forecast and $w_m$ is the vertical velocity due to the flow of air over mountains.

## 3. VERTICAL VELOCITY FORECASTS

The solution of equation (3) by the IBM 704 computer yields values of the vertical velocity associated with the large-scale features of the atmosphere. Small-scale vertical motions, such as those in thunderstorms, are excluded. The flow of air over mountains is another source of vertical motion in the atmosphere, and we have taken it into account by means of the relationship

*Most of the work on this paper was completed while the author was assigned to the Joint Numerical Weather Prediction Unit, U.S. Weather Bureau, Washington, D.C.

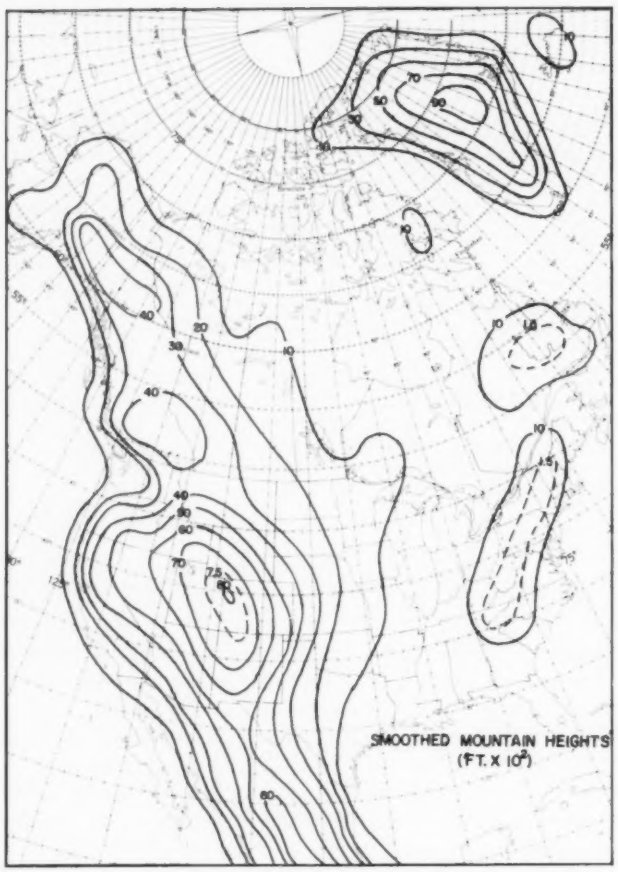


FIGURE 1.—Smoothed contour map of North America (in hundreds of feet).

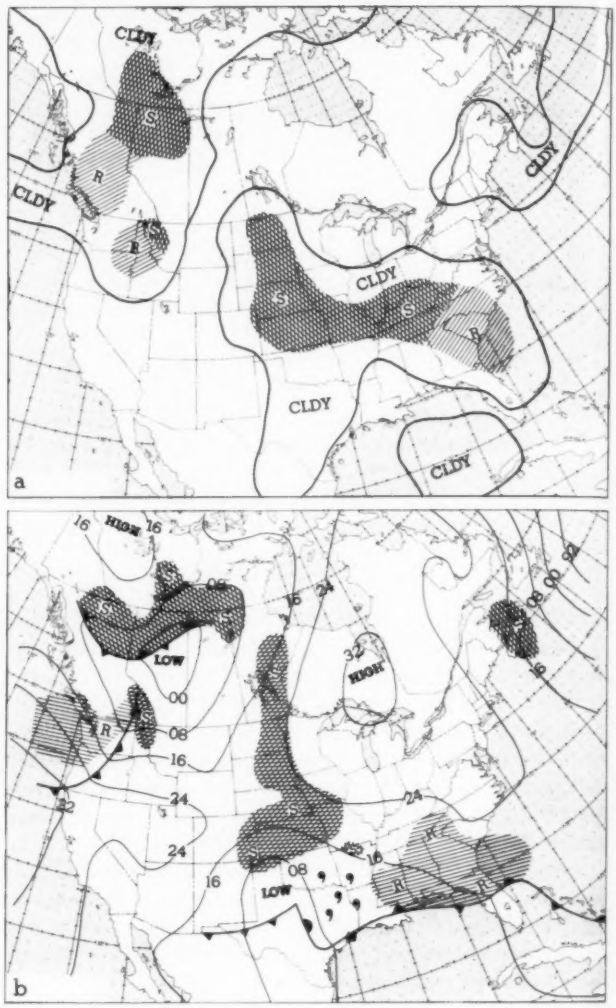


FIGURE 2.—1200 GMT, March 15, 1960. (a) 24-hour forecast of clouds and precipitation; (b) observed sea level pressure and precipitation patterns. R=rain, S=snow.

$$w_m = \mathbf{V}_g \cdot \nabla h \left(\frac{700}{p_g}\right)^{2.5} \tag{5}$$

where $w_m$ is the mountain-produced vertical velocity in cm. sec.$^{-1}$, $\mathbf{V}_g$ is the wind (cm. sec.$^{-1}$) near the ground, $p_g$ is the pressure (mb.) at ground level in the standard atmosphere, and $\nabla h$ is the slope of the ground.

The factor $(700/p_g)^{2.5}$ transforms the vertical velocity at ground level to that at 700 mb. The 700-mb. vertical velocity is assumed to be representative of that in the 1000–500-mb. layer. Estoque [5] suggested the use of the factor $(700/p_g)^{2.5}$, but its theoretical and empirical bases are slight.

The computation of $w_m$ from the right side of equation (5) implies a knowledge of the topography of the Northern Hemisphere. We have made use of a simplified, or smoothed, contour map of the Northern Hemisphere, the North American section of which is shown in figure 1. If this figure is compared with an actual contour map of North America it will be seen that the actual contours bear only the crudest resemblance to those portrayed in figure 1. From this it follows that the numerical clouds and precipitation forecasts in mountain regions can hardly be expected to show the small-scale features characteristic of rough terrain.

## 4. CLOUDS AND PRECIPITATION FORECASTS

After the fields of wind and vertical motion are predicted, equation (4) is solved and the field of moisture is predicted for periods up to 36 hours in advance. In earlier experiments $T_s$ was taken to be the temperature-dewpoint spread at 700 mb. But as that gave unsatisfactory results, it was decided to take the average of the 700-mb. and

850-mb. spreads to represent the moisture in the 1000-mb. to 500-mb. layer. The quantity $\nabla T_s$, equation (4), is determined initially from an analysis of the moisture field. The 700-mb. wind field $\mathbf{V}$ is determined by interpolating between the 850-mb. and 500-mb. winds, both of which are available at hourly intervals from the routine 2-level forecasts.

The weather forecast is derived from an empirical relation, due to Lewis [7], connecting cloudiness and precipitation with vertical velocity and the temperature-dewpoint spread. This relationship, in the form of a table, is stored in the computer's memory.

From the computed values of the vertical velocity, the temperature-dewpoint spread, and Lewis' table, the computer specifies the amount of middle clouds and the occurrence of precipitation at each of the 1977 grid points on the Northern Hemisphere at 1-hour intervals. Figure 2 shows the 24-hour machine forecast of the weather for 1200 GMT, March 15, 1960, together with the observed weather map. The forecast was successful in some regions but failed in others. The snow area (S) from Kansas northward was well predicted, and so was the line separating rain (R) from snow in southeastern United States. But the observed drizzle area centered over eastern Texas was missed completely.

Because the moisture parameter used depends only on the 850- and 700-mb. spreads, the computer cannot predict the occurrence of drizzle and fog, which are associated with lower-level moisture, or cirrus clouds, which are associated with moisture near the 300-mb. to 200-mb. levels.

Another feature of figure 2 deserves mention: the distinction between rain and snow in the forecast. Studies by Wagner [12] and Lamb [6] have shown that the type of precipitation, rain or snow, is highly correlated with the thickness of the 1000-mb. to 500-mb. layer at the time precipitation is occurring. To their statistics data were added from several stationary ships in the Atlantic and Pacific Oceans and from land stations in Alaska and Canada. Then figure 3, showing isolines of equal probability of rain and snow, was prepared and stored in the computer's memory.

When precipitation is predicted, the computer, in effect, refers to figure 3 to determine the type of precipitation. If, at a given point, precipitation is predicted and the thickness is equal to or greater than the value shown on figure 3, the computer prints out R (for rain); if less, it prints out S (for snow).

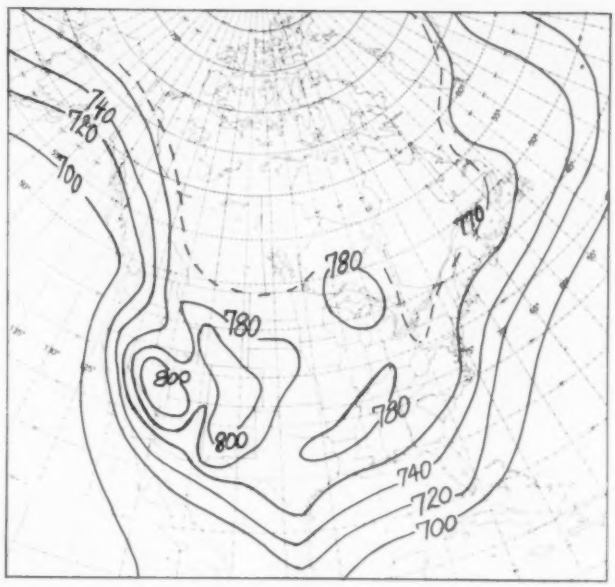


FIGURE 3.—Critical thickness (1000–500 mb.) which determines type of precipitation forecast. Thickness equal to or greater than value shown indicates rain forecast for that point; lesser thickness indicates snow forecast. (780 = 17,800 ft., etc.)

## 5. QUANTITATIVE PRECIPITATION FORECASTING

For some purposes, flood forecasting for example, it is desirable to know the amount of precipitation to expect in the forecast period. To explore the applicability of computer techniques to the solution of the quantitative precipitation forecasting problem we proceeded along the lines suggested by Smagorinsky and Collins [10].

The rate $R$ at which precipitation reaches the ground is

$$R=\int\frac{dr}{\rho_w g dt}\,dp\approx\int_{1000}^{500}\frac{dr}{\rho_w g dt}\,dp$$

where $p$ is pressure, $t$ is time, $r$ is the humidity mixing ratio, and $\rho_w$ is the density of liquid water. The integral should be taken through the entire depth of the atmosphere, but for many practical purposes the result is close enough if the moisture charge in the 1000–500-mb. layer only is considered. The amount of precipitation $A$ accumulated over a time $\Delta t$ is

$$A=\int_0^{\Delta t}R dt\approx\int_0^{\Delta t}\int_{1000}^{500}\frac{dr}{\rho_w g dt}\,dp dt$$

or

$$A\approx\int_0^{\Delta t}\int_{r_{1000}}^{r_{500}}\frac{\omega}{\rho_w g}\,dr dt\approx\frac{\omega}{\rho_w g}\,\Delta r\Delta t \qquad (6)$$

By the time the computer reaches the stage where it is required to produce the quantitative precipitation forecast it already has stored in its memory the hourly values of the vertical velocity, the spread, and thickness at each of the 1977 grid points. The computer now examines each point to see if precipitation has been predicted. If so, it converts the thickness (or mean temperature) to the appropriate saturation mixing ratio, solves equation (6) for $A$, and stores the hourly amount of precipitation for each grid point. The process is repeated for each hour. Finally, the computer adds the amounts and prints out the total precipitation for 12, 24, and 36 hours.

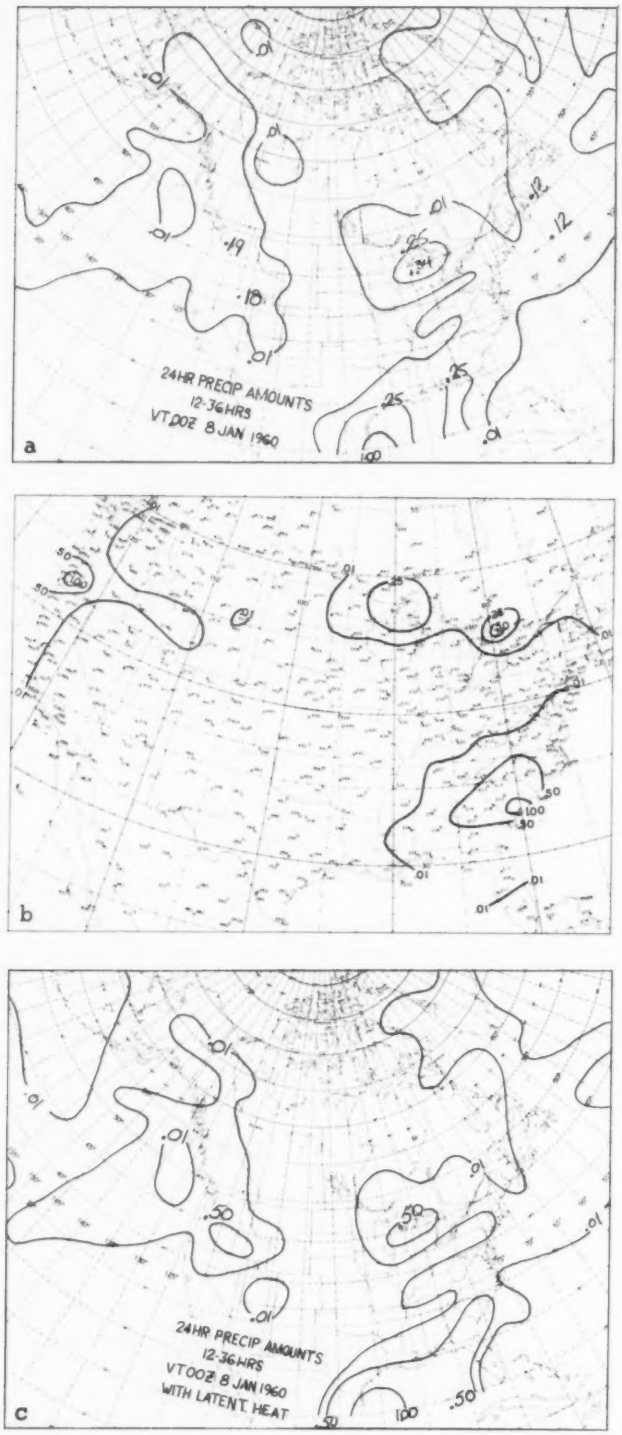


FIGURE 4.—0000 GMT, January 8, 1960. (a) 24-hour quantitative precipitation forecast (inches); (b) observed 24-hour precipitation; (c) 24-hour quantitative precipitation forecast with latent heat included in formula.

Figure 4a shows a 24-hour quantitative precipitation forecast for the period ending 0000 GMT, January 8, 1960. The forecast covers the period from 12 to 36 hours after the time of the data on which the forecast was based. Before comparing the observed precipitation (fig. 4b) with the forecasted, it may be better to discuss the problem of latent heat. Most investigators in the field of quantitative precipitation forecasting have found that current atmospheric models are incapable of predicting enough precipitation. Smagorinsky [9] has demonstrated that this results from the failure to take into account the release of the latent heat of vaporization. Following a suggestion by Smebye [11], the influence of latent heat was approximated.

The essence of Smebye's method is this. First, compute the vertical velocity by the solution of equation (3) and the precipitation amount—a first approximation. Then compute the amount of heat released by the precipitation. This leads to a correction to the vertical velocity, and in turn, results in an additional amount of precipitation. (The released heat is not allowed to change the flow pattern, which it most likely does.)

Figure 4c shows the predicted 24-hour precipitation amount, taking into account the release of latent heat, for 0000 GMT, January 8, 1960. Comparing figure 4c with 4b, one notices, first, that the precipitation forecast for eastern Texas was a complete failure. Over the remainder of the United States there is a fair correspondence between the forecasted and observed precipitation. Considerably more precipitation is predicted when latent heat is taken into account (fig. 4c) than when it is omitted (fig. 4a).

A rough comparison of forecasts made with and without the latent heat effect indicated that the maximum amount of precipitation predicted was about three times greater if the latent heat effect was included. This is in agreement with Manabe [8] who found that, while the ratio of vertical speed in a moist adiabatic atmosphere to that in a dry adiabatic atmosphere is variable, in middle latitudes it usually has a value ranging from 2 to 5.

On further comparison of figure 4b with 4c one finds that the predicted half-inch line in western Oregon is observed in eastern Oregon and Idaho. This is a characteristic error of the model. The use of smoothed mountains leads to predictions of precipitation farther inland than actually observed.

To summarize, this is how the computer makes a quantitative precipitation forecast:

1. Determines, for each of the 1977 grid points, if precipitation is predicted. If no, the process stops. If yes,
2. Notes the 1000–500-mb. thickness value and the total vertical velocity.
3. Reads a table that gives the amount of precipitation per hour as a function of thickness and vertical velocity.

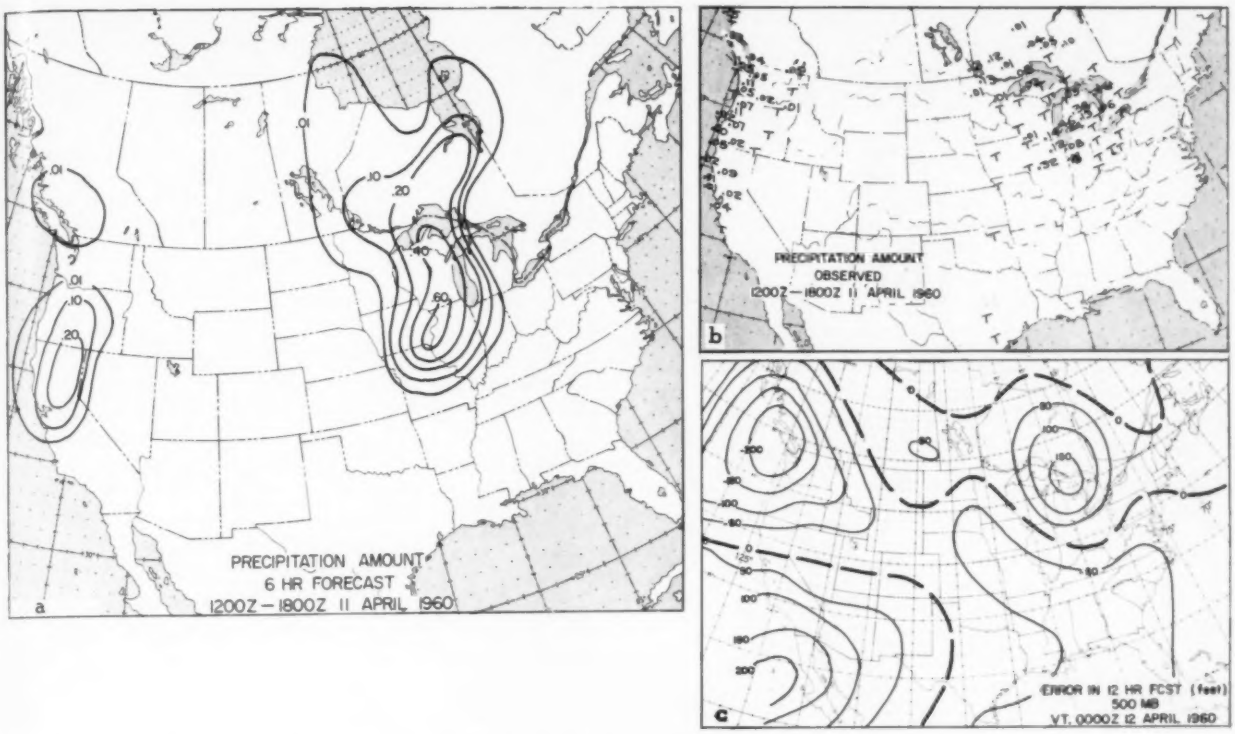


FIGURE 5.—Precipitation 1200–1800 GMT, April 11, 1960. (a) Forecasted; (b) observed. (c) Error in 12-hour 500-mb. forecast (ft.) for 0000 GMT, April 12, 1960 (forecasted minus observed).

4. Stores the hourly precipitation amount for each point.
5. Corrects the vertical velocity by an amount depending on the quantity of heat released by the precipitation.
6. Reads the table again, using the corrected vertical velocity.
7. Stores the new hourly precipitation amount in place of the old.
8. Repeats the process for each hour.
9. Adds the precipitation amounts.
10. Prints the total 12-, 24-, and 36-hour precipitation amounts for each grid point.

## 6. TESTING THE MODEL

Suppose the computer had made a perfect forecast of the 500-mb. flow pattern and the thickness field, would the model give a perfect precipitation forecast? To put it another way: Does the model contain the proper physical ingredients to enable it to predict precipitation correctly? A start was made to write a program that would enable the computer to get a precipitation forecast from a perfect forecast of the fields of flow and thickness (i.e., from observed data), but manpower shortages prevented completion of the job. And so a basic question remains unanswered.

Without much effort, however, one is able to get useful information about the quality of the atmospheric model. Several years of verification had shown that computer-made 24-hour 500-mb. forecasts were very good and that 12-hour forecasts were excellent. Therefore, the assumption was made that 6-hour forecasts were "nearly perfect." Six-hour observed precipitation amounts were then compared with the computed predictions.

Figure 5 shows the observed and predicted 6-hour precipitation amounts for the period 1200 to 1800 GMT, April 11, 1960. The largest amount of precipitation was forecasted in northern Illinois, but observed in Michigan. More precipitation was forecasted than observed in the western United States. The overall forecast may be considered a good one. One reason for the differences between the observed and forecasted precipitation may be found from an examination of figure 5c.

Figure 5c gives the error in the 12-hour 500-mb. forecast for the period 1200 GMT April 11 to 0000 GMT, April 12. The first half of this period corresponds to the 6-hour precipitation period under discussion. It would have been better to have a 6-hour 500-mb. error chart but that is not available. The 12-hour 500-mb. error chart, however, is routinely printed out by the computer. In the area over Michigan the 500-mb. forecast was 150 feet too high. Synoptic experience suggests that a lower 500-mb. height

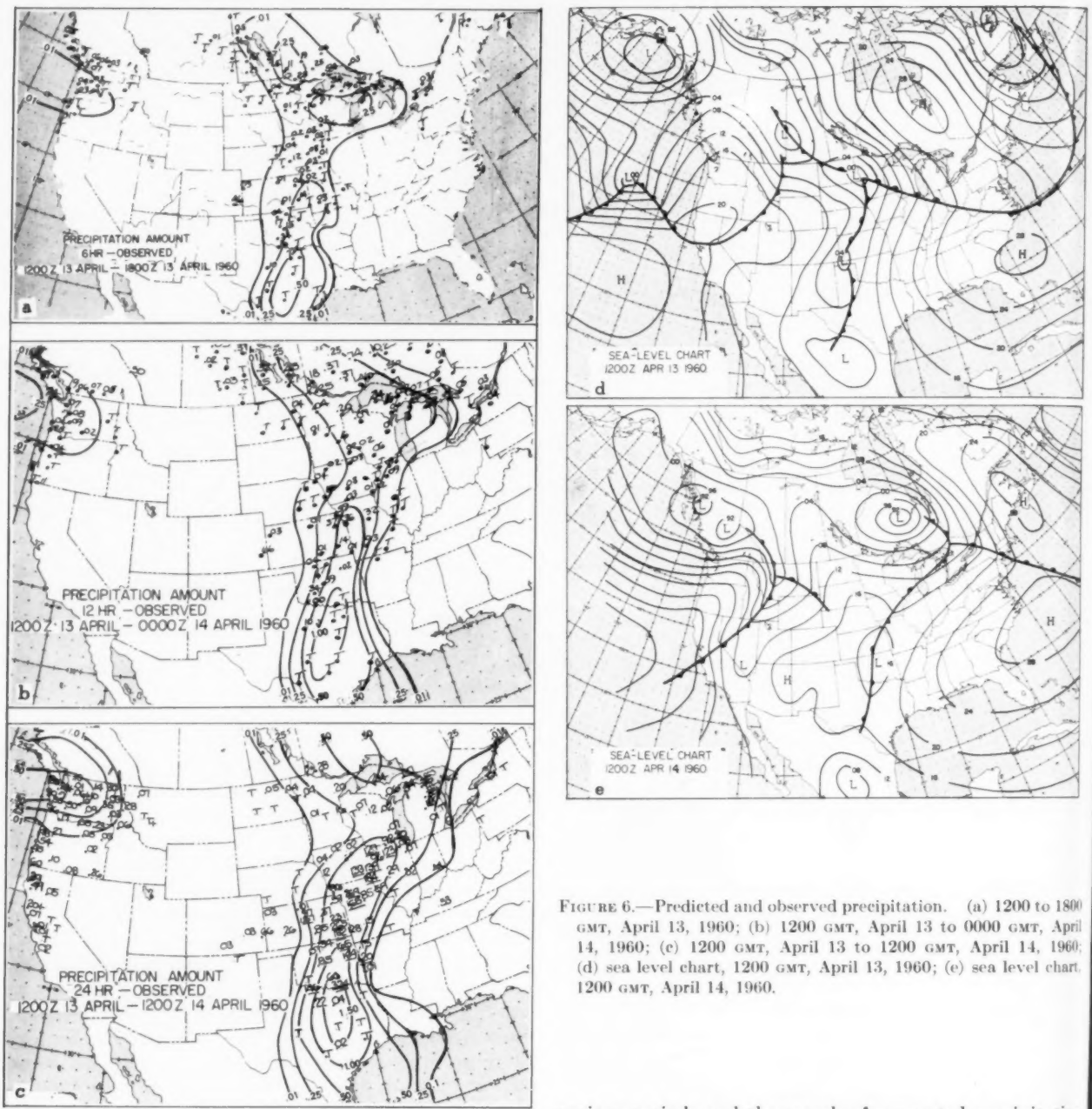


FIGURE 6.—Predicted and observed precipitation. (a) 1200 to 1800 GMT, April 13, 1960; (b) 1200 GMT, April 13 to 0000 GMT, April 14, 1960; (c) 1200 GMT, April 13 to 1200 GMT, April 14, 1960; (d) sea level chart, 1200 GMT, April 13, 1960; (e) sea level chart, 1200 GMT, April 14, 1960.

forecast would have improved the precipitation forecast there. The error chart also shows that our assumption of a nearly perfect 6-hour 500-mb. forecast was, most likely, not altogether correct. In the west, errors in the precipitation forecast are just as likely due to lack of knowledge of the initial conditions over the ocean as to a faulty model.

Since the computer calculates and stores precipitation amounts for each hour, the values may be printed out for various periods and the march of computed precipitation across the country compared with that of the observed precipitation. Figure 6 shows the predicted and observed amounts of precipitation as well as the movements of the precipitation areas for the 24 hours from 1200 GMT, April 13 to 1200 GMT, April 14, 1960. The forecast has caught the main features of the observed precipitation patterns.

From an examination of 6-hour precipitation forecasts, the impression emerges that the precipitation model is basically sound. It is unable to cope with the details of the mountain effect. The lack of information over the oceans and the Gulf of Mexico is sometimes disastrous to

the forecast. A principal difficulty may be the inadequacy of the essentially barotropic model in predicting cyclogenesis with which large amounts of precipitation are associated. Further, the model cannot hope to forecast such small-scale phenomena as individual convective showers and thunderstorms.

## 7. SMALLER-SCALE OROGRAPHIC PRECIPITATION

In western United States, as is well known, the mountains have a strong effect on the distribution of precipitation. Since grid points are about 240 miles apart in the JNWP computational grid, and since the slope of the mountains is determined from the heights of points 480 miles apart, it is clear that the important features of the distribution of precipitation in western United States cannot be predicted.

Aside from the fact that current numerical weather prediction models do not permit the dynamics that are applicable to small-scale orographic motions, the main reason these methods use grid intervals of not less than 200 to 300 miles is that if shorter space intervals are used shorter time intervals must also be used in the integration of the governing differential equations. Short integration time steps mean a longer time to produce a forecast. Machine time is expensive. But as the computation of vertical velocity due to the flow of air over mountains, equation (5), does not involve the solution of a differential equation, Lt. Col. H. A. Bedient of JNWP Unit suggested experimenting with a much smaller grid interval.

Some computations have been made using a grid interval of 40 miles in the States of Washington and Oregon. These States were selected for test because of the rugged character of the country and the large space variation of mean annual precipitation amounts. Consider a saturated moist adiabatic atmosphere with a 700-mb. temperature of −6° C. and a west wind of 20 knots ($V_g$). The precipitation pattern due to the flow of air over the mountains, if these conditions hold for 24 hours, is shown in figure 7. An interesting feature of figure 7 is that it demonstrates that the flow of air over the mountains is sufficient to give heavy rains without the introduction of the latent heat effect. The amounts and pattern of precipitation bear a strong similarity to those frequently observed on the synoptic weather map., i.e., the precipitation is concentrated along the coastal mountains and, farther inland, along the Cascade Range.

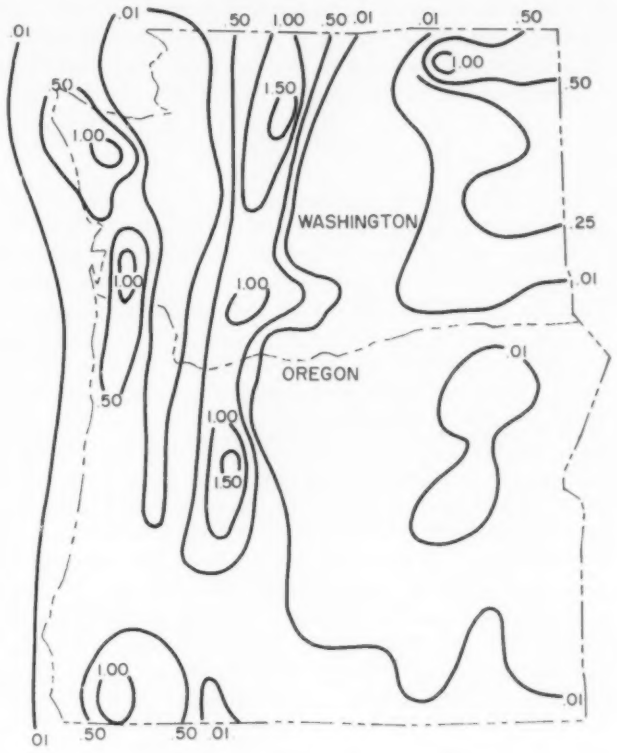


FIGURE 7.—Precipitation amount (inches per day) from a saturated atmosphere with a 700-mb. temperature of −6° C. and a 20-knot west wind at the ground.

## 8. PROBLEMS AND SUGGESTIONS

*Friction.*—All the precipitation forecasts have been made without taking into account the vertical velocity due to surface frictional flow into Lows and out from Highs. However, the friction program has been written and checked out and will be incorporated into the main program shortly. The effect of friction on the 500-mb. flow has recently been taken into account by Cressman [3].

*Showers.*—Much of the summertime rain in the United States falls in showers. It seems best to tackle this problem with a probability forecast. Stanley Doore of JNWP Unit has written a program to enable the computer to print out the probability of the occurrence of showers. His work is based on the studies of Curtis and Panofsky [4].

*Rain and snow.*—The use of the 1000–500-mb. thickness as the only parameter to distinguish between rain and snow needs further examination. The use of another parameter, such as the 850-mb. temperature, may improve the forecast.

Some thought has been given to have the computer predict snow depth—a weather element of critical importance in the winter. It is easy for the computer to keep track of the predicted amount of precipitation that falls as snow. Precipitation amount can be transformed to snow depth by the computer by use of the standard 10 to 1 ratio (snow depth to water equivalent). But difficulties arise if both rain and snow are predicted during the forecast period.

*Multi-level models.*—The present precipitation forecasts depend on the simple atmospheric models now in use. As more sophisticated atmospheric models come into use,

improved forecasts of the fields of flow, temperature, and moisture may be expected. Multi-level models of the atmosphere will be used in the powerful new IBM 7090 computer which was installed in JNWP Unit in mid-1960.

## 9. VERIFICATION

From what little verification has been made of the computer forecasts of precipitation, it seems that so far as "heavy precipitation"—1 inch or more in 24 hours—is concerned, the subjective forecaster is doing better than the computer. The reason for this is not clear. It may be that the latent heat effect is taken into account too crudely, or that the moisture field near the ground has to be considered. But perhaps the trouble is more fundamental. Examination of all the heavy rain cases for April 1960 in the contiguous United States revealed that most of the heavy rains were on so small a scale that they could not possibly have been predicted with the coarse grid used. If further study reveals that this is generally true, a smaller grid interval will have to be used to successfully predict heavy precipitation.

However, if the verification is made on the basis of "precipitation" or "no precipitation", it turns out that the computer-made precipitation forecasts are of about the same quality as subjective forecasts.

## ACKNOWLEDGMENTS

This study could not have been completed without the help of the JNWP staff members, especially Messrs. E. J. Brennan, A. Rosenbloom, J. Arnold, S. Doore, B. Helmick, Lt. Col. H. A. Bedient, USAF, and Dr. G. P. Cressman.

## REFERENCES

1. G. 'Arnason and L. P. Carstensen, "The Effects of Vertical Vorticity Advection and Turning of the Vortex Tubes in Hemispheric Forecasts with a Two-Level Model," *Monthly Weather Review*, vol. 87, No. 4, Apr. 1959, pp. 119–127.
2. E. M. Carlstead, "Forecasting Middle Cloudiness and Precipitation Areas by Numerical Methods," *Monthly Weather Review*, vol. 87, No. 10, Oct. 1959, pp. 375–381.
3. G. P. Cressman, "Improved Terrain Effects in Barotropic Forecasts," *Monthly Weather Review*, vol. 88, Nos. 9–12, Sept.–Dec. 1960, pp. 327–342.
4. R. C. Curtis and H. A. Panofsky, "The Relation Between Large-Scale Vertical Motion and Weather in Summer," *Bulletin of the American Meteorological Society*, vol. 39, No. 10, Oct. 1958, pp. 521–531.
5. M. A. Estoque, "An Approach to Quantitative Precipitation Forecasting," *Journal of Meteorology*, vol. 14, No. 1, Feb. 1957, pp. 50–54.
6. H. H. Lamb, "Two-Way Relationship Between Snow or Ice Limit and 1000–500 mb. Thickness in the Overlying Atmosphere," *Quarterly Journal of the Royal Meteorological Society*, vol. 81, No. 348, Apr. 1955, pp. 172–189.
7. W. Lewis, "Forecasting 700-mb. Dewpoint Depression by a 3-Dimensional Trajectory Technique," *Monthly Weather Review*, vol. 85, No. 9, Sept. 1957, pp. 297–301.
8. S. Manabe, "On the Contribution of Heat Released by Condensation to the Change in Pressure Pattern," *Journal of the Meteorological Society of Japan*, vol. 34, Ser. 2, No. 6, Dec. 1956, pp. 308–320.
9. J. Smagorinsky, "On the Inclusion of Moist Adiabatic Processes in Numerical Prediction Models," *Berichte des Deutschen Wetterdienstes*, vol. 5, No. 38, 1957, pp. 82–90.
10. J. Smagorinsky and G. O. Collins, "On the Numerical Prediction of Precipitation," *Monthly Weather Review*, vol. 83, No. 3, Mar. 1955, pp. 53–68.
11. S. J. Smebye, "Computation of Precipitation from Large-Scale Vertical Motion," *Journal of Meteorology*, vol. 15, No. 6, Dec. 1958, pp. 547–560.
12. A. J. Wagner, "Mean Temperature from 1000 mb. to 500 mb. as a Predictor of Precipitation Type," *Bulletin of the American Meteorological Society*, vol. 38, No. 10, Dec. 1957, pp. 584–590.

# RELATIVE MOTION OF HURRICANE PAIRS

EUGENE W. HOOVER

U.S. Weather Bureau, Washington National Airport, Washington, D.C.

[Manuscript received April 20, 1961]

## ABSTRACT

It is found that the observed relative motion of Atlantic hurricanes occurring simultaneously as pairs is related to the orientation of their line of centers, and that the tendency to approach is more pronounced when the hurricane centers are positioned in an east-to-west through southeast-to-northwest line. Other orientations of hurricane pairs have been associated with a separation of the centers.

The relative motion of centers of pairs separated more than 600 nautical miles is found to be predominantly clockwise. Most of the cases of counterclockwise revolution of these hurricane pairs occurred when the centers were oriented in essentially an east-to-west line. Limited data suggest relative counterclockwise revolution existed in most cases with centers separated less than 600 nautical miles.

It is found that the predominant relative motion of Pacific tropical cyclone pairs in the vicinity of the Philippines is counterclockwise. It is suggested that this difference in relative motion of Pacific tropical cyclone pairs from that of Atlantic pairs may be due to differences in circulation patterns related to geographical features.

## 1. INTRODUCTION

The relative motion of vortices occurring simultaneously as pairs has been studied extensively by Fujiwhara [1]. He found that the relative motion was composed of the counterclockwise revolution of one vortex about another and the tendency for the approach of like circulations. Haurwitz [2] derived a mathematical expression showing that the counterclockwise revolution of one cyclonic vortex with reference to another was directly proportional to the intensity of the circulations and inversely proportional to the square of the distance between the two centers.

In the present study, the theories of Fujiwhara and Haurwitz were tested by observing the behavior of Atlantic hurricane pairs as shown in the convenient annual tracks of North Atlantic tropical cyclones for the period 1886–1959 [3], [4]. There were 5 cases in which the tracks showed hurricane pairs closer than 600 nautical miles. There was a total of 38 cases where two or more hurricanes occurred simultaneously for a period of 24 hours or more, separated by a distance of 1500 nautical miles or less in the area encompassed by the North Atlantic Ocean, the Gulf of Mexico, and Caribbean Sea.

## 2. PROCEDURE

The procedure which was used to determine the relative motion, illustrated in figure 1, is as follows:

(1) Indicate north and draw concentric circles with radii of 600 and 1200 nautical miles on tracing paper.

(2) Check the annual hurricane tracks for overlapping dates of hurricanes.

(3) Place the tracing paper over the track-map so that the center of concentric circles is positioned on the hurricane that was known to exist first, and orient on north at the longitude of this hurricane.

(4) Indicate the relative position and date of the second hurricane.

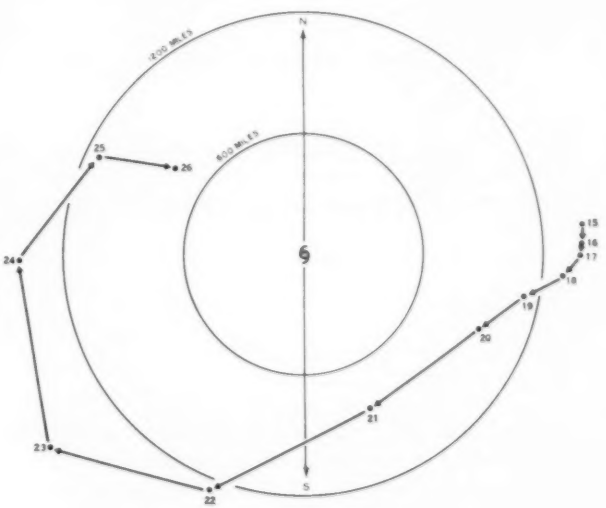


FIGURE 1.—The relative motion of an Atlantic hurricane pair, August 15–26, 1893. The first hurricane is centered at the center of the concentric circles. The path of the second hurricane relative to the first is given by the arrows connecting daily relative position points.

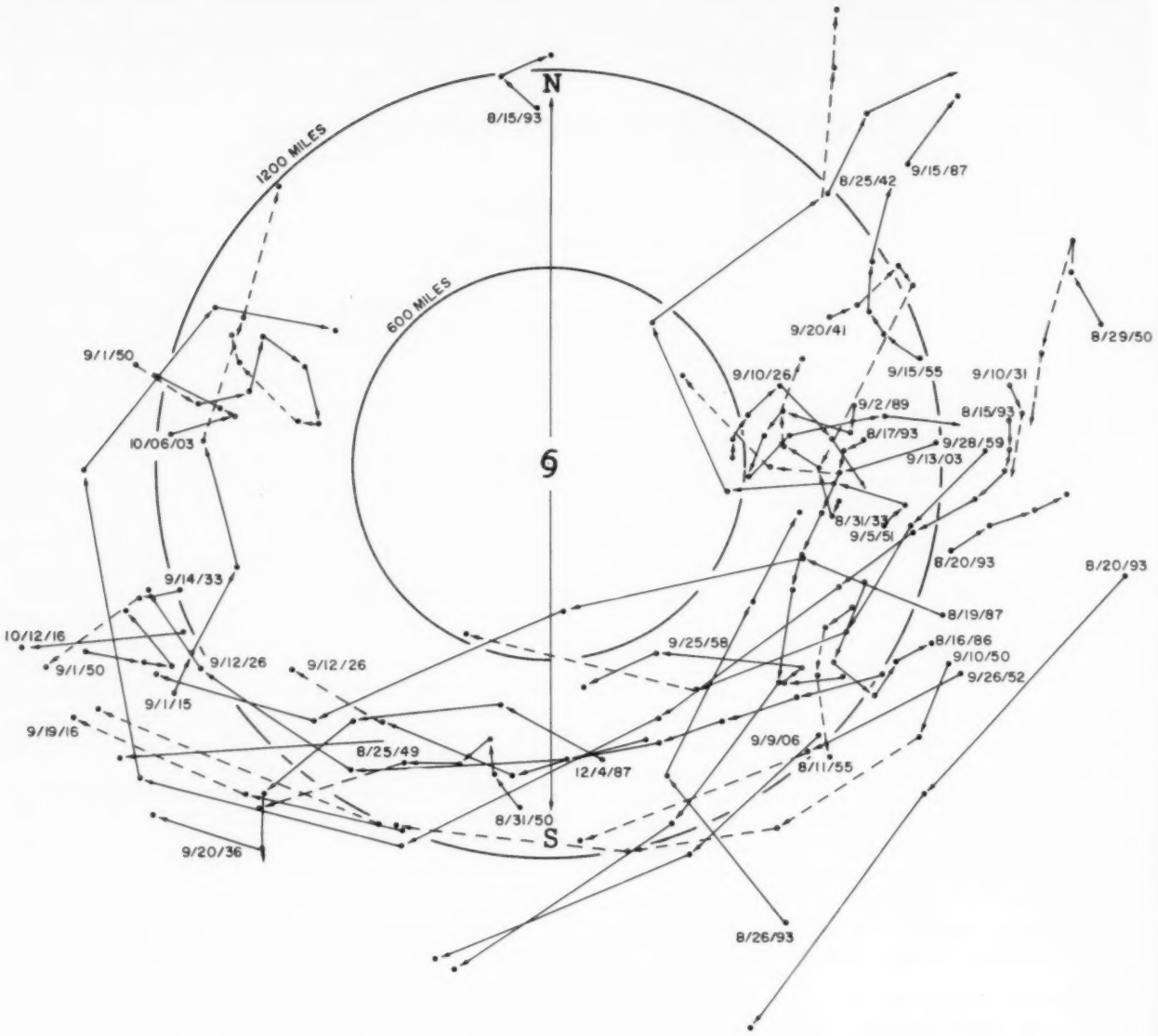


FIGURE 2.—Composite chart of relative motion of Atlantic hurricane pairs, 1886–1959. Dates correspond to first relative positions.

(5) Repeat steps 3 and 4 for each subsequent daily position as long as the tracks are available.

(6) Connect daily positions of relative motion.

The individual tracks, as illustrated in figure 1, were combined on a single chart, figure 2. Dashed lines were used when one or both of the hurricanes diminished below hurricane force. The direction of relative motion is indicated by the arrows.

## 3. RESULTS FOR ATLANTIC HURRICANES

The 38 cases of hurricane pairs contained 145 24-hour periods of relative motion between hurricane pairs. From these periods of relative motion, the following results, as summarized in figure 3, were obtained:

(1) A tendency to separate was observed in 80 periods (55 percent); a tendency to approach in 64 periods (44 percent); indeterminate in 1 period (1 percent).

(2) The maximum segregation of separation periods (81 percent) from the approach periods (19 percent) was obtained from quadrants with center orientation north-northeast to south-southwest.

(3) In the remaining quadrants, the centers were oriented west-northwest to east-southeast; these quadrants contained 58 percent approach periods, 41 percent separation periods, and 1 percent indeterminate.

(4) Clockwise revolving motion occurred in 104 periods (72 percent), counterclockwise in 41 periods (28 percent).

(5) The maximum segregation of clockwise periods (88 percent) from counterclockwise periods (12 percent) was obtained from quadrants with centers oriented north to south.

(6) The periods with east to west quadrant orientation were divided 65 percent clockwise, 35 percent counterclockwise.

In the quadrants whose centers were oriented east-to-west, the average speed of relative motion was 5 knots. Since the direction of relative motion was variable, the mean vector motion was small (approximately 1 knot clockwise approaching).

In the quadrants whose centers were oriented north-to-south, the average speed of relative motion was approximately 10 knots. The direction of the motion was relatively uniform and the mean vector indicated about 7 knots in a clockwise direction.

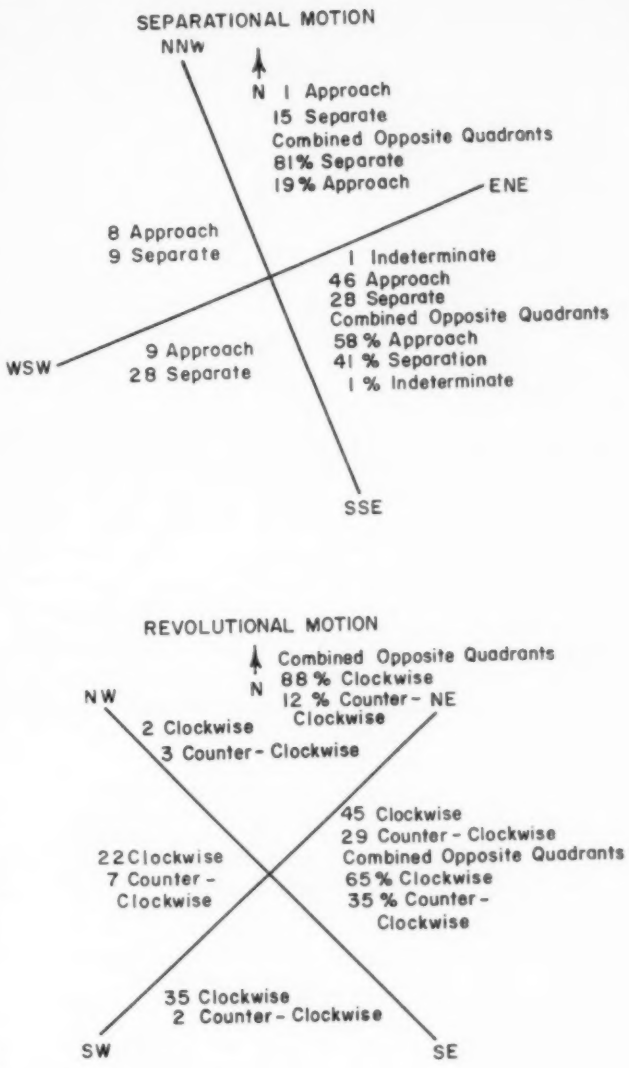


FIGURE 3.—Distribution of relative motion of Atlantic hurricane pairs by quadrants based on orientation of the lines connecting the centers. Percentages for cases in opposite quadrants are combined.

## 4. COMPARISON WITH PACIFIC TROPICAL CYCLONES

There is a difference between the predominant relative motion of simultaneous pairs of tropical cyclones in some areas of the Pacific region and hurricane pairs in the Atlantic. The results of this study show the predominant relative motion is clockwise for simultaneous hurricane pairs in the Atlantic region. The method described here was applied to the Pacific tropical cyclone pairs tabulated by Haurwitz [2] using the center positions indicated on the historical maps, and the results are combined in figure 4. Most of these cases were positioned around the Philippine Islands with one tropical storm centered in the South China Sea and the other in the Pacific, east or northeast of the Philippine Islands. The predominant relative motion of these tropical cyclones was found to be counterclockwise as suggested by Haurwitz [2] and Fujiwhara [1].

The explanation for the difference in the relative motion between tropical cyclone pairs in the Pacific and hurricane pairs in the Atlantic is believed to be a difference in the circulation pattern as suggested by the tropical cyclone track maps. In figure 5, note the double maxima of cyclone tracks in the Western Pacific and China Sea. The maximum to the left extends from the Philippine Islands west across the South China Sea to the coast of Asia. A second maximum of cyclone tracks approaches, then recurves northeast just to the east of the Philippine Islands. The predominant relative motion track in figure 4 is suggested by the relative motion of the two track maxima. If the reference or central point of figure 4 is placed over the track maximum in the South China Sea in figure 5, the second tropical cyclone maximum recurves into the northeast quadrant similar to the relative tracks in figure 4. In the Atlantic area this grouping of tropical cyclone tracks is not in evidence. The most striking feature of the hurricane tracks is the large number that follow a general pattern similar to the idealized track in figure 6. Figure 7 illustrates the relative motion of a

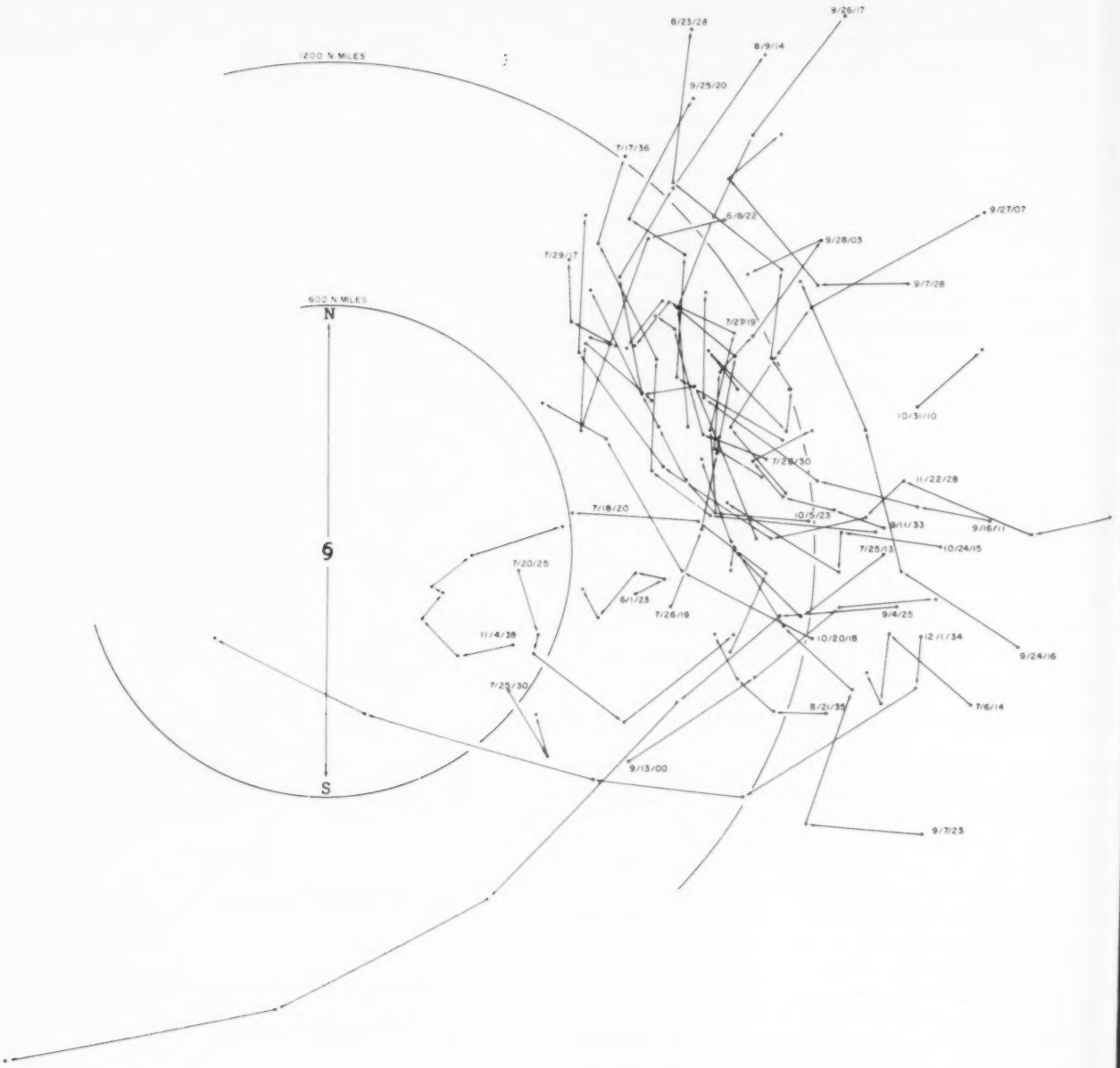


FIGURE 4.—Composite chart of relative motion of western Pacific tropical cyclone pairs (only cases tabulated by Haurwitz [2]). Dates correspond to first relative positions.

simultaneous hurricane pair where both hurricanes follow the idealized track displaced eight days apart. Note the similarity between the predominating pattern in figure 2 and motion in figure 7.

Thus far certain characteristics of tropical cyclone tracks peculiar to the geographical area have been suggested as explanations for the observed difference in the relative motion tracks between figures 2 and 4. It seems proper

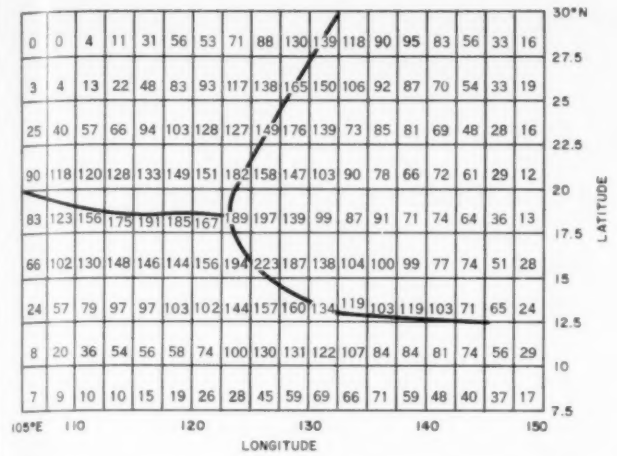


FIGURE 5.—Total number of tropical cyclone tracks passing through each 2.5° latitude-longitude "square," 1884–1953. The heavy lines are loci of maximum numbers. Data from Chin [5].

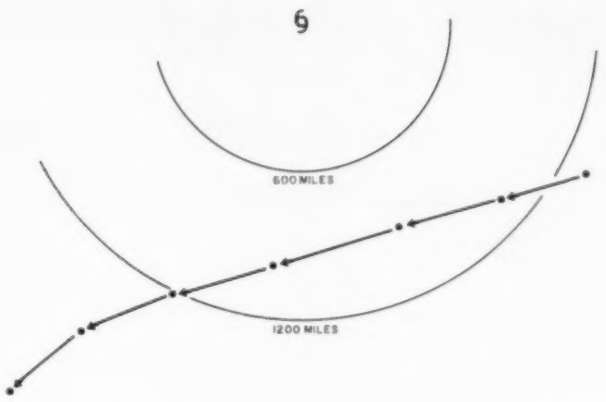


FIGURE 7.—Relative motion of a hurricane pair separated by eight days, both following the idealized track in figure 6.

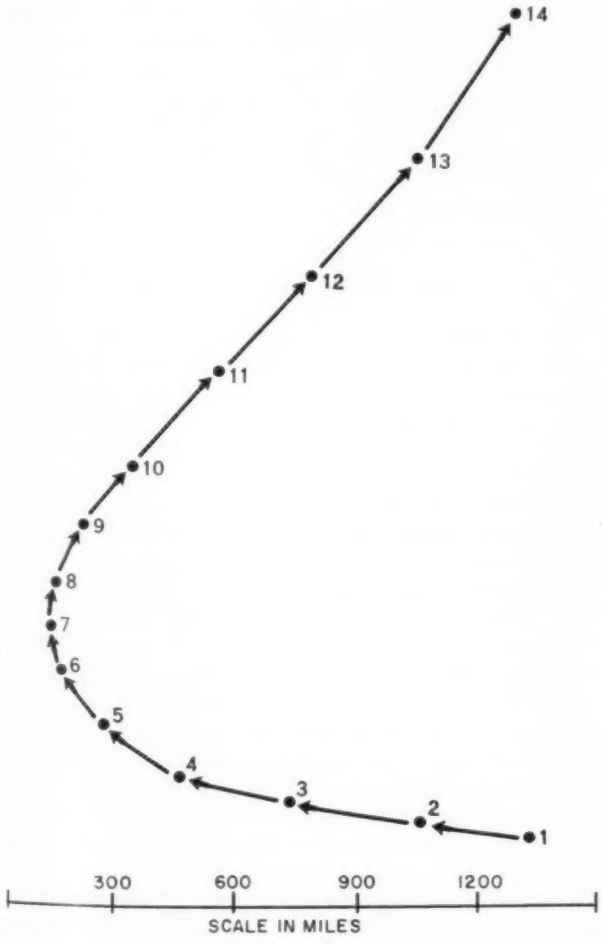


FIGURE 6.—Idealized track suggested by the general pattern of movement of Atlantic hurricanes.

to assume that the tracks are a function of the circulation pattern, which on this scale is likely due to geographical features. However, detailed explanations of the circulation differences are beyond the scope of this paper.

## REFERENCES

1. S. Fujiwhara, "Short Note on the Behavior of Two Vortices," *Proceedings of the Physico-Mathematical Society of Japan*, Third Series, vol. 13, 1913, pp. 106–110.
2. B. Haurwitz, "The Motion of Binary Tropical Cyclones," *Archiv für Meteorologie, Geophysik und Bioklimatologie*, Ser. A, vol. 4, 1951, pp. 73–86.
3. G. W. Cry, W. H. Haggard, and H. S. White, "North Atlantic Tropical Cyclones," U.S. Weather Bureau, *Technical Paper* No. 36, Washington, D.C., 1959, 214 pp.
4. G. E. Dunn and Staff, Weather Bureau Office, Miami, Fla., "The Hurricane Season of 1959," *Monthly Weather Review*, vol. 87, No. 12, Dec. 1959, pp. 441–450.
5. P. C. Chin, "Tropical Cyclones in the Western Pacific and China Sea Area from 1884 to 1955," *Technical Memoir* No. 7, Royal Observatory, Hong Kong, 1958.

# THE WEATHER AND CIRCULATION OF APRIL 1961[1]

## Persistant Blocking in Eastern Canada and Cool Weather in the United States

JAMES F. O'CONNOR

Extended Forecast Section, U.S. Weather Bureau, Washington, D.C.

### 1. WEATHER HIGHLIGHTS

The mild weather of March 1961 in the United States [1] underwent a sharp reversal in April as temperatures changed to below seasonal normals over most sections. Average temperatures also contrasted in many areas with those of April 1960 [2] which had been predominantly mild in the United States. Both Aprils were similar, however, in that each had reversals near mid-month with cooling in the West and warming in the East in the latter part of the month.

It was the coldest April since 1907 in much of the Southeast, as well as the coldest on record in parts of Alabama, where Montgomery reported a monthly average of 60.2° F., the lowest in 89 years. In the West unseasonably low temperatures produced freezing minima on a number of days near the middle and latter parts of the month with damage to orchard crops in many regions. In Montana and Wyoming this was the first month since August 1960 that temperatures averaged below normal.

This was not only a cold month but also a wet one in many parts of the East, drastically retarding spring planting operations in many places. It was the wettest April of record in portions of Alaska, North Dakota, New York, Ohio, and Rhode Island. In North Dakota, Bismarck and Fargo reported the first beneficial excess of precipitation since the first of the year.

By way of contrast, this was the driest April on record in some areas of central and southern Texas. The dryness approached drought conditions there, as well as in other parts of the Southwest such as at Phoenix, Ariz., Point Arguello, Calif., and Reno, Nev., where deficiencies of precipitation have been reported for the past five or six months.

Snow fell in record amounts for April in many places, e.g., Caribou, Maine, Youngstown, Ohio, and Muskegon, Mich., while record 24-hour amounts for April of from 11 to 12 inches were reported at Grand Rapids, Mich., and Duluth, Minn., in association with a slowly moving storm between the 14th and 16th. For the winter season as a whole, record accumulations of snowfall were recorded at Williamsport, Pa., (80.2 in.) and Akron, Ohio, (81.5 in.). In contrast, Green Bay, Wis., had its smallest winter snowfall on record.

A deep storm on the 12th produced the lowest sea level pressure (989 mb.) ever recorded in April at Louisville, Ky. It was accompanied by winds of over 100 m.p.h. at Sullivan and Edisto Islands near Charleston, S.C., and tornado damage at James Island, S.C. Tornado reports were numerous in the last 10 days of the month in the climatologically famed "Tornado alley" extending from Oklahoma to Iowa. Tornadoes were also numerous, particularly on the 12th and 15th in the Southeast, where the expectancy is much less than in the Mid-West.

Moderate to major flooding continued in various parts of the Mississippi Basin, in many of the same areas which were in flood during the preceding month [1].

### 2. THE MONTHLY CIRCULATION

The monthly average circulation at 700 mb. (fig. 1) and at sea level (fig. 2) for April 1961 was featured by strong blocking in eastern Canada and the polar regions with additional blocking in the Pacific. This was reflected in above normal height departures in these areas at 700 mb. (fig. 1) and a strong High centered near the the North Pole at sea level (fig. 2). Mean 700-mb heights over Baffin Island averaged 460 feet above normal, the largest departure in the hemisphere this month. A departure of this magnitude in the Canadian area has been exceeded only once in any April since 1933. A departure of 610 feet was observed in April 1953 [3] which was similar to this April in respect to the coolness over much of the United States, as well as other features.

Figure 3 shows the well-marked changes in the 700-mb circulation (in excess of the normal changes) which occurred between March and April 1961. Large height rises in the Gulf of Alaska and falls over the Great Lakes set up an abnormally strong flow of cool air from northwestern Canada into the southeastern United States. Strong rises in the Baffin Island area almost completely reversed the flow in this area, while strong height falls near the United Kingdom reflected a cessation of the blocking which occurred there during March [1]. The

[1] Descriptions of the weather of May, June, and July 1961 will appear in the August, September, and October issues of the *Monthly Weather Review*, respectively.

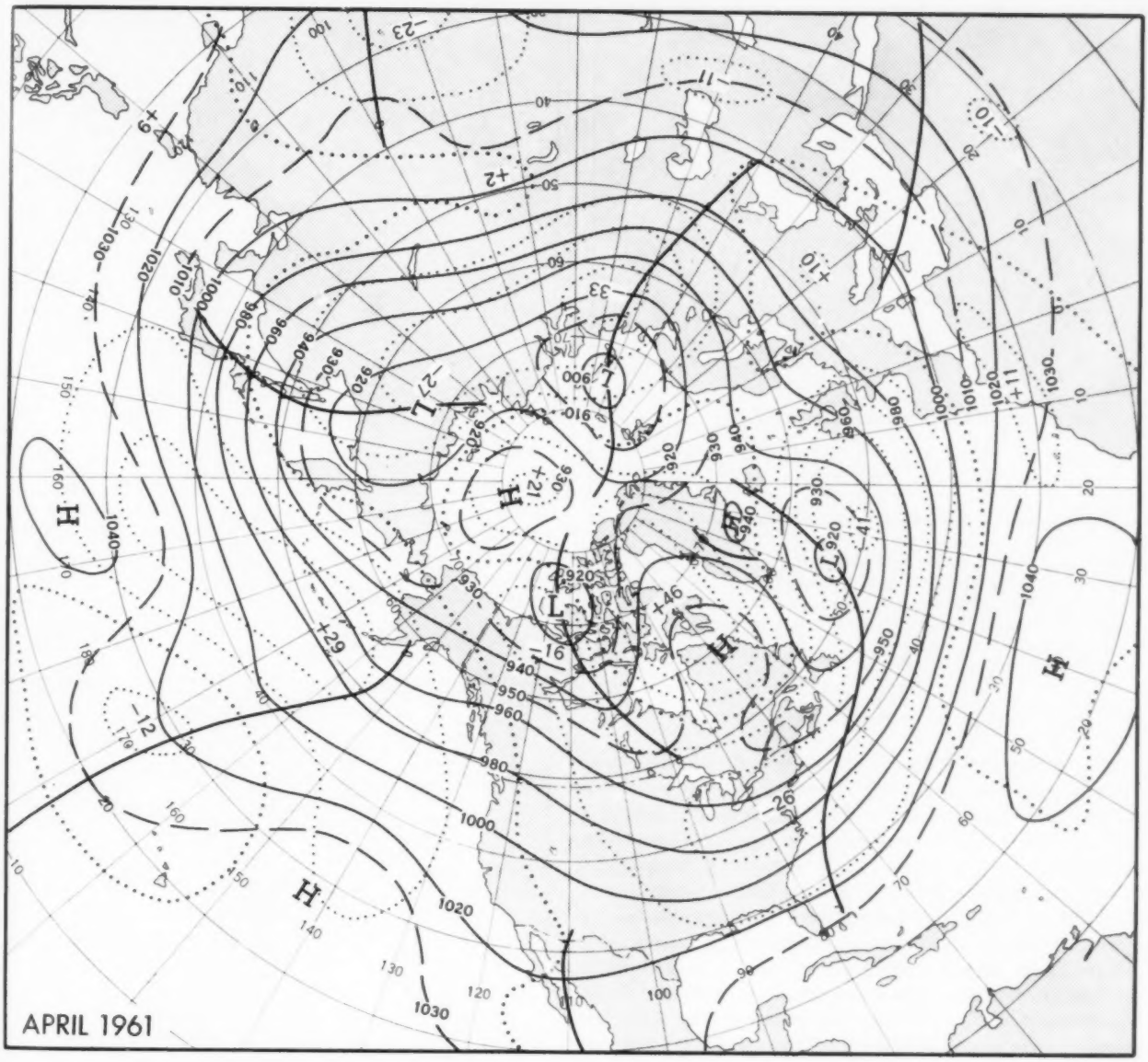


FIGURE 1.—Mean 700-mb. contours (solid) and departures from normal (dotted) (both in tens of feet) for April 1961. Blocking of near record intensity in eastern Canada had a major influence on weather in the United States.

retrogression of this block to North America is evident in the movement of a height rise area, which was located just south of Greenland in March (fig. 6 of [1]), to the Baffin Island area in April (fig. 3), and subsequently, westward across Canada as shown in figure 4.

Despite extensive blocking in the western sector of the hemisphere (0°–180° W.), the average speed of the westerlies between latitudes 35° N. and 55° N. was almost exactly normal in April (8.3 m.p.s. at 700 mb. and 2.4 m.p.s. at sea level). The diminution in wind speeds (about 7 m.p.s. below normal at 700 mb.) associated with blocking occurred primarily in southeastern Canada and the North Atlantic, as well as in the central Pacific, but it was compensated by much stronger than normal westerlies in the Atlantic, where 700-mb. wind speeds averaged as much as 21 m.p.s., or about twice the normal speed, between 35° N. and 45° N. In the subtropics (20° N.–35° N.) wind speed indices also averaged near normal at both sea level and 700 mb. Only in the polar (55° N.–70° N.) wind speed averages was the anomalous

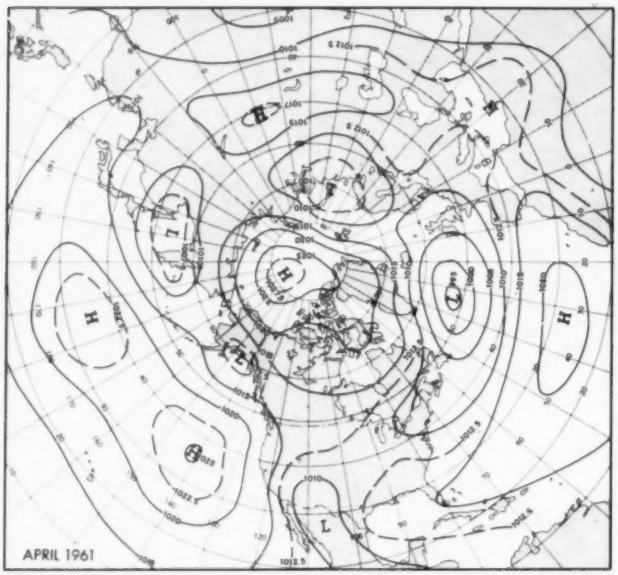


FIGURE 2.—Mean sea level isobars (with intermediate isobars dashed) (in millibars) for April 1961. Widespread anticyclonic activity dominated the polar region, while the marked trough from the southern Rockies to New England reflects the locus of vigorous cyclonic activity.

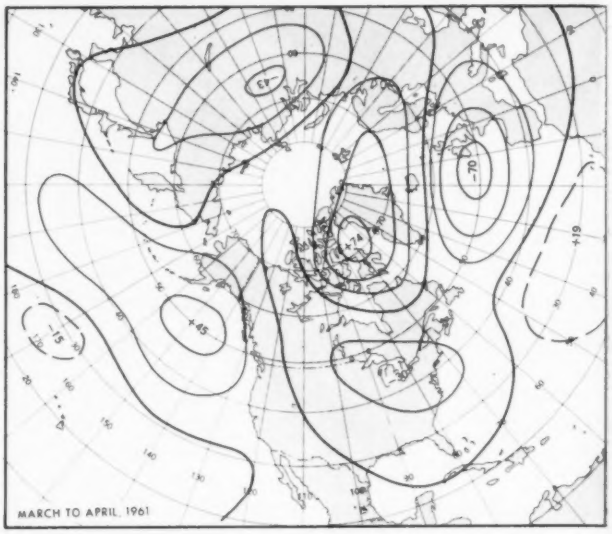


FIGURE 3.—Anomalous 700-mb. height changes (tens of feet) between March and April 1961 with zero line heavier. Falls over the Great Lakes and rises in the eastern Pacific produced a sharp reversal in the circulation and associated temperature regime over large areas.

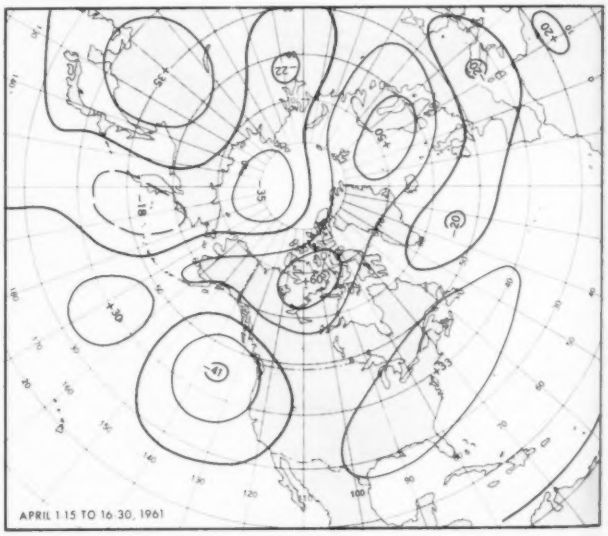


FIGURE 4.—Mean 700-mb. height changes (tens of feet) between the first and last halves of April 1961 (see fig. 5). Lowering of heights in the eastern Pacific and increase of heights east of the Rockies were associated with cooling over the Rockies and warming to the east in the latter half of the month.

nature of the circulation clearly revealed. At 700 mb., for example, the westerlies averaged 1.1 m.p.s. below normal, while at sea level the easterlies averaged 3.2 m.p.s. or twice the normal value for April. This abnormality was related to the excessive easterly components of the average flow, relative to normal, in eastern North America and the North Atlantic. This is revealed by figure 1 which shows the axis of positive height departures located at 70° N. in eastern Canada and Greenland, while the axis of negative departures extended from 50° N. in the Atlantic to 40° N. in North America. The mean sea level pressure averaged at each latitude in the 0°–180° W. sector showed above normal pressures north of about 55° N. and below normal pressures to the south, a similar profile to that shown in figure 1 of [3] for April 1953.

The eastern Canadian block was associated not only with a marked weakening of westerlies in this area, but also, as revealed by figure 1, with an actual high center at 700 mb. in the monthly average. This was a noteworthy abnormality in view of the fact that eastern Canada is the location of a deep cyclonic center of action in the long-period circulation averages. No closed high centers in the monthly average circulations at 700 mb. have heretofore been observed in this area in any April in the historical files of Extended Forecast Section which date back to 1933, although about 10 cases with 5-day mean high circulations in this area were observed between 1947 and 1958. On a daily basis, high centers aloft in this area were observed on over half the days during this month, in addition to ridge conditions on some other days.

The abnormality of the circulation in Canada is dramatized by the extreme temperature departures from

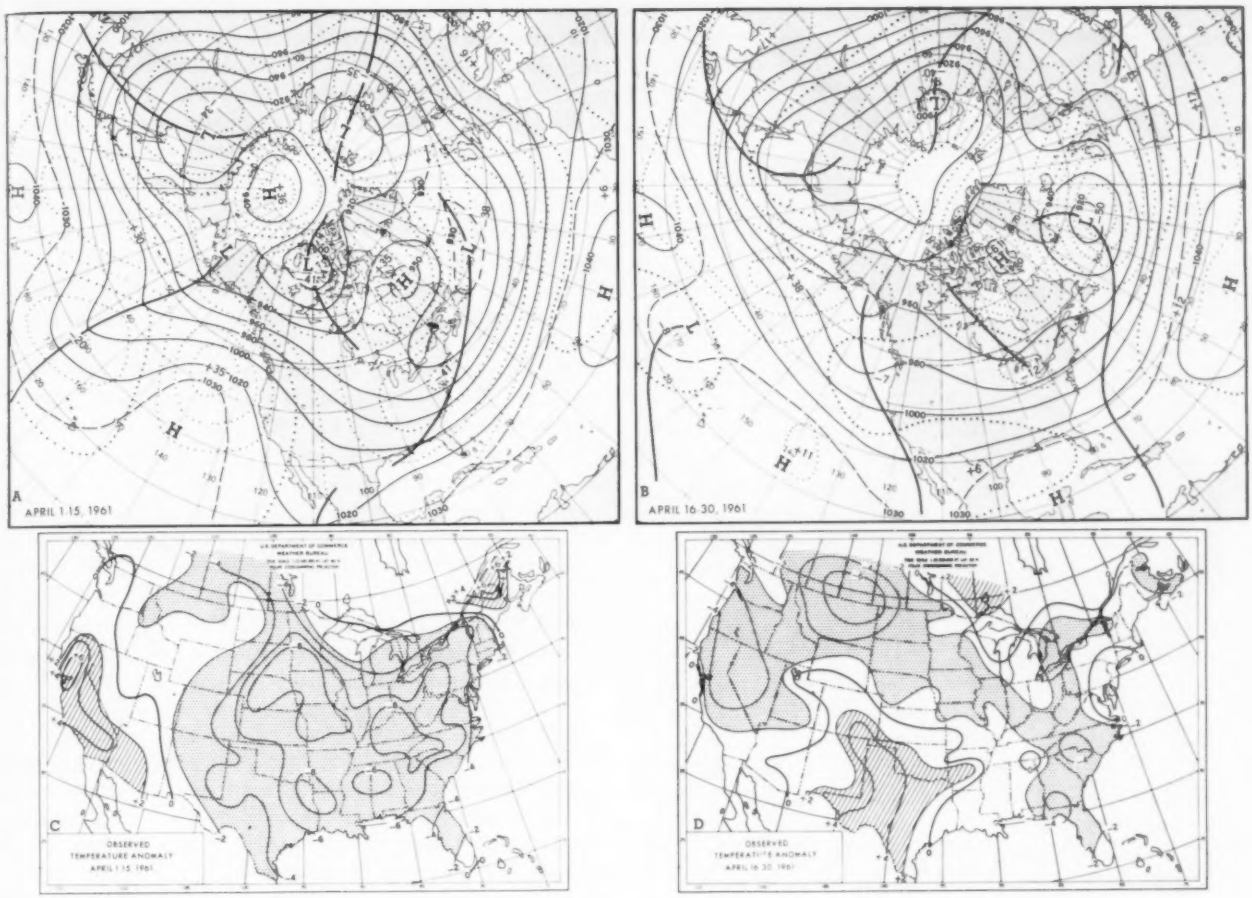


FIGURE 5.—(A) (B) Mean 700-mb. contours (solid) and height departures from normal (dotted) (both in tens of feet) for April 1–15, and April 16–30, 1961, respectively. (C) (D) Mean temperature departure from normal (°F.) for April 1–15, and April 16–30, 1961, respectively. Trough development along the west coast permitted warming east of the Rockies and cooling in the Far West during the second half of the month.

normal. Temperatures for the month averaged as much as 12° F. above normal in southeastern Canada and over 12° F below normal in northwestern Canada. Extreme dryness in eastern Canada also characterized the area of persistent blocking anticyclonic circulation.

In the Pacific the zone of above normal heights centered in the Aleutians was a manifestation of recurrent propagation of anticyclonic vorticity, tending to maintain cyclonic activity at lower latitudes northwest of Hawaii.

## 3. THE HALF-MONTHLY CIRCULATIONS

Although both halves of April 1961 were characterized by blocking in eastern North America and the north Pacific, continuity of long-period retrogression of major height change centers at higher latitudes was still evident. Figure 4 shows the height changes which occurred between the first and last halves of April. Comparing these with figure 3, it appears that the Baffin Island block, which had previously retrograded from the North Atlantic, continued westward across Canada, while the Gulf of Alaska block retrograded toward the central Pacific. Replacing the retrograding Gulf of Alaska block in the second half of the month was a 410-foot height fall center off the Pacific Northwest coast, in precisely the location of a strong ridge in the first half of the month.

Figures 5 A and B show the circulations in the first and last halves of the month with the 700-mb. height departures superimposed. The northern part of the full-latitude trough of the first half-month in the central Pacific sheared and was forced eastward by progression of the Asiatic trough at higher latitudes. The sheared trough subsequently combined with the low-latitude

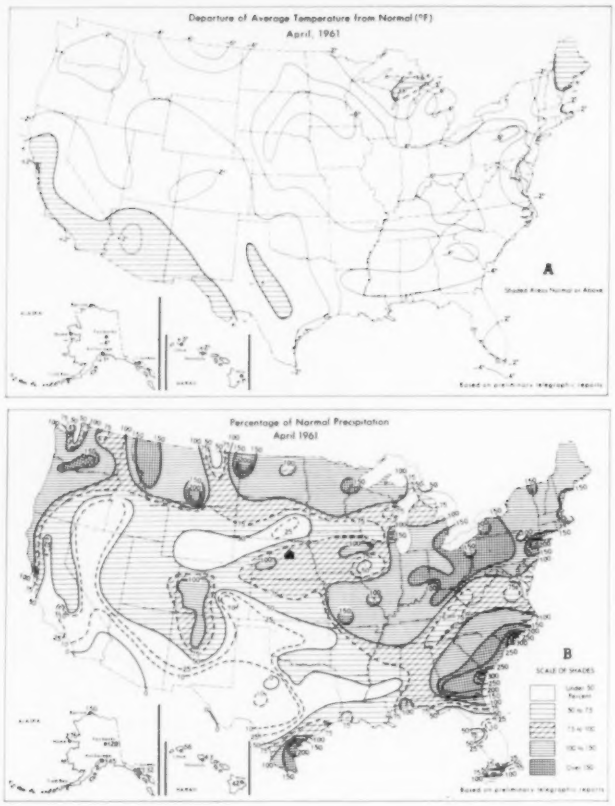


FIGURE 6.—(A) Mean temperature departures from normal (°F.) for April 1961. (B) Percentage of normal precipitation for April 1961. (From [4].)

trough near Baja California. The lowering of heights associated with this trough amalgamation along the west coast was reflected downstream in the pattern of rising heights over the Middle Atlantic States in figure 4. These rises resulted in considerable filling of the eastern United States trough in the last half of the month. However heights still remained below normal with depressed westerlies in the East, a common manifestation of blocking conditions at higher latitudes.

## 4. AVERAGE WEATHER IN THE UNITED STATES

### TEMPERATURE

Temperatures averaged cooler than normal over most of the United States except Hawaii, Maine, and parts of the Southwest, as shown in figure 6A. The coolest air, relative to normal, extended from Montana southeastward to the Appalachians, ranging to 6° F. or more below normal in upper Montana, the northern Plains, Pennsylvania, the Ohio Valley, and the southern Appalachians. This pattern was in close agreement with the negative height departures at 700 mb. (fig. 1) and the direction of anomalous flow from western Canada and Alaska. This flow had additional support from the abnormally strong ridge in the eastern Pacific which helped transport cold polar air southward into the United States.

Persistence of the temperature pattern from the previous month, expressed as a percentage of 100 stations not changing by more than one class (out of five) was only 32, compared with average March to April persistence of about 65 percent from 1942 to 1960. This comparison dramatizes the magnitude of the change in regime over North America, due in part to retrogression of blocking from its position over the Atlantic during the previous month.

The average temperature departures for the first and last halves of April are shown in figures 5 C and D. Marked cooling in the Far West and warming in the East are explained in large part by the lowering of heights and trough development near the west coast, and rising heights with resulting partial filling of the trough near the east coast, shown by the height change pattern in figure 4. The relatively larger warming over Texas, where temperatures rose to well above normal in the latter half of the month, may be due, at least in part, to the extreme dryness there, tending to make this region act as a heat source.

### PRECIPITATION

Precipitation this April (fig. 6B) was heavier than normal throughout most of the northern border States, and also from the middle Mississippi Valley across Ohio to the Northeastern States. Another area of very heavy precipitation included Georgia and the Carolinas. Above normal precipitation also occurred in the southern part of the Continental Divide and extreme southern Texas. Elsewhere precipitation was mostly less than normal, with dry conditions approaching drought in many parts of the Southwest and Southern Plains, as well as in parts of the Florida peninsula where the driest April on record was reported. The heavy precipitation areas were closely associated with the prevailing depressed tracks of cyclonic activity, which was generally of a vigorous nature. These tracks are clearly suggested by the trough in the monthly sea level chart (fig. 2) and the negative height departure pattern of the 700-mb. contours (fig. 1). Very heavy precipitation, much of it in the form of snow, occurred in Alaska and was related to below normal temperatures and frequent storminess, as indicated by the mean Low there at sea level (fig. 2).

## 5. WEATHER EVENTS BY 5-DAY PERIODS

### APRIL 1–5

During this period an extremely deep trough aloft near the east coast combined with an abnormally strong ridge near the west coast to bring much cooler air than normal to the eastern half of the United States, with average temperature departures as much as 10° F. in the Appalachian area. The West enjoyed warmer conditions, ranging

to 10° F. above normal in California and parts of Nevada. Hottest temperatures for so early in the spring were reported in some areas such as Yuma, Ariz., where temperatures reached 104° F. Precipitation was generally moderate in eastern and northern sections, although rains in excess of an inch fell in parts of New England in connection with a deep storm that emerged from the Gulf States.

APRIL 6–10

During this period retrogression of large-scale circulation features over the United States was accompanied by an influx of much colder than normal air into western and central sections, ranging on the average to 16° F. below normal in the Central Plains, with above normal temperatures in the country confined to the extreme corners. Heavy precipitation, totaling from ½ inch to well over an inch, occurred in many places from Nevada eastward to the east coast during the passage of a vigorous Low from the southern Rockies to the Mid-Atlantic coast. Snowfall ranging up to 12 inches fell in the Central Plains, and rains up to 2 inches along the Gulf coast accompanied this storm system.

APRIL 11–15

Below normal temperatures persisted during this period from coast to coast, with widespread heavy precipitation over most sections of the country (except the dry Southwest) due to a deep trough in the central part of the country with a strong ridge off the west coast. Temperatures averaged as much as 10° F. below normal in the Central Plains.

The heavy precipitation, over an inch generally in the East and ranging to 3 and 4 inches in the Southeast, accompanied by tornadoes and severe windstorms, was produced by a rapidly deepening storm which traversed this area from the southern Rockies. This storm produced over a foot of snow in some places in the Central Plains, and farther east it yielded the record low pressure of 989 mb. at Louisville, Ky., on the 12th. On this day Huron, S. Dak., recorded a minimum temperature of 6° F., the lowest ever recorded there in April.

Another deep storm traversed the upper Mississippi Valley on the 14th and 15th, bringing heavy precipitation to that area, including about a foot of snow.

APRIL 15–19

In this period shearing of the central Pacific trough carried its northern portion eastward into the Gulf of Alaska, which forced the eastern Pacific ridge inland over the Rockies and the central United States trough eastward to the Appalachians. This eastward motion produced warming to above normal temperatures west of the Continental Divide, while below normal temperatures continued to dominate the country east of the Rockies, averaging as much as 11° F. below normal in some parts. The coldest temperatures for so late in the season occurred in parts of Texas and Louisiana, especially on the 16th.

The warmer air in the West spread eastward from the Rockies, reaching the Mississippi Valley on the 19th. Temperatures ranged up to 21° F. above normal in the Dakotas, with an all time high temperature for so early in spring of 83° F. on the 19th at Denver, Colo. Another mass of very cool Pacific air, as much as 16° F. below normal in Oregon, followed in the wake of this warm air, reaching Salt Lake City on the 19th, accompanied by heavy precipitation in the Pacific Northwest.

Precipitation was heavy from the Mississippi Valley eastward from the same deep storm system of mid-month which slowed down over the Great Lakes Region.

APRIL 20–24

This was the only extended period during the month which departed radically from the monthly mean circulation and temperature regime. During this time a deep mean trough was situated in the Far West with a stronger than normal ridge in the East. Blocking still persisted in eastern Canada, however, but was somewhat diminished in strength. Because of the prevailing southwesterly flow over much of the United States, precipitation was generally heavy from coast to coast north of about 37° N. However, it was largely dry to the south, except in California where heavy rains associated with the deep coastal mean trough extended southward into the southern part of that State.

Temperatures were above normal east of the Continental Divide, averaging as much as 15° F. above normal at Oklahoma City, while, in the West, temperatures averaged as much as 12° F. below normal in Nevada and California. These conditions were favorable for above normal tornado activity in the central sections of the country.

On the 23d the cool Pacific air was centered near Ely, Nev., where temperatures averaged 20° F. below normal that day, while the leading edge of the cool air advanced across the North Central States to the Great Lakes. At this time very warm temperatures, ranging up to 17.5° F. above normal near Amarillo, Tex., stretched eastward to the Mid-Atlantic States, just south of a strong jet stream and polar front. By the 24th the cool Pacific and Canadian air stretched from the southern Continental Divide to the upper Great Lakes, with an active tornado-producing wave cyclone traveling across Iowa toward the Great Lakes. Temperatures in the warm air reached 18° F. above normal in Ohio at this time.

APRIL 25–30

In this period the circulation again reverted to the characteristic monthly regime of trough in the East and ridge in the West, with cooler than normal air practically from coast to coast, averaging as much as 13° F. below normal in the Dakotas and Minnesota. Precipitation during the period was heavy in the East and in most northern border areas.

On the 25th the cool air spread from the lower Great

Lakes region southwestward to Texas, reaching 14° F. below normal in Arizona, while another mass of very cool Canadian air entered Montana. The warm air in the East at this time was attended by a temperature of 91° F., or 20° F. above normal, at Richmond, Va. This was reminiscent of the record warmth in April 1960 when the temperature reached a record 96° on the 26th. These strongly contrasting air masses were associated with another active frontal cyclone which traveled from the Panhandle to the Great Lakes. By the 27th the cool air had swept eastward and stretched from coast to coast, ranging to 19° F. below normal in North Dakota. On the 28th and 29th, warm air was again spreading over the Rockies and southeastward into Texas, where temperatures reached 15° F. above normal on the 30th. On the last day of the month another influx of cold Canadian air entered the North Central States, with temperatures as much as 16° F. below normal in North Dakota.

## REFERENCES

1. J. F. Andrews, "The Weather and Circulation of March 1961—Another Mild Month in the United States," *Monthly Weather Review*, vol. 89, No. 6, June 1961, pp. 205–210.
2. J. F. O'Connor, "The Weather and Circulation of April 1960—A Sharp Mid-Month Drop in the Zonal Westerlies Accompanied by a Temperature Reversal in the Contiguous United States," *Monthly Weather Review*, vol. 88, No. 4, Apr. 1960, pp. 158–166.
3. W. H. Klein, "The Weather and Circulation of April 1953—A Cold Stormy Month with a Low Index Circulation," *Monthly Weather Review*, vol. 81, No. 4, April 1953, pp. 115–120.
4. U. S. Weather Bureau, *Weekly Weather and Crop Bulletin, National Summary*, vol. XLVIII, Nos. 18 and 19, May 1 and 8, 1961.

U.S. GOVERNMENT PRINTING OFFICE: 1961